

UNCLASSIFIED

AD NUMBER
AD820380
NEW LIMITATION CHANGE
TO Approved for public release, distribution unlimited
FROM Distribution authorized to U.S. Gov't. agencies and their contractors; Critical Technology; AUG 1967. Other requests shall be referred to Air Force Flight Dynamics Laboratory, Wright-Patterson AFB, OH 45433.
AUTHORITY
5 Apr 1972, ST-A per AFFDL ltr

THIS PAGE IS UNCLASSIFIED

AD890380

AFFDL-TR-67-74

GUST DESIGN PROCEDURES BASED ON POWER SPECTRAL TECHNIQUES

JOHN C. HOUBOLT

*AERONAUTICAL RESEARCH ASSOCIATES OF PRINCETON, INC.
PRINCETON, NEW JERSEY*

TECHNICAL REPORT AFFDL-TR-67-74

AUGUST 1967

This document is subject to special export controls and each transmittal to foreign governments or foreign nationals may be made only with prior approval of the Air Force Flight Dynamics Laboratory (FDTR), Wright-Patterson Air Force Base, Ohio 45433.

AIR FORCE FLIGHT DYNAMICS LABORATORY
DIRECTORATE OF LABORATORIES
AIR FORCE SYSTEMS COMMAND
WRIGHT-PATTERSON AIR FORCE BASE, OHIO

NOTICE

When Government drawings, specifications, or other data are used for any purpose other than in connection with a definitely related Government procurement operation, the United States Government thereby incurs no responsibility nor any obligation whatsoever; and the fact that the Government may have formulated, furnished, or in any way supplied the said drawings, specifications, or other data, is not to be regarded by implication or otherwise as in any manner licensing the holder or any other person or corporation, or conveying any rights or permission to manufacture, use, or sell any patented invention that may in any way be related thereto.

Copies of this report should not be returned unless return is required by security considerations, contractual obligations, or notice on a specific document.

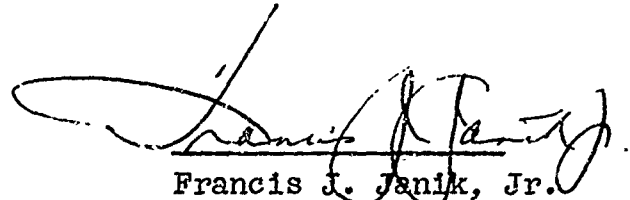
FOREWORD

This report was prepared by Aeronautical Research Associates of Princeton, Inc., Princeton, New Jersey under Air Force Contract AF33(615)-2878, BPSN:5(61136702-62405334). The contract was initiated under Project No. 1367, "Structural Design Criteria, Task No. 136702, "Aerospace Vehicle Structural Loads Criteria".

The work was administered under the direction of the Air Force Flight Dynamics Laboratory, Research and Technology Division, Air Force Systems Command, Wright-Patterson Air Force Base, Ohio, Mr. Paul L. Hasty (FDTR), Project Engineer.

The work reported in this study was conducted by Aeronautical Research Associates of Princeton, Inc. with Dr. John C. Houbolt as principal investigator, and covers the period April 1966 to April 1967.

This technical report has been reviewed and is approved.



Francis J. Janik, Jr.
Chief, Theoretical Mechanics
Branch
Structures Division

ABSTRACT

Further developments of gust design procedures based on power spectral techniques are presented. A number of topics are considered, and presentation is in the nature of a series of interrelated small reports under one cover. Generalized load exceedance curves are considered theoretically, and certain significant properties of these curves are established. It is shown that response and design considerations may be expressed in terms of three basic parameters: P the proportion of time in turbulence, σ_c the gust severity, and a shape parameter which defines the generalized exceedance curves. Over a dozen different families of theoretical exceedance curves are generated. The basic response and environmental parameters that are of concern in design are discussed, and the use of composite values of these parameters as might be involved in mission considerations is shown. The composite gust intensity value σ_c , and the related scale value, L , still represent unsettled questions. A reexamination of some previous airline operational data in terms of generalized exceedance curves is included.

Recommendations on four specific design procedures are given. One of the design procedures, based primarily on the response parameters A and N_0 , incorporates the results of computational studies that were performed on certain existing aircraft as a means for establishing design boundaries. The problem of determining the probability of exceeding given load levels in flights of specified duration is investigated. Areas and parameters which are considered to have weakness or uncertainty are indicated, and recommendations are accordingly made for appropriate future research effort. Consideration of the effect of filtering on deduced scale value is included in an Appendix.

This abstract is subject to specific export controls, and each transmittal to foreign governments or foreign nationals may be made only with prior approval of the Air Force Flight Dynamics Laboratory (AFFDL), Wright-Patterson Air Force Base, Ohio 45433.

9. Probability of Exceedance for Given Flights..... 45

10. Conclusions and Recommendations..... 55

Appendix A - Effect of Filtering on L 59

References..... 63

ILLUSTRATIONS

FIGURE	PAGE
1. Universal Exceedance Curves.....	69
2. Comparison of Different Possible Exceedance Curves.....	76
3. A Composite "Universal" Exceedance Curve; Case j.....	77
4. The Case j Composite Universal Exceedance Curve for Various α	78
5. Case k Composite Exceedance Curves.....	79
6. Case l Composite Exceedance Curves.....	80
7. Exceedance Curve Obtained by Superposition; Case m	81
8. Variation of P With Altitude.....	82
9. Proportion of Time in Turbulence for a Given Type Mission.....	83
10. Tentative σ_c Values.....	84
11. Example Showing Evaluation of Composite A_c	85
12. σ_c Increase Due to Increased Severe Turbulence Encounter.....	86
13. Sensitivity of N to Errors in A , σ_c , N_0 and P ...	87
14. Example Exceedance Curves Illustrating Effect of Errors.	88
15. Effect of Altitude on Universal Curve Shape.....	89
16. Effect of Increased Severe Turbulence Encounter on Universal Curve Shape.....	90
17. Reanalysis of Airline Operations Data.....	92
18. Generalized Exceedance Curves as Derived From the Flight Data.....	98
19. Airplane Computational Results for N_0 vs. $\frac{X}{A}$ Approach..	99
20. Illustrative N_0 vs. $\frac{X}{A}$ Dependence on Flight Conditions.....	100
21. Gust Design by Comparison (Note, Stresswise Adding Metal Lowers A).....	101

ILLUSTRATIONS (Cont'd)

FIGURE	PAGE
22. Design Based on Stipulated σ_c , P, and T	102
23. Master Design Chart for Load Exceedance.....	103
24a. Distribution Function for Repeat Time; Case a.....	104
24b. Distribution Function for Repeat Time; Case b.....	105
25a. Probability of Exceeding Load Level x in Time T ; Case a.....	106
25b. Probability of Exceeding Load Level x in Time T ; Case b.....	107
26. Probability of Not Exceeding Load Level x in Time T .	108
27. Effect of Filtering on L Values.....	109

TABLES

I. Equations for Universal Exceedance Curves.....	65
II. Reanalysis of Airline Data	
(a) Basic Results.....	66
(b) A and σ_c for Various L Values.....	67

SYMBOLS

A	structural parameter; $\sigma_x = A\sigma_w$
$f()$	functional notation, generally representing nondimensional exceedance curve
$F_x(\omega)$	Fourier transform of variable x
h	altitude
L	scale of turbulence
m	number of aircraft in fleet
n	total number of times load level x is crossed with positive slope
n_0	total number of zero crossings with positive slope
n_L, n_u	total number of crossings with positive slope at limit and ultimate loads
N	number of times per second load level x is crossed with positive slope
N_0	number of zero crossings per second with positive slope
$p(x)$ $p(x, \dot{x})$ $p(x, t)$	} various probability distribution functions
P	proportion of time spent in turbulence
$P(x, T)$	probability of reaching x in time T
$q(\sigma)$	probability distribution function of σ
r	ratio; also rate of climb or descent
t	time
T	various flight times, including lifetime value
T_1, T_2	time spent in turbulence
T_x	average time to repeat x
V	flight velocity

SYMBOLS (Cont'd.)

$w(t)$	vertical gust velocity
x	response variable, used generally in the sense of being an increment due to gusts
Δx_L	load level increment giving limit load
Δx_u	load level increment giving ultimate load
x_{l-g}	l-g load level
α	constant used in defining universal curves
λ	wavelength
σ	r.m.s. value
σ_c	composite r.m.s. value of vertical gust velocity
σ_f	r.m.s. value after filtering
σ_t	truncated r.m.s. value
σ_{tc}	composite truncated r.m.s. value
σ_w	r.m.s. value of vertical gust velocity
σ_x	r.m.s. value of variable x
$\sigma_{\dot{x}}$	r.m.s. value of variable \dot{x} ; the dot denotes a time derivative
$\phi(\Omega)$	power spectrum
ω	angular frequency
Ω	spacial frequency, $\frac{\omega}{V}$

Note:

$$\Omega = \frac{\omega}{V} = \frac{2\pi}{\lambda}$$

$$\phi(\Omega) = L\phi(L\Omega) = V\phi(\omega)$$

SECTION 1

INTRODUCTION

Under contract with the Air Force Flight Dynamics Laboratory, Aeronautical Research Associates of Princeton has been developing procedures for designing aircraft for gust encounter based on power spectral techniques. Reference 1 reports the preliminary findings of these studies. In particular, four possible design procedures covering various degrees of sophistication were brought out. This report presents the results of a continuing phase of effort aimed at evolving further the procedures, as well as investigating other aspects of the spectral approach to gust response and design problems. The presentation given herein is in the nature of a series of small reports, covering a variety of interrelated topics which pertain to the subject of gust loads analysis of aircraft.

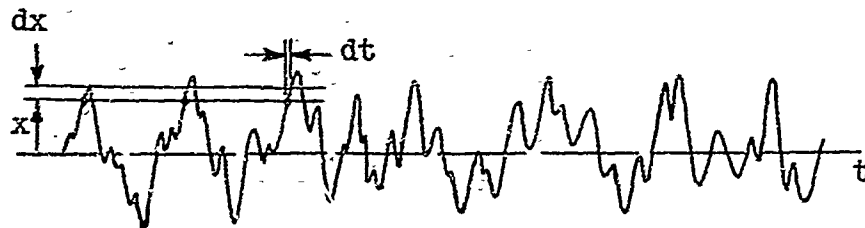
As was brought out in Reference 1, related work has simultaneously been carried out by some of the aircraft companies, sponsored also by the Air Force Flight Dynamics Laboratory and under monitorship by Dr. J. C. Houbolt, the principal investigator of the present investigation. These were computational studies of certain existing gust critical airplanes that were designed by the discrete-gust technique, and were aimed at establishing for these aircraft some of the basic response parameters that are significant in a power spectral design approach. The results, References 8, 9, and 10, are incorporated herein as one of the means for guiding the choice of spectral design numbers and design boundaries. It is well to repeat here one of the underlying theses that is being followed, namely, that of applying a possible new procedure in retrospect manner to proven gust critical aircraft with the concept that if they had been designed originally by the new procedure, safe designs would have also resulted.

SECTION 2

THEORY FOR LEVEL CROSSINGS. $N(x)$

This section gives some of the basic theory that is associated with level or threshold crossings for random time history functions. Application is then made to the gust loads case, with the view toward developing further the concept of "universal load exceedance curves" that is brought out in Reference 1. It is shown, in quite general form, that load exceedance considerations need only involve three basic environmental factors. A new and remarkable moment property of the level crossing curves is also established which is of governing importance in the mathematical description of these curves and which should be of marked significance in the interpretation and use of flight data on load exceedance.

General Formulation.- A derivation of the general equation for determining the number of level crossings is given first, using an approach which is slightly different than that used by Rice in Reference 2. Consider a random function of time as depicted in the following sketch:



We wish to establish the statistical estimate for the average number of crossings of the level x . For any one crossing, the amount of time to cross the interval dx is

$$dt = \frac{dx}{|\dot{x}|}$$

In a total time T , the total time spent in the incremental area dx is, by definition

$$\Delta T = T_p(x, \dot{x}) dx$$

where p represents the joint-probability distribution function of the random function x and its time derivative \dot{x} . The total number of dx crossings in time T is thus

$$dn = \frac{\Delta T}{dt} = T |\dot{x}| p(x, \dot{x}) dx$$

We now find the contribution from all possible \dot{x} 's by integrating with respect to \dot{x} , thus

$$n = T \int_{-\infty}^{\infty} |\dot{x}| p(x, \dot{x}) d\dot{x}$$

The probability density function is supposed symmetric, and, therefore, the contribution from negative x should be the same as for positive x ; the equation may thus be written

$$n = 2T \int_0^{\infty} \dot{x} p(x, \dot{x}) dx \quad (1)$$

This equation yields the total number of crossings, both upward and downward, of the level x . The number of upward crossings (or the number of downward crossings for negative x) is given with the factor 2 suppressed. Thus, suppressing the 2 and putting the equation on a per unit time basis, we obtain the following general form for the number of upward crossings per unit time of the level x

$$N(x) = \frac{n}{T} = \int_0^{\infty} \dot{x} p(x, \dot{x}) d\dot{x} \quad (2)$$

This equation is true regardless of the form of p . Specific analytical expressions for $N(x)$ may be found by substituting in any plausible and convenient expression for the joint distribution function p . In general, these joint distribution functions need only have the following constraints or properties:

$$\begin{aligned} 1 &= \int_{-\infty}^{\infty} \int_{-\infty}^{\infty} p(x, \dot{x}) dx d\dot{x} \\ \sigma_x^2 &= \int_{-\infty}^{\infty} \int_{-\infty}^{\infty} x^2 p(x, \dot{x}) dx d\dot{x} \\ \sigma_{\dot{x}}^2 &= \int_{-\infty}^{\infty} \int_{-\infty}^{\infty} \dot{x}^2 p(x, \dot{x}) dx d\dot{x} \\ p(x) &= \int_{-\infty}^{\infty} p(x, \dot{x}) d\dot{x} \end{aligned} \quad (3)$$

In addition, we limit ourselves to only those p functions which are symmetrical in both the x and \dot{x} directions.

A study of these equations indicates that $p(x, \dot{x})$ must be of the form

$$p(x, \dot{x}) = \frac{1}{2\pi} \frac{1}{\sigma_x \sigma_{\dot{x}}} g\left(\frac{x}{\sigma_x}, \frac{\dot{x}}{\sigma_{\dot{x}}}, \alpha\right) \quad (4)$$

where g is a nondimensional function which is described completely by means of a "shape" parameter α , and by the nondimensional independent variables x/σ_x and $\dot{x}/\sigma_{\dot{x}}$, which involve σ_x and $\sigma_{\dot{x}}$, the r.m.s. values of x and \dot{x} . The factor $1/2\pi$ is included simply as an aid to be used later in defining the basic frequency parameter N_0 . (Note the symmetric properties of p can be explicitly brought out by writing g in the functional form $g\left(\frac{x^2}{\sigma_x^2}, \frac{\dot{x}^2}{\sigma_{\dot{x}}^2}, \alpha\right)$ but for simplicity the square notation will be omitted.) Substitution of this equation for p into Equations 3, and introducing the notation

$$\xi = \frac{x}{\sigma_x} \quad (5a)$$

$$\eta = \frac{\dot{x}}{\sigma_{\dot{x}}} \quad (5b)$$

gives the following properties of g

$$1 = \frac{1}{2\pi} \int_{-\infty}^{\infty} \int_{-\infty}^{\infty} g(\xi, \eta, \alpha) d\eta d\xi \quad (6)$$

$$1 = \frac{1}{2\pi} \int_{-\infty}^{\infty} \int_{-\infty}^{\infty} \xi^2 g(\xi, \eta, \alpha) d\eta d\xi \quad (7)$$

$$1 = \frac{1}{2\pi} \int_{-\infty}^{\infty} \int_{-\infty}^{\infty} \eta^2 g(\xi, \eta, \alpha) d\eta d\xi \quad (8)$$

$$p(x) = \frac{1}{2\pi} \frac{1}{\sigma_x} \int_{-\infty}^{\infty} g(\xi, \eta, \alpha) d\eta \quad (9)$$

Application to Gust Encounter - The Three Basic Environmental Factors σ_x , P , and α . - In application to the airplane gust encounter problem, Equation 2 applies, of course, only during turbulence encounter. To make the equation yield results which give the average level crossing rate based on entire flight time, we multiply by T_t , the total time spent in turbulence, and divide by T , the total flight time; the result is

$$N(x) = P \int_0^{\infty} \dot{x} p(x, \dot{x}) d\dot{x} \quad (10)$$

where $P = T_t/T$ denotes the proportion of time spent in turbulence. Substitution of Equation 4 into this equation yields

$$N(x) = P \frac{\sigma_{\dot{x}}}{2\pi\sigma_x} \int_0^{\infty} \frac{\dot{x}}{\sigma_{\dot{x}}} g\left(\frac{x}{\sigma_x}, \frac{\dot{x}}{\sigma_{\dot{x}}}, \alpha\right) d\frac{\dot{x}}{\sigma_{\dot{x}}} \quad (11a)$$

$$= PN_0 f\left(\frac{x}{\sigma_x}, \alpha\right) \quad (11b)$$

This equation is of fundamental significance. Apart from N_0 , which is related to the structural response characteristics of the aircraft, it shows that the level crossing history of an aircraft in gust is dependent on only three basic parameters: P , the proportion of time in turbulence; σ_x , the severity parameter; and α the shape parameter of the curve $f\left(\frac{x}{\sigma_x}\right)$.

It is noted that the equation is derived through general consideration only. Concepts of an atmospheric model consisting of a series of patches (see Reference 3), or involving the assumption of Gaussian distribution, need not be introduced. Instead the concept is advanced that the gust encounter experience of an aircraft can be described completely in terms of an overall distribution curve of the type given by Equation 4, or, alternatively, by Equation 11. These two equations form the basis for developments contained in this report.

Some general observations pertaining to the applicability of Equation 11 might serve well at this point. First, x represents any variable of concern, either input or output response. If x is a response variable, then its r.m.s. value is related to the p.m.s. gust value through the well-known expression

$$\sigma_x = A\sigma_c$$

The "severity" σ_x is thus related directly to the composite severity σ_c of the gusts through the parameter A . The practical evaluation of the structural response quantities A and H_0 by spectral techniques is considered in Reference 1 and 3.

Secondly, we note, without detailed elaboration, that complete stationarity is not a necessary prerequisite for the random variable x . Stationarity of H_0 is implied but the local r.m.s. value (as defined on a patch sense basis) need not be. Varying H_0 values are easily taken into account by a superposition technique.

Thirdly, it may be remarked that the observations suggested by Equation 11 are also supported by practical considerations. Thus, if one reflects and tries to single out the main factors which govern gust loads experience, it seems plausible that the logic would narrow down to the following three questions:

- 1) What is the time spent in turbulence?
- 2) What is the severity?
- 3) What is the general shape of any chosen load-describing curve?

These three questions are reflected by Equation 11.

In the next section it will be shown that the first moment of the area under the $N(x)$ curve about the origin (considering the right-hand plane only) is of significant practical importance. Thus with Equations 4 and 10 we write the following for later use

$$\int_0^{\infty} xN(x)dx = PN_0\sigma_x^2 \int_0^{\infty} \int_0^{\infty} \frac{x}{\sigma_x} \frac{\dot{x}}{\sigma_{\dot{x}}} g\left(\frac{x}{\sigma_x}, \frac{\dot{x}}{\sigma_{\dot{x}}}, \alpha\right) d\frac{\dot{x}}{\sigma_{\dot{x}}} d\frac{x}{\sigma_x} \quad (12)$$

General Results and Basic Moment Property For a Practical Subclass. - If we restrict our attention to a certain practical class of random functions where, at least, the function and the first derivative are continuous, then further properties of note may be deduced in general. Specifically, suppose the functions are described by joint-distribution functions wherein the independent variables always appear in the combination

$$\frac{x^2}{\sigma_x^2} + \frac{\dot{x}^2}{\sigma_{\dot{x}}^2} = r^2$$

We introduce the change of variable

$$\xi = \frac{x}{\sigma_x} = r \cos \theta$$

$$\eta = \frac{\dot{x}}{\sigma_{\dot{x}}} = r \sin \theta$$

Then for a single integration in the η direction

$$\eta = \sqrt{r^2 - \xi^2}$$

$$d\eta = \frac{r dr}{\sqrt{r^2 - \xi^2}}$$

and for double integration, we have, through the Jacobian

$$d\xi d\eta = r dr d\theta$$

With these relations, Equations 6, 7, 11, and 12 become

$$L = \int_0^{\infty} r g(r, \alpha) dr$$

$$1 = \frac{1}{2} \int_0^{\infty} r^3 g(r, \alpha) dr$$

$$\frac{N(x)}{PN_0} = \int \frac{x}{\sigma_x} rg(r, \alpha) dr$$

$$\int_0^{\infty} x \frac{N(x)}{PN_0} dx = \frac{\sigma_x^2}{2} \int_0^{\infty} r^3 g(r, \alpha) dr$$

From the first and third of these equations, we see that

$\frac{N(x)}{PN_0}$ or $f(x, \alpha)$ of Equation 11 must have the property

$$\frac{N(0)}{PN_0} = f(0, \alpha) = 1 \quad (13)$$

while the second and fourth indicate that

$$\int_0^{\infty} x \frac{N(x)}{PN_0} dx = \sigma_x^2 \quad (14)$$

Equation 14 is of fundamental interest and significance. Geometrically it indicates that the first moment of the area under the right-hand side of the normalized exceedance curve must equal σ_x^2 , a fact evidently not known before. This fact and Equation 13 place important restraints on the form that the exceedance curve can take, and are most useful in establishing analytical expressions for the exceedance curve, as will be seen. These two properties should also be very helpful in the interpretation of experimental data; in fact, if in the deduction of exceedance curves from flight data it is found that these properties are not met, particularly the moment property, then it may be surmised that there is something wrong with the data evaluation or interpretation. It is noted that Equation 14 is exact if N_0 is invariant

with time, but represents a good approximation when N_0 varies slightly and in slow fashion with time, as is found generally in the gust response case.

SECTION 3

SPECIFIC LOAD EXCEEDANCE CURVES

Derivation Procedures.- At least three different procedures may be used for deriving specific load exceedance curves as described in the following.

Direct means:

In this procedure, a form of $p(x, \dot{x})$ satisfying Equations 6, 7, and 8 is assumed. Substitution into Equation 10 leads then directly to the result for $N(x)$. As an example, a case often quoted and used is based on the assumption that x and \dot{x} obey a joint-normal or Gaussian distribution. In this instance, p is given by

$$p(x, \dot{x}) = \frac{1}{2\pi} \frac{1}{\sigma_x \sigma_{\dot{x}}} e^{-\frac{x^2}{2\sigma_x^2}} e^{-\frac{\dot{x}^2}{2\sigma_{\dot{x}}^2}}$$

Substitution of this equation into Equation 10 and the last of Equations 3 yields

$$N(x) = PN_0 e^{-\frac{x^2}{2\sigma_x^2}} \tag{15}$$

$$p(x) = \frac{1}{\sqrt{2\pi}} \frac{1}{\sigma_x} e^{-\frac{x^2}{2\sigma_x^2}} \tag{16}$$

which are noted to be a form of Rice's results.

It is significant to note that a Gaussian assumption is not essential in the treatment of gust loads, as has been the general belief or the underlying assumption in previous studies. Any plausible form of $p(x, \dot{x})$ may be used. As a specific example, if

$$p(x, \dot{x}) = \frac{1}{2\pi\sigma_x\sigma_{\dot{x}}} \frac{\frac{\alpha}{\sigma_x^2}}{\left[1 + \frac{1}{2(\alpha-1)}\left(\frac{x^2}{\sigma_x^2} + \frac{\dot{x}^2}{\sigma_{\dot{x}}^2}\right)\right]^{\alpha+1}}$$

then the following equation results for $N(x)$

$$\frac{N(x)}{PN_0} = \frac{1}{\left[1 + \frac{1}{2(\alpha-1)} \frac{x^2}{\sigma_x^2}\right]^\alpha}$$

By summation of Gaussian cases:

Although not necessary, the technique described in Reference 1 for the composite gust model consisting of the encounter of a number of Gaussian patches of turbulence with varying r.m.s. values of intensity is, of course, still valid. The intensity values of the various Gaussian patches are characterized by a probability density distribution $q(\sigma)$ with properties

$$\begin{aligned} \int_0^{\infty} q(\sigma) d\sigma &= 1 \\ \int_0^{\infty} \sigma^2 q(\sigma) d\sigma &= \sigma_x^2 \end{aligned} \quad (17)$$

The variable σ corresponds to the σ_x used in Equations 15 and 16; the σ_x given by Equation 17 refers to the r.m.s. value of all the patches linked together. With q chosen, we use Equations 15 and 16, with the subscript x dropped, and arrive at the composite results given by

$$p(x) = \frac{1}{\sqrt{2\pi}} \int_0^{\infty} q(\sigma) \frac{1}{\sigma} e^{-\frac{x^2}{2\sigma^2}} d\sigma \quad (18)$$

$$N(x) = PN_0 \int_0^{\infty} q(\sigma) e^{-\frac{x^2}{2\sigma^2}} d\sigma \quad (19)$$

As is proper, it may be shown that the composite density curve must satisfy

$$1 = \int_{-\infty}^{\infty} p(x) dx$$

$$\sigma_x^2 = \int_{-\infty}^{\infty} x^2 p(x) dx \quad (20)$$

Dual but equivalent definitions for the composite r.m.s. value of x are noted to be given by Equations 17 and 20.

To illustrate this procedure, we use the well-known case where q is assumed to be

$$q(\sigma) = \sqrt{\frac{2}{\pi}} \frac{1}{\sigma_x} e^{-\frac{\sigma^2}{2\sigma_x^2}}$$

Substitution of this equation into Equation 19 gives the familiar result

$$N = PN_0 e^{-\frac{x^2}{\sigma_x^2}} \quad (21)$$

By summation timewise:

Reference 1 indicated that equivalent composite results could also be obtained by assuming that the σ_x in Equation 15 is expressed by a timewise variation instead of by a distribution q . In this case the composite results are given by the equations

$$p(x) = \frac{1}{\sqrt{2\pi}} \frac{1}{t_2 - t_1} \int_{t_1}^{t_2} \frac{1}{\sigma} e^{-\frac{x^2}{2\sigma^2}} dt$$

$$N(x) = \frac{PN_0}{t_2 - t_1} \int_{t_1}^{t_2} e^{-\frac{x^2}{2\sigma^2}} dt \quad (22)$$

where σ is some chosen function of time.

As a simple example, suppose

$$\sigma^2 = \frac{a}{t}$$

Substitution into Equation 22 yields the result

$$H(x) = PN_0 \frac{2a}{t_2 - t_1} \frac{1}{x^2} \left(e^{-\frac{x^2 t_1}{2a}} - e^{-\frac{x^2 t_2}{2a}} \right)$$

The constant a is established from the fact that the r.m.s. value is given by

$$\sigma_x^2 = \frac{1}{t_2 - t_1} \int_{t_1}^{t_2} \sigma^2 dt$$

or

$$\sigma_x^2 = \frac{a}{t_2 - t_1} \log \frac{t_2}{t_1}$$

Additional Moment Properties. - Further information on moment properties, specifically the relationships between the various order moments of the area under the p , q , and N curves about the origin, can be derived by suitable manipulations of Equations 18 and 19. Because of the symmetry of the p and N curves, odd-order moments are taken using the right-hand plane only; even-order moments consider both right and left halves. Thus, from Equations 18 and 19, the following equalities may be derived

$$\int_{-\infty}^{\infty} \frac{N}{PN_0} dx = 2\pi \int_0^{\infty} x p(x) dx = \sqrt{2\pi} \int_0^{\infty} \sigma^2 q(\sigma) d\sigma$$

$$\int_{-\infty}^{\infty} x^2 \frac{N}{PN_0} dx = \pi \int_0^{\infty} x^3 p(x) dx = \sqrt{2\pi} \int_0^{\infty} \sigma^3 q(\sigma) d\sigma$$

$$\int_{-\infty}^{\infty} x \frac{N}{PN_0} dx = \frac{3\pi}{2} \int_0^{\infty} x^5 p(x) dx = 3\sqrt{2\pi} \int_0^{\infty} \sigma^5 q(\sigma) d\sigma$$

$$\int_{-\infty}^{\infty} x^n \frac{N}{PN_0} dx = 1 \cdot 3 \cdot 5 \cdots (n-1) \frac{2\pi}{2^{n/2} (\frac{n}{2}!)} \int_0^{\infty} x^{n+1} p(x) dx$$

$$= 1 \cdot 3 \cdot 5 \cdots (n-1) \sqrt{2\pi} \int_0^{\infty} \sigma^{n+1} q(\sigma) d\sigma, \quad n \text{ even}$$

$$\int_0^{\infty} x \frac{N}{PN_0} dx = \int_0^{\infty} x^2 p(x) dx = \int_0^{\infty} \sigma^2 q(\sigma) d\sigma = \sigma_x^2$$

$$\int_0^{\infty} x^3 \frac{N}{PN_0} dx = \frac{2}{3} \int_0^{\infty} x^4 p(x) dx = 2 \int_0^{\infty} \sigma^4 q(\sigma) d\sigma$$

$$\int_0^{\infty} x^5 \frac{N}{PN_0} dx = \frac{8}{3 \cdot 5} \int_0^{\infty} x^6 p(x) dx = 8 \int_0^{\infty} \sigma^6 q(\sigma) d\sigma$$

$$\int_0^{\infty} x^n \frac{N}{PN_0} dx = \frac{2^{\frac{n-1}{2}} (\frac{n-1}{2}!)}{1 \cdot 3 \cdot 5 \cdots n} \int_0^{\infty} x^{n+1} p(x) dx$$

$$= 2^{\frac{n-1}{2}} (\frac{n-1}{2}!) \int_0^{\infty} \sigma^{n+1} q(\sigma) d\sigma, \quad n \text{ odd}$$

The fifth expression is noted to be the important moment property that was brought out by Equation 14. These moment relations are valid essentially for only the class of functions wherein at least the function x and its first derivative are continuous.

Analytical Forms for N and p.- As derived from the foregoing considerations, a number of specific analytical expressions for the "universal" curves for $N(x)$ and $p(x)$ are presented in this section. Three forms are considered.

General form:

A large number of specific analytical expressions were derived by means of Equation 10 or through use of Equations 18 and 19. Some of the more interesting results obtained are shown in Table I as the first nine entries. Figure 1 gives plots of the associated exceedance curves. For some of the cases, $q(\sigma)$ is also shown on the figures. The first three cases are noted to be the same cases as those given in Reference 4, except that here results are given in generalized form.

A comparison of the various cases is given in Figure 2; the specific curve chosen from each case was arbitrary. This comparison indicates that all the curves may be considered to represent various deviations about a basic reference curve

defined by $e^{-\frac{x}{\sigma}}$. If a given universal curve falls above this reference curve at low x values, then it must fall below at high x values; if below at low x , then it must be above at high x . In general, the position of the "tail", or portion of the curve at high values of x , is seen to be very sensitive to the initial position or trend. This tendency is simply reflecting the property given by Equation 14. The fact that the curves appear to have large deviations from one another at large x is, of course, due to the use of semi-log plots; the effect, however, is of much importance in load exceedance and design considerations.

Composite forms:

In the development of the universal exceedance curves of Figure 1 and in taking into consideration the form suggested by flight data, it was observed that a desirable curve would be

one which fell essentially along the $e^{-\frac{x}{\sigma}}$ curve for a wide range of x and which would then depart in upward fashion from this trend at large x . A universal curve of special interest and having these characteristics was therefore developed through use of a composite technique. The curve is shown in Figure 3 and is derived from Equations 13 and 14 as follows.

Assume the upper and lower portions of the curve are given respectively by simple exponential and power laws according to the expressions

$$\begin{aligned} \frac{N}{PN_0} &= e^{-ax} & , x < x_1 \\ &= \frac{b}{x^\alpha} & , x > x_1 \end{aligned}$$

and assume that the two portions join with equal height and slope at the joining point x_1 . These two joining conditions allow for the solution of a and b and yield the result

$$\frac{N}{PN_0} = e^{-\alpha \frac{x}{x_1}}, \quad x < x_1 \quad (23a)$$

$$= \left(\frac{x_1}{ex}\right)^\alpha, \quad x > x_1 \quad (23b)$$

We now invoke relation 14 to solve for x_1 , and find that

$$x_1 = \frac{\alpha \sigma_x}{\sqrt{1 + \frac{\alpha+2}{\alpha-2} e^{-\alpha}}} \quad (23c)$$

Condition 13 is automatically satisfied by the exponential function choice. Equations 23 thus form the universal curve shown in Figure 3. The equations and associated curves applying for various values of α are given below and in Figure 4, where f_a and f_b are used in shorthand way to denote the two portions of $\frac{N}{PN_0}$:

$$\alpha = 6, \quad f_a = e^{-1.0025 \frac{x}{\sigma_x}}$$

$$f_b = \left(\frac{5.985\sigma_x}{ex}\right)^6 = \left(\frac{2.2\sigma_x}{x}\right)^6$$

$$\alpha = 7, \quad f_a = e^{-1.000818 \frac{x}{\sigma_x}}$$

$$f_b = \left(\frac{6.994274\sigma_x}{ex}\right)^7 = \left(\frac{2.57\sigma_x}{x}\right)^7$$

$$\alpha = 8, \quad f_a = e^{-\frac{x}{\sigma_x}}$$

$$f_b = \left(\frac{8\sigma_x}{ex}\right)^8 = \left(\frac{2.94\sigma_x}{x}\right)^8$$

$$\alpha = 9, \quad f_a = e^{-\frac{x}{\sigma_x}}$$

$$f_b = \left(\frac{9\sigma_x}{ex}\right)^9 = \left(\frac{3.31\sigma_x}{x}\right)^9$$

$$\alpha = 10, \quad f_a = e^{-\frac{x}{\sigma_x}}$$

$$f_b = \left(\frac{10\sigma_x}{ex}\right)^{10} = \left(\frac{3.68\sigma_x}{x}\right)^{10}$$

A study of this set of universal curves in the light of flight data indicates that only the larger values of α are of practical concern. For these larger values it is noted that x_1 is given in good approximation by

$$x_1 = \alpha\sigma_x$$

and thus Equations 23a and 23b read simply

$$\frac{N}{PN_0} = e^{-\frac{x}{\sigma_x}}, \quad \frac{x}{\sigma_x} < \alpha \quad (24a)$$

$$\frac{N}{PN_0} = \left(\frac{\alpha\sigma_x}{ex}\right)^\alpha, \quad \frac{x}{\sigma_x} > \alpha \quad (24b)$$

Strictly speaking, to preserve the moment relation given by Equation 14, the coefficient of unity in the exponent of Equation 24a should be minutely larger than one (as given by 23c); the difference between plotted results when using unity or the precise value cannot be detected, however, and so the use of unity for practical purposes is justified. The combination of Equations 24 thus forms a remarkably simple and easy to apply universal curve for load exceedances. Its ease of application will be seen in some of the subsequent design applications. Equations 24 also include another case that has been of special interest; that is, when $\alpha = \infty$ the result is simply

$$\frac{N}{PN_0} = e^{-\frac{x}{\sigma_x}}$$

This is noted to be Case a of Table I.

Cases k and l represent two other interesting composite forms that were derived through use of Equations 13 and 14 and which show characteristics similar to Case j just discussed; plots are given in Figures 5 and 6. Case k is noted to be a refined version of the form

$$\frac{N}{N_0} = P_1 e^{-\frac{x}{\sigma_{x1}}} + P_2 e^{-\frac{x}{\sigma_{x2}}}$$

which has been referred to often in previous studies. The newer developments of the present report have been used to express the equation in a form that is compatible with the other cases.

Superposed forms:

After performing the work covered in the preceding sections, which had the underlying aim of developing reasonably simply analytical expressions for the exceedance curves, and which at the same time yielded desired shape characteristics, the following fact was realized. Any number of different exceedance curves can be added together by coefficients which sum to unity to yield yet another exceedance curve. Specifically, in terms of two different chosen exceedance curves f_1 and f_2 , the following applies in general

$$\frac{N}{PN_0} = f\left(\frac{x}{\sigma_x}\right) = (1 - \alpha) f_1\left(\frac{x}{\sigma_x}\right) + \alpha f_2\left(\frac{x}{\sigma_x}\right)$$

Case m of Table I, and associated Figure 7, illustrate this technique. This case was formed from Cases a and d and is of special interest. It is quite simple analytically, and, in the light of available flight exceedance data, shows good shape characteristics.

With the variety of cases presented in Table I, the question naturally arises as to what forms are most appropriate for practical use. In partial answer to this question, we must admit that at the present time not enough experimental data exist in true generalized exceedance form to allow a selection to be made (or to associate form with mission type).

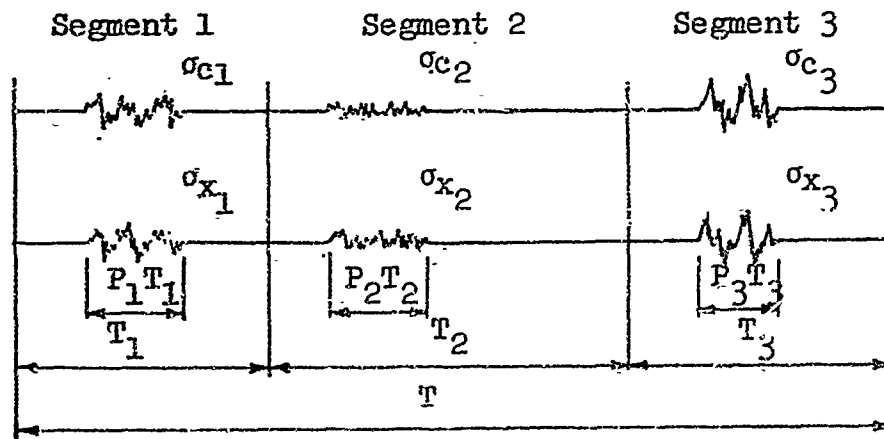
A study made subsequently in this report using a limited amount of flight data indicates which of the forms appear to be favored. On the basis of the information available at the present time, Cases j and m are preferred choices.

SECTION 4

BASIC PARAMETERS FOR DESIGN

In general there are five basic parameters which are involved in the consideration of gust loads. Two are the basic structural response parameters A and N_0 , and three are the basic environmental parameters brought out by Equation 11, namely P , $\sigma_x = A\sigma_c$, and α . These parameters, with the exception of α , are discussed in this section. Because of their close tie-in, A and σ_x are discussed together. A sixth parameter, the scale of turbulence L , may also be mentioned. The scale L and the parameters A and σ_c are so interrelated, however, that only two of the three may be considered independent. Thus comments on the scale value will also be made when appropriate in the discussion of A and σ_x . A further discussion of scale, particularly the effect that filtering of time history gust data has on deduced scale value, is given in the appendix.

All of the subsequent discussion is based on the fact which is demonstrated by Equation 11 that each one of the parameters N_0 , P , and σ_x may be considered to be a composite value of all the flight experience. These composite values may be established conveniently by assuming that the flight of an aircraft is expressed in terms of various flight segments as depicted in the following sketch:



The segments are arbitrary and may represent, for example, climb, cruise, and descent - or any other convenient and appropriate breakdown. The model, somewhat analogous to the discrete-gust patch model concept discussed in Reference 3, corresponds to a condensed version of a mission approach. In the development of this report, the determination of exceedance

curves for each segment is obviated, yet generality and a feel for the sensitivity of mission results to the individual segments can still be retained, as will be seen.

General relationships which apply to this model and which are to be used throughout the developments to follow are

$$PT = P_1 T_1 + P_2 T_2 + P_3 T_3 \quad (25)$$

$$\sigma_c^2 = \frac{1}{PT} (P_1 T_1 \sigma_{c1}^2 + P_2 T_2 \sigma_{c2}^2 + P_3 T_3 \sigma_{c3}^2) \quad (26)$$

$$\sigma_x^2 = \frac{1}{PT} (P_1 T_1 \sigma_{x1}^2 + P_2 T_2 \sigma_{x2}^2 + P_3 T_3 \sigma_{x3}^2) \quad (27)$$

where, for convenience in writing, consideration has been limited to three segments.

Additional basic relationships involving the structural parameter A are

$$\sigma_{x_n} = A_n \sigma_{c_n} \quad (28a)$$

$$\sigma_x = A \sigma_c \quad (28b)$$

The Frequency Parameter N_0 - The total number of upward zero crossings for the model would be

$$n_0 = P_1 T_1 N_{01} + P_2 T_2 N_{02} + P_3 T_3 N_{03}$$

From this equation the composite N_0 follows simply as

$$N_0 = \frac{n_0}{PT} = \frac{1}{PT} (P_1 T_1 N_{01} + P_2 T_2 N_{02} + P_3 T_3 N_{03}) \quad (29)$$

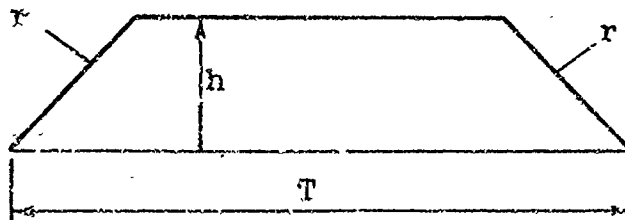
The basic spectral formula for evaluating the individual N_0 's is given in Reference 1.

The Composite Proportion of Time Parameter P.- Some past efforts have attempted to establish the average amount of time that is spent in turbulence, and particularly the variation with altitude. Results vary considerably, References 5, 6, and 7. Because different analytical techniques were used, there is some question on the reliability of the results. In an attempt to ascertain appropriate values of P, consultation was made with various airplane pilots. One in particular, Norman A. Murphy, who has many years of flight experience involving crop dusting, charter, and corporate flying, presented a picture on proportion of time which is considered truly amazing. He verified that geographic location and season were, of course, dominant factors influencing gust encounter. For an overall coverage, however, Mr. Murphy suggested a breakdown involving daytime (8 a.m. - 8 p.m.) and nighttime (8 p.m. - 8 a.m.) operation. The results he gave, purely from mental reflection, are shown in Figure 8. Since these results are not dependent on a specific analytical reduction procedure, they are considered the most reliable yet shown.

As an illustration of how the values of P shown in Figure 8 may be used in mission consideration, consider the daytime values to be represented by the solid straight line segments which are defined as follows:

$$\begin{array}{ll}
 P = .8 e^{-.1623 \frac{h}{1000}} & 0 \leq h \leq 15,000 \\
 P = .07 & 15,000 \leq h \leq 30,000 \\
 P = e^{-.0886 \frac{h}{1000}} & 30,000 \leq h
 \end{array} \quad (30)$$

These equations may be combined with any assumed mission in accordance with Equation 25 to yield the effective value of P. Because of the analytical form assumed for the P's, exact integration can be used in place of a summation convention. For example, the results found from Equations 30 and the assumed mission



are the following

$$0 \leq h \leq 15,000,$$

$$P = .8 \frac{2}{Tra} + .8 \left[1 - \frac{2}{Tra} (1 + ah) \right] e^{-ah}$$

$$15,000 \leq h \leq 30,000,$$

$$P = .8 \frac{2}{Tra} + .07 \left[1 - \frac{2}{Tra} (1 + 15,000a) \right]$$

(31)

$$30,000 < h,$$

$$P = .8 \frac{2}{Tra} + .07 \frac{2}{Tra} \left(\frac{a}{b} - 1 + 15,000a \right) +$$

$$\left[1 - \frac{2}{Trb} (1 + bh) \right] e^{-bh}$$

where $a = \frac{.1623}{1000}$, $b = \frac{.0886}{1000}$ and where r is the rate of climb and descent, here considered equal. Figure 9 shows the results obtained from these equations. These results represent expected average values of P for the assumed mission for daytime operation. Because of the similarity of day and nighttime curves shown in Figure 8, estimates of P for operations which represent a combination of day and nighttime flights may be made quite easily from Figure 9 through use of a simple reduction factor. Thus, for a combination of half daytime and half nighttime flights, P may be estimated simply by multiplying the value shown in Figure 9 by .6. For all nighttime operation a factor of .3 appears reasonably good.

The opinion is given here that values of P for operations which use turbulence-avoidance procedures, as practiced generally by the commercial airlines, are probably not too much less than the values given in the preceding paragraph. Usually the intent of avoidance procedures is to avoid mainly the severe turbulence, and this type contributes only a small amount to P . The principal effect of avoiding the severe turbulence probably shows up more as a change in the value of the shape parameter α , as examples later in the report will show.

Results for P were given in Reference 1 for a different assumed basic variation with altitude, but no equations were given. The variation considered was given by the exponential form

$$P = P_0 e^{-ah}$$

Consideration of the basic climb-cruise-descent type mission led to the following equation:

$$\frac{P_m}{P_0} = \frac{2}{Tra} \left(1 - e^{-ah_m} \right) + \left(1 - \frac{2ah_m}{Tra} \right) e^{-ah_m}$$

where h_m is the mission cruise altitude. This equation gives the results shown in Figure 4 of Reference 1, Vol. II (the subscript m is dropped on both P and h in the figure). The results given are for the assumed values of $P_0 = .2$ and $a = .08/1000$.

The Composite Severity Parameter σ_x and the Related Parameter A .- The composite severity parameter σ_x is given by Equation 27. From the basic relations 28, this severity value becomes

$$\sigma_x^2 = \frac{1}{PT} (P_1 T_1 A_1^2 \sigma_{c_1}^2 + P_2 T_2 A_2^2 \sigma_{c_2}^2 + P_3 T_3 A_3^2 \sigma_{c_3}^2) = A^2 \sigma_c^2 \quad (32)$$

In application, the A_n 's and σ_{c_n} 's of this equation cannot be treated independently at the present time because they are closely linked together by the turbulence scale value L . The values of A are strongly dependent on the scale value used in the chosen gust spectral equation and, in the consideration of flight data, it has not been possible thus far, because of instrumentation limitations, to separate the effects of σ_c and L . Thus, neither σ_c or L , or the variation of these quantities with altitude, are really known at this time. We must await better flight test data to ascertain their values. In the meantime, the approach given in Reference 1, making use of the truncated value of gust intensity, is suggested.

The truncated value of intensity, as associated with the area under the spectrum beyond a frequency Ω_t , is given by

$$\sigma_t = \frac{.885 \sigma_w}{(L \Omega_t)^{1/3}}$$

(Note, σ_t and Ω_t here replace the σ_1 and Ω_1 as used in

Reference 1, and σ_w is the gust intensity of one of the patches that make up the composite value σ_c .) In general, σ_t is given with good accuracy by the flight data, and so the best that can be said about σ_w and L is that they are some combination that satisfies this relation. Without some additional piece of information, no unique values can be established. (Some bounds exist, of course, on σ_w ; i.e., it cannot be smaller than σ_t nor is it larger than the mean square value of the raw time history data of gust velocity.) Lacking specific information on σ_w , we can treat σ_t as the basic gust intensity variable. Concepts of a distribution curve for σ_t , similar to that used in Equations 18 and 19, and a variation of σ_{t_c} with altitude, similar to that given for σ_c in Figure 3 of Reference 1, Vol. II, are equally valid; σ_{t_c} represents the composite value of σ_t , analogous to the use of σ_c as the composite value of σ_w . We may write, therefore,

$$\sigma_{t_c} = \frac{.885\sigma_c}{(L\Omega_t)^{1/3}} \quad (33)$$

On the basis of the limited information that exists, and also as partially guided by the results that were obtained in the reexamination of some airline data as given later in this report, we assume the following: that $\sigma_{t_c} = 2.45$ for an associated $\Omega_t = .003$. These assumptions lead to the σ_c values shown in Figure 10. This figure is tentatively suggested for design purposes.

An equivalent procedure for treating σ_c is the following. If σ_c is eliminated between Equations 28b and 33, we find that

$$\begin{aligned} \sigma_x &= A \frac{(L\Omega_t)^{1/3}}{.885} \sigma_{t_c} \\ &= A_1 \sigma_{t_c} \end{aligned} \quad (34)$$

Reference 1 indicates that A_1 is fairly insensitive to L . Thus, as an alternative to the use of Figure 10, design could make use of Equation 34, with $\sigma_{t_c} = 2.45$ for $\Omega_t = .003$ as the tentative choice for the truncated gust intensity value.

In this form the necessity of considering L is virtually eliminated.

The composite value of A is of interest and may be derived directly from Equations 26 and 32; the result is

$$A^2 = \frac{\sigma_x^2}{\sigma_c^2} = \frac{\gamma_1 A_1^2 + \gamma_2 A_2^2 + \gamma_3 A_3^2}{\gamma_1 + \gamma_2 + \gamma_3} \quad (35a)$$

where $\gamma_n = \frac{P_n T_n}{PT} \sigma_{c_n}^2$. If $\sigma_{c_1} = \sigma_{c_2} = \sigma_{c_3}$, as is suggested in Reference 1, and in the preceding paragraphs, the solution for A is simply

$$A^2 = \frac{P_1 T_1}{PT} A_1^2 + \frac{P_2 T_2}{PT} A_2^2 + \frac{P_3 T_3}{PT} A_3^2 \quad (35b)$$

Thus, Equations 35 provide for the fairly easy evaluation of the effective or composite value of A for use in load exceedance considerations. An illustration of the application of Equation 35b to a fairly complex type mission is shown in Figure 11; the numbers given near the bottom of the figure show which of the segments contribute most to the composite value of A .

With respect to the concept of using an increased σ_c value when increased severe turbulence encounter is contemplated, it should be mentioned that the results given in Figure 5 of Reference 1, Vol. II, are slightly in error; the correct values should be the square root of the values shown. The equation appropriate to the figure is derived as follows. Consider the sequential encounter of turbulence of intensity σ_1 for a time T_1 and of σ_2 for a time T_2 ; the total time of turbulence encounter is thus $T = T_1 + T_2$. The composite mean square value is given by

$$\begin{aligned} \sigma_c^2 &= \frac{1}{T} \int_0^T w^2 dt \\ &= \frac{1}{T} \left(\int_0^{T_1} w_1^2 dt + \int_{T-T_2}^T w_2^2 dt \right) \\ &= \frac{1}{T} (T_1 \sigma_1^2 + T_2 \sigma_2^2) \end{aligned}$$

This may be rearranged to give

$$\frac{\sigma_c^2}{\sigma_1^2} = \frac{1 + \frac{T_2}{T_1} \left(\frac{\sigma_2}{\sigma_1}\right)^2}{1 + \frac{T_2}{T_1}} \quad (36)$$

The correct values of σ_c/σ_1 as obtained from this equation are given in Figure 12 (note P_1 and P_2 of Figure 5 in Reference 1, Vol. II, are replaced here respectively by T_1 and T_2).

Errors and Sensitivity to A and N_0 .- The sensitivity of N to possible errors in A or N_0 , or to errors in σ_c and P, is of interest. One way to show this sensitivity is to assume that A or N_0 may be in error by a given percentage and to determine how much N has changed as a result. Figure 13 shows typical results; the figure shows the percentage change in N due to an assumed 10 percent error in either A or σ_c , or N_0 or P. In Figure 14, error effects are brought out in another way; number of exceedances as might be obtained in a specific case are shown for base values of A, N_0 , σ_c , and P, and for values of these parameters which are assumed to be in error \pm 10 percent. The main effect noted from these figures is that small errors in A or σ_c can lead to large errors in N. A 10 percent error in either N_0 or P gives a 10 percent error in N, but a 10 percent error in A or σ_c can lead to errors in N of several hundred percent. These observations emphasize the fact that A and σ_c are the critical parameters and need to be established as accurately as possible, but that in comparison, approximate estimates suffice for N_0 and P. It is noted that errors in A or σ_c can be likened to the use of a different α curve. Thus the choice of α and the accuracy by which A can be established are closely interrelated.

SECTION 5

EFFECT OF MISSION ON SHAPE OF EXCEEDANCE CURVE

The four possible design procedures that were advanced in reference 1 are to be discussed further in a subsequent section on DESIGN. The subject of mission design merits some additional clarifying thoughts however, and this consideration is given in this section. The mission design procedure that is being followed here, as in reference 1, represents a departure from that explored in the past. Here we do not necessarily build up the mission curve by adding together the curves from all the various assumed flight segments. We simply choose a single universal curve to represent the mission. For example, in Figure 4, the curve for $\alpha = 8$ may be stipulated as the curve applying to Mission A, while the curve $\alpha = 6$ may be chosen to represent Mission B. Thus, in the mission approach under consideration here we simply specify one of the universal curves (which actually may be established by experience on another aircraft). In addition, we need values of σ_c and P . These may be established in two ways: (1) by stipulation, or (2) they may be calculated through mission segment considerations by Equations 25 and 26 (note σ_c and P may be established on a segmented basis even though the N curves are not handled in this way). With the universal curve, σ_c and P chosen, the design curve is completely specified (except for the value of turbulent scale L , which is handled as discussed in connection with Equations 33 and 34.

As a matter of interest, the effect of mission on the shape of the mission universal curve is demonstrated by the following treatment. Consider a mission composed basically of three different segments, an ascent, cruise, and descent portion. We may construct a universal curve applying to the whole mission in a manner analogous to the segmented mission approach, but here, we assume that each segment is governed by the same basic universal curve, say one of the curves in Figures 4 or 7. We write for convenience that $N(\)/PN_c = f(\)$; the composite curve for load exceedance then follows as

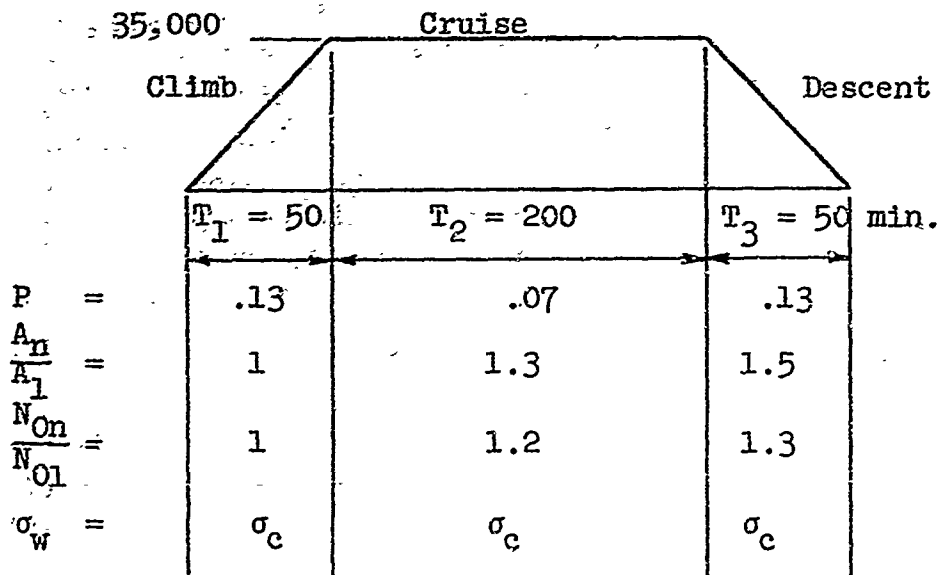
$$n = P_1 T_1 N_{01} f\left(\frac{x}{\sigma_{x1}}\right) + P_2 T_2 N_{02} f\left(\frac{x}{\sigma_{x2}}\right) + P_3 T_3 N_{03} f\left(\frac{x}{\sigma_{x3}}\right) \quad (37)$$

The analysis and equations that apply for determining the composite values P , σ_c , σ_x , and N_c are given in the preceding section. Through these equations Equation 37 may be written in the universal form

$$\frac{n}{PN_0} = \frac{N}{PN_0} = \epsilon_1 f\left(\frac{x}{\sigma_x} \frac{\sigma_x}{\sigma_{x1}}\right) + \epsilon_2 f\left(\frac{x}{\sigma_x} \frac{\sigma_x}{\sigma_{x2}}\right) + \epsilon_3 f\left(\frac{x}{\sigma_x} \frac{\sigma_x}{\sigma_{x3}}\right) \quad (38)$$

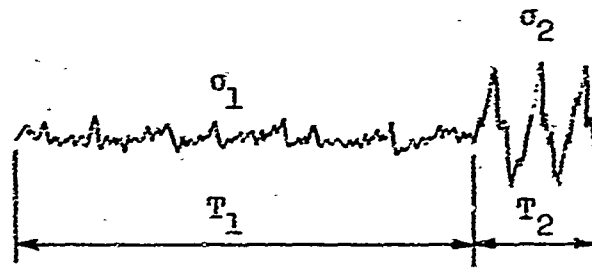
where $\epsilon_i = (P_{iH}/PT)(N_{On}/N_0)$

Altitude Effect. - To see how the shape of the universal curve might be influenced by mission, Equation 38 was applied to the assumed high altitude mission shown in the following sketch:



Note that the gust velocity is assumed to be invariant with altitude. Results obtained using the $\alpha = 8$ curve of Figure 4 as the basic universal curve are shown in Figure 15. The $\alpha = 8$ universal curve is shown also and is labeled zero altitude, since this curve is precisely the result that would be obtained for an assumed "zero altitude" mission. A comparison of results and referral to Figure 4 indicates that the main effect of altitude is to yield a universal curve having a slightly lower value of α .

Turbulence Intensity Effect. - The effect on shape of increased operation in severe type turbulence can be demonstrated in a similar way. Consider, for example, an operation having turbulent encounter as shown in the following sketch



If this model is analyzed in a manner analogous to that used for Equation 38, the following result is obtained

$$\frac{N}{PN_0} = \frac{1}{1 + \frac{T_2}{T_1}} \left[f\left(\frac{x}{A\sigma_c} \cdot \frac{\sigma_c}{\sigma_1}\right) + \frac{T_2}{T_1} f\left(\frac{x}{A\sigma_c} \cdot \frac{\sigma_c}{\sigma_2}\right) \right] \quad (39)$$

where $\frac{\sigma_c}{\sigma_1}$ is given by Equation 36, and where $\frac{\sigma_c}{\sigma_2} = \frac{\sigma_c}{\sigma_1} \frac{\sigma_1}{\sigma_2}$.

Figure 16(a) shows the universal curves that are obtained in this case for various values of T_2/T_1 and σ_2/σ_1 , arbitrarily choosing the Case (a) universal curve of Figure 1 as the basic curve. With reference to Figure 4, we see that the tendency to shift to curves having lower values of α is much more pronounced in this instance than for the altitude case. These tendencies and trends suggest that a reasonable scheme for selecting the universal curve to use in design application could be of the nature indicated by the following listing:

	Case j	Case m
1. Normal low altitude mission	$\alpha = 8$.005
2. Normal high altitude mission	$\alpha = 7.5$.01
3. Extended flight through severe turbulence	$\alpha = 6$.04

The numbers given here are not necessarily recommended choices; they are intended mainly to indicate the general trends or behavior. It should be noted that the discussion here is centered mainly on the shape of the curve; each mission may have different composite values of σ_c and P , and they, of course, individually have a marked influence on the load exceedance history, as much or more so than the shape factor. In the examples given, these values were suppressed in the role of normalizing factors so as to emphasize the shape effect.

Figure 16(b) is an extension of the results of Figure 16(a) to show that as the assumed operation approaches complete severe turbulence encounter, $T_1 \rightarrow 0$, the universal curve returns to the same form as that for no severe turbulence encounter, $T_2 \rightarrow 0$. The load history for the high ratios of T_2/T_1 will, of course, be much more severe than for the low ratios of T_2/T_1 .

because σ_c is greater, even though the shapes of the universal curves are essentially the same as for the case $T_2/T_1 = 0$. The most marked change in shape is noted to occur when only a small amount of severe turbulence is involved.

SECTION 5

REEXAMINATION OF OPERATIONAL DATA

The applicability of the universal curves of Figure 4 was tested by applying the curves to the flight operational data given in Reference 4. Part of this reexamination consisted of reevaluating the values of A and N_0 that applied to the airplanes, because only crude estimates of these parameters were used in the reference report; the rigid body results given in Section 5 of Reference 1, Vol. II, were used for this purpose. Results of the test are shown in Figure 17; associated values of the various parameters that were evaluated and deduced, such as P , σ_c , α , are listed in Table II.

The fitting of the universal curves given by Equation 24 and pictured in Figure 4 involved two kinds of fit: (1) at least two of the leftmost data points fell on the straight line section of the universal curve, Operations 1, 2, 3, 4, 5, 6; (2) only one point fell on the straight portion so that the joining point of the two portions was between the first and second point, Operations 7 and 8.

The results for A and σ_c in Table II (a) apply to an assumed scale $L = 1000$ ft. In Table II(b) the results for other choice of L are given as well. The wide variation shown in the deduced value of σ_c , depending on the value of L used, demonstrates the role and importance of knowing the scale value. As another interesting point to be seen, the table shows also the influence of flight route on the amount of time spent in turbulence; specifically, the largest values of P are seen to be associated with geographic locations where more turbulence is generally to be expected.

Some comments on the success of the reexamination follow. The matching of the flight data with the universal curve chosen is perhaps the best ever seen. There is no arbitrariness about fitting the curves. Further, it appears that the curves provide a consistent and reliable means for deducing the values of P and σ_c that apply. It is noted also that in the case of Equations 24, the properties of exponential and powers laws are such as to make the fitting of the analytical expressions to the data a rather easy task. With the encouraging success indicated here, it is considered desirable to examine in future work the applicability of the various generalized exceedance curves to other flight data.

Many aids may be devised to simplify the task of fitting a chosen universal curve to flight data. One is to plot exceedance values against x^4 on log-log paper to judge whether the data tend to behave as a power law at high x ; the use of

the fourth power is arbitrary, but the choice helps to reduce the steepness of the curves and aids in fairing. Another aim is the following: convert the exceedance values to a N/N_0 basis, divide the variable x by several assumed values of σ_x , multiply the N/N_0 values by e^{-x/σ_x} and plot the results against x/σ_x . The value of σ_x which causes the data points to lie along a horizontal line at low x is the deduced flight value; the value where this horizontal line intersects the vertical axis is the P value. To find the α value, multiply the chosen universal curves also by e^{-x/σ_x} and plot; then lay the flight results over these modified analytical curves so that the chosen flight horizontal line overlays the horizontal line for the analytical curves (which should be unity). The value of α is then found by interpolation by noting where the flight values at high x/σ_x fall relative to the various analytical curves.

This reexamination, using the curves of Figure 4, was made before the curves of Figure 7 (and some of the other cases) had been established. It is expected, however, that equal success and similar P and σ_x values would have been found if the curves of Figure 7 had been used.

A summary of the generalized exceedance curves as derived from the flight data is given in Figure 18 as a matter of interest. We conclude this section with an observation that is in the nature of a warning. We should not draw any hard conclusions from this reanalysis, or from the summary given in Figure 18 for the following reasons. First, only a limited amount of data has been considered here. Secondly, the exceedance data used is, strictly speaking, not of the proper kind; the data represents a certain type of peak count analysis, but whether the specific count analysis used represents the results that would be obtained by a level crossing analysis - on which the exceedance curves are based - is not known. Therefore, we cannot judge at this time which family (or families) of generalized curves represents flight exceedance the best. We should also keep in mind the following thought in any future analysis: any exceedance analysis should also include data at low x values because knowledge of the behavior of the exceedance data at low and intermediate x can be very valuable in predicting how the exceedance curves should behave at very large x , where data is usually nonexistent. Stated in another way, the behavior of the exceedance curve at large x is very strongly dependent on whether the curve at low values of x is convex, straight, or concave, when viewed from above (on the basis of a semi-log plot).

SECTION 7

DESIGN PROCEDURES

In the light of the newer developments that have been found in this phase of study, we examine, in this section, the four design procedures that were advanced in Reference 1. Essentially, the four procedures still appear sound. Some of the numbers are altered slightly herein; other numbers still cannot be fixed with certainty until better and more appropriately analyzed flight data become available.

The discussion is presented for the most part using a general notation for the universal exceedance curve. In places, Equation 24 is used to give specific illustration.

In the lifetime T of the airplane, the number n of exceedances of level x is (see Equation 11)

$$n = TN(x) = PTN_0 f\left(\frac{x}{\sigma_x}, \alpha\right) \quad (40)$$

where

$$\sigma_x = A\sigma_c$$

Most of the discussion to follow is given on the basis of limit load considerations; a treatment of ultimate load is also given, however, to show that some insight on the nearness to or possibility of ultimate load encounter can be gained, even though possible complications, such as nonlinear structural and aerodynamic behavior, are not considered.

At limit load, $x = \Delta x_L$, we wish the expected number of exceedances, as given by Equation 40, to be equal to or less than a specified number n_L ; thus

$$PTN_0 f\left(\frac{\Delta x_L}{\sigma_x}, \alpha\right) \leq n_L \quad (41)$$

In terms of Equation 24b, this relation reads specifically

$$PTN_0 \left(\frac{\alpha \sigma_x}{ex}\right)^\alpha \leq n_L \quad (42)$$

Design Based on N_0 vs. x/A .- For safe design, Equations 40 and 41 indicate the following functional relation between N_0 and x/A :

$$N_0 \leq \frac{n}{P T \left(\frac{x}{A \sigma_c} \right)^\alpha} = F \left(\frac{x}{A} \right)$$

With Equation 40, this would read specifically

$$N_0 \leq c_1 \left(\frac{x}{A} \right)^\alpha \quad (43)$$

As mentioned in Reference 1, c_1 can be established by assigning values to n , P , T , σ_c , and α , or it may be found in empirical manner by applying the equation in retrospect manner to past gust-critical airplanes that have proved themselves airworthy by many years of successful operation. Let us examine what the second of these two ways indicates. In Figure 19, we plot the results of the computational studies that are presented in References 8, 9, and 10. We see the expected "shot gun" pattern of points and note that they establish a reasonably well-defined left-hand border, as was anticipated and hoped. Equation 43 was used to establish the three border curves shown; the curves, representing $\alpha = 7, 8, \text{ and } 9$, were all arbitrarily made to pass through the point $x/A = 52.5$, $N_0 = 1$. Specifically, the chosen borders are given by the equation

$$N_0 = \left(\frac{x}{52.5A} \right)^\alpha \quad (44)$$

It is noted that, because of the general steepness of the curves, the border itself is not too critically dependent on the value of α chosen. Note also that quite similar borders would be established if other specific forms of the exceedance curve had been used.

The results shown in the figure are for computations based on a scale $L = 1000$ ft. If, however, the results for other L values are plotted using $\frac{x}{A} \left(\frac{1000}{L} \right)^{1/3}$ as the abscissa, as based on the indications of Equation 34, then similar patterns with the same left-hand boundary are found. It would appear desirable, therefore, to use the abscissa which includes the L factor, since the necessity for specifying

L. thereby becomes obviated.

An important point to note in this procedure is the following. In the consideration of various flight conditions, it is possible that one or more flight conditions may give combinations of N_0 and x/A for a specific structural design point that falls to the left or unsafe side of the design border, while all other flight conditions yield values which fall to the right or safe side. The composite value combination of N_0 and x/A , as given by Equations 29 and 35b may, however, still fall on the safe side. A procedure as follows is therefore suggested. Evaluate N_0 and x/A for various flight conditions, and, if the points all fall on the safe side, the design may be judged safe; there is no need to establish composite or mission values. If some of the points fall on the unsafe side, then determine the composite values of N_0 and x/A ; in all likelihood, these will fall on the safe side, thus indicating a safe design. If the composite values fall on the left side, the design should, of course, be judged unsafe.

Figure 20 presents some of the airplane computational results to illustrate these situations. For the RB-57, stress point 9 appears safe for all four flight conditions assumed. For stress point 13 however, a combination for N_0 and x/A is obtained which falls just to the left of the design border. The flight condition for this case is 5% fuel at 50,000 ft. altitude. In this situation the design may be judged safe without establishing the composite values of N_0 and x/A , since the amount of time spent in this apparent critical flight condition is surely quite small. A similar situation is found to occur for stress point 1 for the B-58, whereas for stress point 3, results fall on the safe side for both flight conditions investigated. The results shown for the KC-135 are seen to be safe, and serve also to show the spread in points due to various flight conditions.

In general, the concept of using past aircraft to establish a design border for this N_0 vs. x/A approach appears successful. The use of composite values of N_0 and x/A when necessary makes the approach quite attractive and versatile. The nature of the results found suggest, in fact, a simplification worthy of consideration. As noted, the design borderline is characterized by a marked steepness, so much so that it appears a vertical line design border might serve just as well for practical purposes. From the results shown in Figure 19, we might choose, for example, a vertical line at an abscissa value of 55. Design could then be couched in the following concise phrasing; design for gusts shall be

such as to satisfy $\frac{1}{A} \left(\frac{1000}{L} \right)^{1/3} \geq 55$. This approach is, of course, the $\eta\sigma_w$ approach advanced in Reference 3; it is analogous to the discrete-gust approach and has simplicity as one of its merits. These results also bring out again a point that was discussed in a previous section, namely, that A is predominant in design, and that relatively, N_0 has a secondary role.

Design Based on Comparison.- The comparison chart that follows from Equation 40 and which takes the place of Figure 6 in Reference 1, Vol. II, is given in Figure 21. The curves shown are based on Equation 42. This method is still considered good. Not only is it good for comparing one aircraft design to another design, but it should be especially good for comparing the adequacy of the design at one point of an airplane with the design at another point of the same airplane. This latter point deserves much attention. Thus, some other procedure may be used to evaluate or fix the design at a given critical reference point on the wing, for example, and then use can be made of the comparison technique to check other points along the wing or elsewhere. When applied in this way to the same design, there is no concern over what the values of P, T, and σ_c (or L) should be. Again, composite values as given by Equations 25, 26, 29, and 35b, may be used if desired or needed.

Design Based on Stipulated σ_c , P, and T.- In this procedure, we specify the values of σ_c , P, T, and L to be used for design (and a particular universal exceedance curve); we also fix the number n_L of limit load encounters acceptable. Values of A and N_0 are computed for various flight conditions and, for simplicity, may first be checked individually. If some are found to be on the unsafe side for certain flight conditions, then, as in the previous two approaches, composite values of A and N_0 (and P) may be used to test acceptability from a mission point of view. Design can be examined completely and directly on the chosen universal exceedance curve, as is indicated in Figure 22. For limit load, Equation 41 indicates

$$\frac{n_L}{PTN_c} \geq f\left(\frac{\Delta X_L}{A\sigma_c}, a\right)$$

The left-hand side of this relation fixes the level of the horizontal line a. For a design to be considered satisfactory, level a must be equal to or above point A. Ultimate load encounter may also be treated, at least in a

rough sense, by introducing the number m of airplanes in the fleet. We do not wish to encounter an ultimate load during the lifetime of the fleet and thus, on the basis that Equation 40 also applies in approximate fashion to ultimate loads, we have

$$n_u = 1 > mPTN_0 f \left(\frac{\Delta x_U}{A\sigma_c}, \alpha \right)$$

or

$$\frac{1}{mPTN_0} > f \left(\frac{\Delta x_U}{A\sigma_c}, \alpha \right)$$

In this case, the left-hand side fixes the level of the horizontal line b . The example numbers shown in Figure 22 serve to illustrate the procedure.

The "master design" chart form suggested in Reference 1 may also be used in an alternative way to assess the design. Figure 23 illustrates the form, using Equation 24b with $\alpha = 8$ to establish the curves. This particular form was suggested because of the analogy to and possible use for fatigue considerations, as brought out in Reference 1.

The following comments are intended to be of a general nature, and indicate one means for establishing the number of limit load encounters that might be appropriate for design use. The process is admittedly open to some question since ultimate load aspects are involved, and since the numbers found are dependent on the particular exceedance curve chosen, but at least order of magnitude values should be indicated. If Equation 24b and the abscissa relations shown on Figure 22 are used, the following simple relation for the ratio of the number of limit load encounters to the number of ultimate load encounters is found

$$\frac{n_L}{n_u} = \left(\frac{1.5r + .5}{r} \right)^\alpha$$

This relation yields the results

r or $\frac{\Delta x_L}{x_{1-g}}$	$\alpha = 6$	7	8	9	10
1	64	128	256	512	1024
1.5	38	70	128	234	430
2.0	29	50	88	154	270

Statistically, these numbers indicate the number of limit load encounters that may be expected for the fleet for one expected ultimate load encounter; for example, 512 are indicated for the case of $r = 1$ and $\alpha = 9$. From these numbers and a consideration of airplane fleet size, we can establish the number of limit load encounters per airplane that is reasonable to use for design. Thus, for the example ratio of 512, the following relation between fleet size m and limit load encounters n_L per airplane must be preserved so as not to exceed (statistically) one ultimate load encounter of the fleet

m	n_L
64	< 8
128	< 4
256	< 2
512	< 1
1024	< $\frac{1}{2}$

These numbers simply reflect the fact that if more airplanes are involved, then the chances of encountering ultimate load increase. Other exceedance curves would indicate different numbers, but we must await better experimental evidence to judge which curve is the most realistic to use.

Design Based on Mission Approach (Utilizing exceedance curves for each segment).— The mission approach, in which exceedance curves are established for each assumed mission segment and then summed, is not developed further herein as a design tool. A supplemental report to this report is intended, however, to cover additional developments and newer ideas on this approach. In reading the subsequent discussion, the following thought should be kept in mind. Most of the observations are made here in a negative vein; positive aspects will be dealt with in the supplemental report. The lack of support indicated here is not because the mission approach is felt to be improper. The principal investigator of the present report, in fact, first advanced the use of generalized ex-

ceedance curve in a mission approach in Reference 11, and restated the concept in Reference 3. The approach is still considered good, but unfortunately not enough information exists as yet to place it on an acceptable firm basis.

At the present time the segmented mission approach is recommended not as a direct design tool, but rather as a means for assessing how the character of the expected load history is changed if the aircraft is utilized in different ways. There are several reasons for these observations. The main reason is that too many uncertainties still exist with respect to the input quantities. In the treatment of physical problems in which uncertainty exists, there is sometimes a tendency to add yet another ingredient to the problem in the belief that the situation is made clearer. In reality though, the problem has been made all the more uncertain. At present, the segmented approach, while potentially a very powerful tool, has many of these aspects. In particular, when evaluated on the basis of the number of statistical variables involved, the approach has four independent variables; these may be stated in various ways, but a common way expresses them as 2 proportion of time values, and 2 gust severity values. While attempts have been made to establish these values, they are still very uncertain.

The approaches given herein can accomplish everything that can be done with the segmented approach, but in a much abbreviated way, and with fewer variables. Corresponding to the four variables mentioned, there are only three, or less, involved in the approaches of this report - specifically P , σ_c , and α (for the N_0 vs. x/A approach, there are none). The uncertainty of a fifth variable, which is common to all procedures, the scale L , has also been removed to a large extent. In a sense the uncertainties that exist with all the specific generalized exceedance curves of the mission approach are here lumped together into a single curve described by the parameter α . The underlying thought is that instead of summing together, say, 10 different curves, each of which has a degree of uncertainty, why not choose a single curve representing the sum, which, even though it too may be somewhat uncertain, is at least guided or constrained more directly by past experience results.

An illustration of the pitfall that may be encountered if design is made on a mission basis is afforded by back reference to Figure 1/e. These results were obtained from three different airplanes of the same type that were utilized in three different ways, but at essentially the same mission altitude. The question suggested by these results is: how might a mission have been conceived for design that could have covered the load histories actually experienced? A mission covering the lowest curve might have been conceived only to find that the results given by the top curve were obtained in utilization of the aircraft. The answer is that the mission conceived must cover all possible future uses of

the aircraft, and if this is the case, we might just as well select a single exceedance curve to begin with that, if anything, is on the conservative side.

A point made by a friend serves well. He states the case, "I have the graph of the load experience of an airplane locked up in my desk. You compute by mission consideration what the load history is, and we will compare results". He knows that if he gives the graph out first that computations can always be tailored so that the computed results agree well with the flight results. The ability to predict actual load histories is, however, still quite questionable. The main reason is that the input quantities are not consistent and reliable.

As mentioned previously, the mission segment procedure can, nevertheless, be used at the present time for investigating how the loads might be influenced by different uses of the aircraft. The results given in Figures 15 and 16 are illustrative of this procedure.

SECTION 8

CONSIDERATION OF STRUCTURAL INTERACTION EFFECTS

The exceedance considerations discussed so far in this report apply to any response quantity which can be treated separately. It is known, however, that there are often points in aircraft structures where the strength is governed by structural interaction boundaries; that is, the strength depends on the combination of two stresses, such as an axial stress and a shear stress. The problem of determining the number of times a given interaction boundary is exceeded is therefore present.

The means for determining the expected number of exceedances of a given structural interaction boundary has been developed in a separate study. The procedure is general but quite simple, and exact solutions have been obtained for certain cases. A report covering the study is under preparation and thus no further discussion will be given here.

SECTION 9

PROBABILITY OF EXCEEDANCE FOR GIVEN FLIGHTS

In the development of this report there is no explicit consideration given to establishing probability of failure or the probability levels of exceeding certain loads, such as limit load. The reason is that there is no need to do this. There may be interest and concern, however, in the question of what is the probability of exceeding a certain load level in a given number of hours of routine flight, or for flights such as extended operation through known severe turbulence conditions. An analysis of this probability problem is given in this section. The results are basic and apply in general to the probability of failure or the probability of survival for structures exposed to random loading. Three solutions are presented.

A fundamental ingredient to all solutions is the average repeat time for a given load level. From the generalized exceedance Equation 11, this value is

$$T_x = \frac{1}{N} = \frac{1}{PN_0 f} \quad (45)$$

where f is understood to represent the function $f\left(\frac{x}{\sigma_x}, \alpha\right)$.

We ask then, what is the probability that the load level x will be exceeded in time T .

The first solution is approximate. We assume that T is very small compared to T_x . Then the probability of exceedance is simply

$$\begin{aligned} P(x, T) &= \frac{T}{T_x} \\ &= TPN_0 f \end{aligned} \quad (46)$$

The solution obviously breaks down when T approaches or exceeds T_x . (Note in this presentation the distinction between the functional notation $P(x, T)$ for the probability and the proportion of time P should be kept in mind; \bar{P} will be used throughout the remainder of this section to denote the proportion of time P .)

The second solution follows the line of reasoning used in a private communication from Prof. B. Etkin. Let T be divided into a sequence of small intervals Δt such that

$T = n\Delta t$ and that $\Delta t \ll T_x$, and assume that the probability of x being reached in any particular interval is independent of whether x was reached in any other interval. The probability of reaching x in Δt is therefore

$$P(x, \Delta t) = \frac{\Delta t}{T_x}$$

so that the probability that x will not be reached in Δt is

$$Q(x, \Delta t) = 1 - P = 1 - \frac{\Delta t}{T_x}$$

By the assumption of independent events the probability that x will not be reached in the n successive intervals is

$$\begin{aligned} Q(x, n\Delta t) &= \left(1 - \frac{\Delta t}{T_x}\right)^n \\ &= \left(1 - \frac{T}{nT_x}\right)^n \end{aligned}$$

For n very large, and by the known relation that

$$\lim_{n \rightarrow \infty} \left(1 - \frac{a}{n}\right)^n = e^{-a}$$

the value for Q becomes

$$Q(x, T) = e^{-\frac{T}{T_x}}$$

From this relation the probability that x is reached in time T is found to be

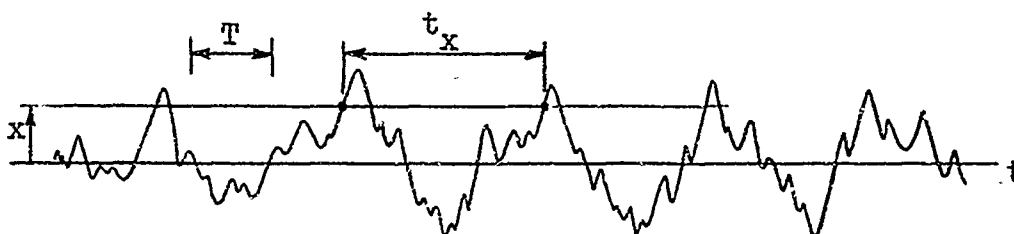
$$P(x, T) = 1 - e^{-\frac{T}{T_x}}$$

With Equation 45 this yields the desired result for P

$$P(x,T) = 1 - e^{-TPN_0 f(x)} \quad (47)$$

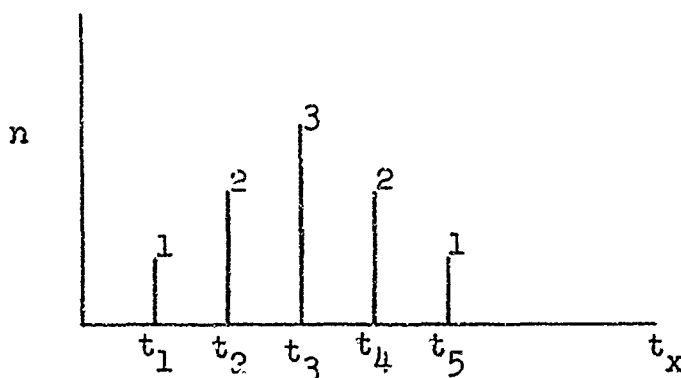
This equation is noted to be associated with the Poisson distribution.

It is questionable whether Equation 47 properly represents the actual characteristics of a random function. For one thing the equation is based on the average repeat time, but in reality the repeat time is variable and must be characterized by a distribution function. Secondly, the equation does not yield the correct results when applied to a deterministic function such as a sine wave, as is the belief that it should. A development which overcomes both of these objections is the following. Consider the random function shown in the following sketch

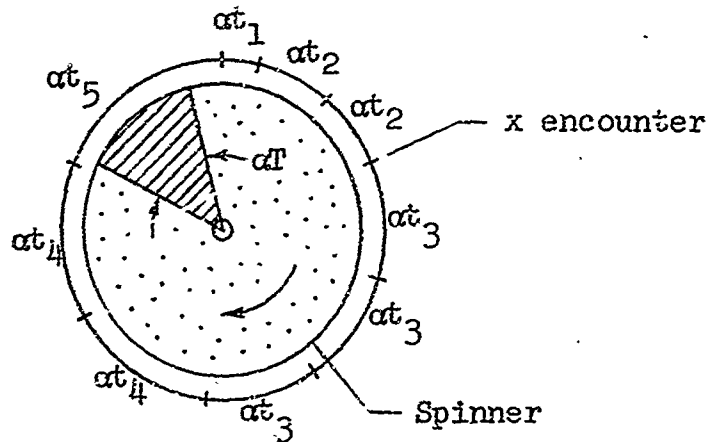


We are interested in the probability of whether the level x will be experienced in a given time interval T . By way of illustration we first analyze the situation on the basis that t_x is characterized by a discrete value distribution; afterwards a continuous distribution function for t_x is considered.

Suppose that the individual t_x values are read over a long time interval and that when these values are grouped in interval brackets, that the following specific distribution diagram is found



To find the probability of encountering x in time T we can make use of a probability wheel of the following type



The factor α is inserted simply to convert the time values to angle notation, such that

$$2\pi = \alpha \sum_i n_i t_i$$

Assume, for illustration purposes, that

$$t_3 < T < t_4$$

Then, through the consideration of many repeated spins of the dial, the probability that the shaded area will not cover an x encounter in a single try is

$$Q(x, T) = \frac{2(t_4 - T) + (t_5 - T)}{t_1 + 2t_2 + 3t_3 + 2t_4 + t_5} \quad (48)$$

The probability of encountering x is thus

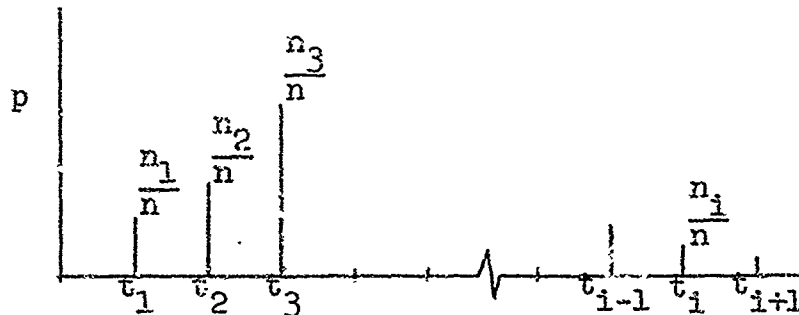
$$P(x, T) = 1 - Q(x, T) = 1 - \frac{2(t_4 - T) + (t_5 - T)}{t_1 + 2t_2 + 3t_3 + 2t_4 + t_5}$$

The average repeat time is found from the first moment of the n diagram, or specifically

$$T_x = \frac{t_1 + 2t_2 + 3t_3 + 2t_4 + t_5}{1 + 2 + 3 + 2 + 1} \quad (49)$$

$$= t_3 \quad \text{if} \quad t_i = i\Delta T$$

A generalization of this elementary model may be made as shown by the following density plot and equations



where

$$n = n_1 + n_2 + n_3 + \dots$$

$$p_i = \frac{n_i}{n}$$

$$\sum_i p_i = 1 \quad (50)$$

In analogy to Equations 48 and 49, and for $T < T_1$, we may write the probability of not encountering x as

$$Q(x, T) = \frac{n_1 (t_1 - T) + n_{i+1} (t_{i+1} - T) + n_{i+2} (t_{i+2} - T) + \dots}{n_1 t_1 + n_2 t_2 + n_3 t_3 + \dots}$$

OF

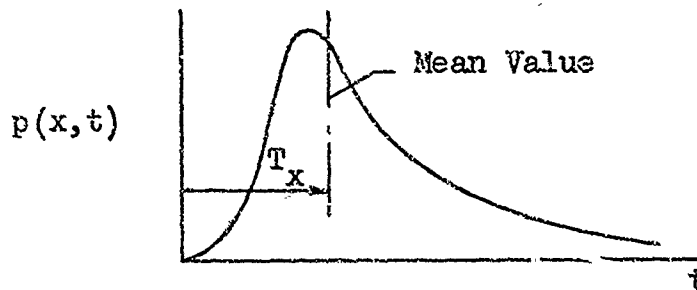
$$Q(x,T) = \frac{p_1 (t_1 - T) + p_{i+1} (t_{i+1} - T) + p_{i+2} (t_{i+2} - T) + \dots}{p_1 t_1 + p_2 t_2 + p_3 t_3 + \dots}$$

$$= \frac{\sum_{j=1}^{\infty} p_j (t_j - T)}{\sum_{j=1}^{\infty} p_j t_j} \quad (51)$$

and the average repeat time T_x as

$$T_x = \frac{\frac{n_1}{n} t_1 + \frac{n_2}{n} t_2 + \dots}{\frac{n_1}{n} + \frac{n_2}{n} + \dots} = \sum_{j=1}^{\infty} \frac{n_j}{n} t_j \quad (52)$$

In the limiting case as the interval $\Delta T = t_i - t_{i-1}$ becomes small, the p distribution may be expressed in continuous form as shown in the following sketch



which by Equations 50 and 52 has the properties

$$\int_0^{\infty} p(x,t) dt = 1 \quad (53a)$$

$$\int_0^{\infty} t p(x,t) dt = T_x \quad (53b)$$

The generalized Q equation becomes

$$Q(x,T) = \frac{\int_0^{\infty} (t - T)p(x,t)dt}{\int_0^{\infty} tp(x,t)dt} = \frac{1}{T_x} \int_T^{\infty} (t - T)p(x,t)dt$$

We have finally, therefore, that the probability of encountering x in a time T is given by the equation

$$P(x,T) = 1 - Q(x,T) \\ = 1 - \frac{1}{T_x} \int_T^{\infty} (t - T)p(x,t)dt \quad (54)$$

This relation is general and should apply to all stationary functions whether random or not. The precise form of p depends on the nature of the random variable; for a sine wave p becomes a Dirac function at the period of the wave.

The nature of p for gust encounter loads is not known as yet, but estimates of P can nevertheless be made by assuming various forms of p. Two choices have been studied; they are

Case a,

$$p(x,t) = \frac{n}{T_x \Gamma(n)} \left(\frac{nt}{T_x}\right)^{n-1} e^{-\frac{nt}{T_x}}$$

Case b,

$$p(x,t) = ate^{-b(t-t_1)^2}$$

The second case is presented in form only because the coefficients a and b are defined by rather lengthy expressions involving exponentials and erf(). Figure 24 shows the graphical nature of these distribution functions. The results found from Equation 54 for these two cases are shown in Figure 25, along with the results indicated by Equations 46 and 47.

To bring out better the behavior of the curves near $P = 1$, probability of not exceeding are given in Figure 26. The results obtained for extreme values of either n or k are noted to be of special and remarkable interest. Case a, yields Equation 46 for $n = \infty$, and Equation 47 for $n = 1$, whereas Case b, gives Equation 46 for $k = \infty$ and for $t_1 = -\infty$ yields the $n = 2$ result for Case a.

The results are general. In application to the gust loads, it is noted that the results are presented in terms of the average repeat time as given by Equation 45.

Although information is not available at this time to judge the validity, the results given by Equation 54 look very satisfying. The associated curves given in Figure 25 appear as generalizations to Equation 47. It is noted also that the distribution functions p approach a Dirac function as the parameters n and k become large, and hence apply to a sinusoid as a limiting case; the corresponding probability curves pass in the limit to the approximation given by Equation 46, which is correct for a sine wave. Although there is no supporting evidence, it is felt that the probability curves in the range of $n = 10 - 20$ in Figure 24(a) and $k = 2 - 2.5$ in Figure 24(b) apply to the gust load exceedance case.

The results given in Figure 25 can be used in several ways to determine the probability of exceeding certain loads. One of course, is on the basis of routine flying. Perhaps a more significant use, however, is with respect to establishing probabilities for a certain flight, or succession of flights, into known severe turbulence conditions. Results can be quite startling. Two examples illustrate the point. Consider that a design was made using the following values:

$$\frac{\Delta x_L}{A} = 16$$

$$\bar{P} = .08$$

$$T = 15,000 \text{ hrs.} = 54 \times 10^6 \text{ sec.}$$

$$N_0 = 1.05$$

$$n_L = 5$$

and that the $\alpha = .005$ curve of Figure 7 was the universal exceedance curve used for design. The $k = 2$ curve of Figure 25(b) is chosen to determine probabilities.

Example 1:

We wish to establish the probability of encountering

a load equal to half the limit load in 10 hours of routine flight; for this instance we have

$$f\left(\frac{x}{\sigma_x}\right) = f(8) = 4 \times 10^{-4}$$

$$\begin{aligned} \frac{T}{T_x} &= \bar{P}PN_0 f\left(\frac{x}{\sigma_x}\right) = .08 \times 10 \times 3600 \times 1.05 \times 4 \times 10^{-4} \\ &= 1.21 \end{aligned}$$

From Figure 25(b) we find $P = .955$. In addition we wish now to determine the time to reach this same probability level if flight is made completely in turbulence that is 2.5 times as severe as the average. In the latter instance $\bar{P} = 1$, σ_x is 2.5 times as large or $\frac{x}{\sigma_x} = \frac{8}{2.5} = 3.2$, $f(3.2) = 4.2 \times 10^{-2}$, and $\frac{T}{T_x}$ must be the same to yield the same probability, hence

$$\bar{P}PN_0 f\left(\frac{x}{\sigma_x}\right) = 1.05T \times 4.2 \times 10^{-2} = 1.21$$

or

$$T = 27.5 \text{ sec.}$$

In summary, for this example, it takes 10 hours of normal routine flying to yield a probability of .955 that a load level one-half the limit load value will be reached, but only 27.5 sec. of flying in turbulence which is 2.5 times as severe as the average to achieve the same probability.

Example 2:

We wish to determine how much time can be flown continuously in turbulence that is 2.5 as severe as the average to obtain the same probability of encountering limit load as is obtained in flying routinely for a time equal to the design life of the airplane. For the lifetime routine flight we have

$$\begin{aligned} \frac{T}{T_x} &= \bar{P}PN_0 f(16) = .08 \times 54 \times 10^6 \times 1.05 \times 1.1 \times 10^{-6} \\ &= 5 \end{aligned}$$

The associated probability is practically 1. For the severe turbulence flight to have the same probability we have, with

$\bar{P} = 1, \frac{x}{\sigma_x} = \frac{16}{2.5} = 6.4, f(6.4) = 1.667 \times 10^{-3}$, the following relation

$$\frac{T}{T_x} = 5 = \bar{P} T N_0 f\left(\frac{x}{\sigma_x}\right) = 1.05T \times 1.667 \times 10^{-3}$$

and so

$$T = 47.7 \text{ min.}$$

These examples serve to show the value of a probability of exceedance analysis, and indicate that probability considerations of the type illustrated can be quite useful in judging whether a specific flight in known severe conditions should be made or not.

SECTION 1

CONCLUSIONS AND RECOMMENDATIONS

The conclusions and recommendations that are indicated by this study dealing with the development of power spectral methods for designing aircraft for gusts are listed in this section.

First, as a general observation, the use of spectral techniques for gust design appears sound and feasible, and it is recommended that such a procedure be incorporated in design specifications. This recommendation does not mean that the discrete-gust design technique should be abandoned. The attitude taken toward the discrete-gust method is that because of its basic simplicity it still may be used to rough out the design in the early stages; the power spectral technique then serves the purpose of checking on the design or uncovering unusual response aspects which cannot be brought out rationally by the discrete-gust technique. We might summarize the use of the power spectral approach as follows: (1) If sufficient structural and aerodynamic information is available early in the design stage, then design by the power spectral approach, (2) If the phasing of the design is such as to preclude making use of the spectral approach initially, then rough out the design by the discrete-gust procedure and subsequently make a detailed check by the power spectral approach, (3) Even if not used initially for a given design, the power spectral method represents a powerful tool to determine how the expected load history may be influenced or changed if the airplane is used in different ways or in a manner different from that originally contemplated.

With respect to future study effort, the following observations are made:

- 1) The values of σ and L are still uncertain and should be established more rationally.
- 2) The questionable reliability of the derived gust history records at low frequencies is one of the principal reasons for the state indicated in item (1); thus, a much better appreciation of record content must be established.
- 3) The operational statistics of various aircraft should be examined to evaluate which form (or forms) of the many generalized exceedance curves presented appears to represent load experience the best.
- 4) The study mentioned in item 3 should also include an examination of whether the shape of the exceedance curves can be correlated with mission category.

- 5) Load level crossing studies should be made of gust response records; results should be correlated with previous, used peak count procedures. Any level crossing study should also include the range of low x values, since information in this range may provide a valuable clue as to how the tail of the exceedance curves should behave.
- 6) Additional values of N_0 and x/A should be established for other gust critical aircraft as a means for providing further substantiation to the results and design boundary given in Figure 19.
- 7) Gust response records should be evaluated to establish experimental distribution functions for repeat time as used in the probability study given in Section 9.

With respect to the spectral design procedures, the following recommendations are made:

- 1) The design based on the plot of N_0 vs. $\frac{x(1000)}{A(L)}^{1/3}$ and represented by Figure 19, is the recommended first choice as a design procedure. Composite mission values of A and N_0 may be used if necessary. This procedure is just about as simple as can be conceived, yet which retains all the basic rational elements of the problem. Serious consideration should be given to adopting the further simplification of this procedure - that of specifying the lower limit to $\frac{x(1000)}{A(L)}^{1/3}$ only, which on Figure 19 is a vertical line.
- 2) Design based on the universal curve and specified (or composite) values of σ_c , P , and T (Figures 22 or 23) is recommended as a second choice. As mentioned, uncertainties still exist as to what values of σ_c , P , and L should be used. The procedure, however, provides for additional relevant design information, such as load information for fatigue considerations.
- 3) The comparison technique is not included in an order of choice basis. This procedure is considered a valuable adjunct to any procedure that is being used. It is valuable in evaluating the design at various locations on a given aircraft, and in many instances can itself serve to be the complete design tool.

- 4) The segmented mission approach involving the use of an exceedance curve for each mission segment is not included as a design procedure at this time. The main reason is that too many uncertainties still exist with respect to the input quantities. The use of this procedure as a means for assessing how the expected load history is affected by different aircraft utilization is, however, recommended. Further developments on this approach are to be covered in a supplemental report.

APPENDIX A

EFFECTS OF FILTERING ON L

Evidence is that the time histories of gust velocities as derived from airplane flight data contain long wavelength contaminations of uncertain magnitude and frequency range. Knowledge of this low frequency "noise" is important because its presence has a major influence on the values of σ_c and L that are deduced. As an example, in Reference 8, it is shown that scale values of over 50,000 ft. are found in some cases from the raw time history records of derived gust velocities; such values appear to be unreasonably out of line. Because of the dependence of σ_c and L on record authenticity, the principal investigator of this report has recommended often that long still air flight tests which include deliberate pilot induced maneuvers be conducted with the instrumented airplane. The records obtained from such flights should give a good indication of what can be believed and what cannot in the gust records. In the absence of these studies, other means for combating the apparent low frequency noise have been used. One of these methods consists of arbitrarily filtering out the low frequency components. The effect that such filtering has on the deduced values of scale should, however, be appreciated more. An analysis is therefore given in the following, which indicates the general effect of filtering.

Consider a raw time history of a random variable $y(t)$. The time history obtained by passing this raw function through a low pass filter is

$$y_f(t) = \int_{-\infty}^{\infty} y(\tau) h(t-\tau) d\tau$$

where h describes the filter characteristics (although not necessary, we assume that the filter used has symmetrical characteristics so that phase distortion is not introduced). The time history with low frequency components removed would thus appear

$$Y(t) = y(t) - \int_{-\infty}^{\infty} y(\tau) h(t-\tau) d\tau$$

The Fourier integral transform of this equation is

$$F_Y(\omega) = F_X(\omega) - F_X(\omega) H(\omega)$$

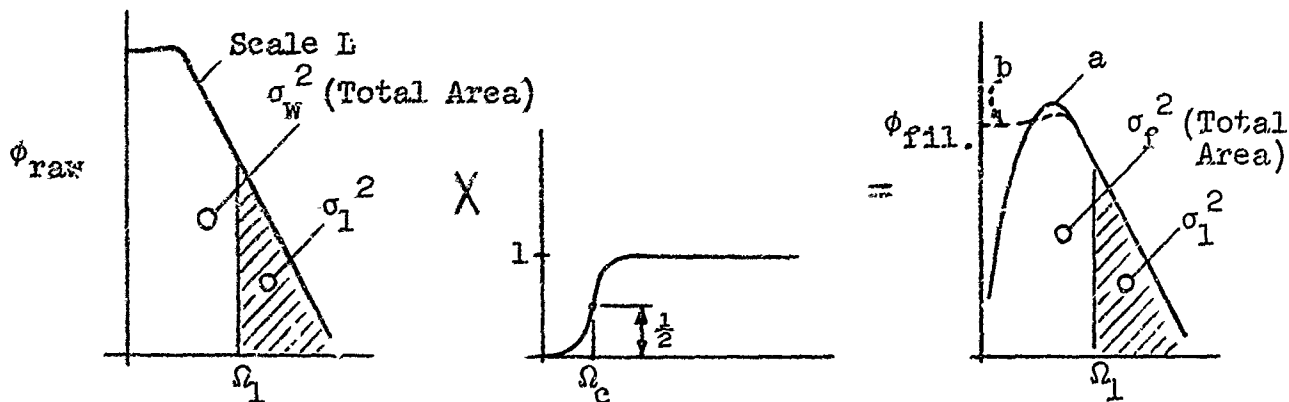
where H is the filter frequency response. The spectrum for Y then follows as

$$\phi_Y(\omega) = |1 - H(\omega)|^2 \phi_X \quad (A1)$$

To establish the effect of filtering on the deduced value of scale L , we make use of Equation 6 of Reference 1, Vol. II, giving the truncated r.m.s. value σ_1 , namely,

$$\sigma_1 = \frac{.885\sigma_W}{(L\Omega_1)^{1/3}} \quad (A2)$$

and postulate the equivalence shown in the following sketches.



The spectrum on the left applies to the raw data, and on the assumption that these data represent real gust information, we fit our chosen analytical spectrum equation (say, Equation 4, Vol. II, Reference 1) and deduce an apparent or "raw" scale L . The second sketch represents the filter transfer function. In accordance with Equation A1, curve a in the third sketch represents the spectrum of the filtered time history. The quantity σ_f^2 denotes the mean square value of the filtered time history. We assume, however, that spectrum a is replaced by an "equivalent" spectrum b , on the basis that b represents the real world situation much better than a ; stated from another viewpoint, if we had a means for precisely extracting the contamination from the raw data, then the filtered data would presumably lead to spectrum b , not a .

The Fourier integral transform of this equation is

$$F_Y(\omega) = F_y(\omega) - F_y(\omega) H(\omega)$$

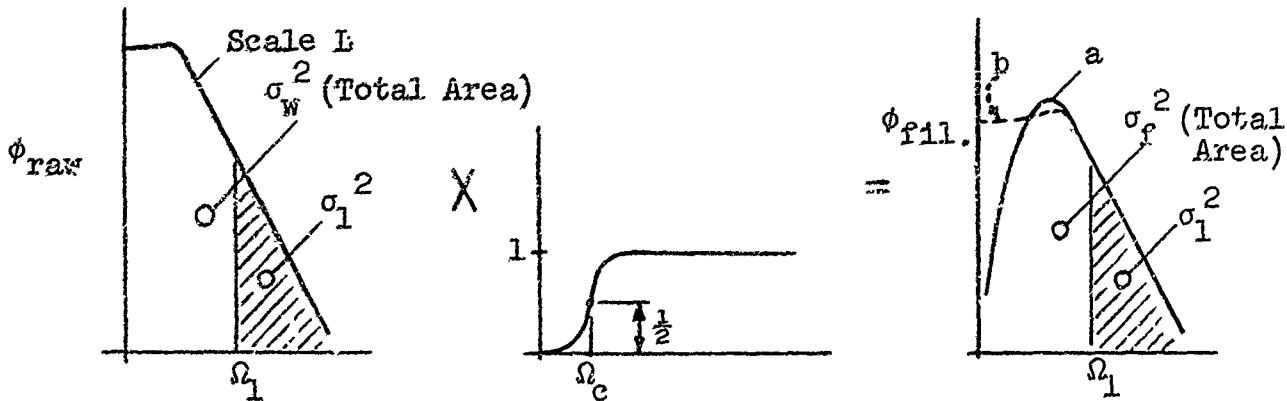
where H is the filter frequency response. The spectrum for Y then follows as

$$\phi_Y(\omega) = |1 - H(\omega)|^2 \phi_y \quad (A1)$$

To establish the effect of filtering on the deduced value of scale L , we make use of Equation 6 of Reference 1, Vol. II, giving the truncated r.m.s. value σ_1 , namely,

$$\sigma_1 = \frac{.885\sigma_w}{(L\Omega_1)^{1/3}} \quad (A2)$$

and postulate the equivalence shown in the following sketches.



The spectrum on the left applies to the raw data, and on the assumption that these data represent real gust information, we fit our chosen analytical spectrum equation (say, Equation 4, Vol. II, Reference 1) and deduce an apparent or "raw" scale L . The second sketch represents the filter transfer function. In accordance with Equation A1, curve a in the third sketch represents the spectrum of the filtered time history. The quantity σ_f^2 denotes the mean square value of the filtered time history. We assume, however, that spectrum a is replaced by an "equivalent" spectrum b , on the basis that b represents the real world situation much better than a ; stated from another viewpoint, if we had a means for precisely extracting the contamination from the raw data, then the filtered data would presumably lead to spectrum b , not a .

The equivalent spectrum is defined as one which has the shape given by the analytical expression adopted, which has a mean square value σ_f^2 and which passes through the same data points at the high frequency end, and hence has the same truncated value σ_1 . The scale value L_f associated with this equivalent spectrum must then satisfy an equation similar to Equation (A2), specifically

$$\sigma_1 = \frac{.885\sigma_f}{(L_f\Omega_1)^{1/3}} \quad (A3)$$

Division of Equation A2 by Equation A3 leads then to the following relation defining the scale L_f which effectively characterizes the filtered data

$$L_f = \left(\frac{\sigma_f}{\sigma_w}\right)^3 L$$

This simple equation can be used to show the effect of filtering on the deduced scale value. Results are shown in Figure 27 for two different assumed ideal filters. The following equations define the filters chosen

Case 1

$$h = \frac{.643\omega_c}{2} e^{-.643\omega_c |t|}$$

$$|1 - H(\omega)|^2 = \left[\frac{\left(\frac{1.554\omega}{\omega_c}\right)^2}{1 + \left(\frac{1.554\omega}{\omega_c}\right)^2} \right]^2$$

Case 2

$$h = \frac{1}{\pi} \frac{\sin \omega_c t}{t}$$

$$\begin{aligned} |1 - H(\omega)|^2 &= 0 && \omega < \omega_c \\ &= 1 && \omega > \omega_c \end{aligned}$$

Note, $\Omega = \frac{\omega}{v}$, Ω_c corresponds to ω_c , and $\frac{\omega}{\omega_c} = \frac{\Omega}{\Omega_c}$.

Note that the scale L_f associated with the filtered data drops off rapidly as the filter cutoff frequency Ω_c is increased, and more significantly that at the higher Ω_c 's the values of L_f become the same regardless of the value of the raw scale L . There is perhaps a significant implication in these results. If we consider, for example, that the information contained in the raw data for frequencies below $\Omega_c = .0005$ (wavelengths greater than $\lambda_c = 2\pi/\Omega_c = 12,560$) is all contamination, then we see that scale values on the order of 1200 ft. are indicated. We see from these results the importance of establishing whether the information given by the raw time history is real or not. The results also suggest the warning: do not arbitrarily filter the data unless definite guidelines are on hand to guide the filtering and unless the effects of filtering on the end results are fully understood.

REFERENCES

1. Houbolt, J.C. "Preliminary Development of Gust Design Procedures Based on Power Spectral Techniques." Technical Report AFFDL-TR-66-58, Vol. I and II. September, 1966
2. Rice, S. O. "Mathematical Analysis of Random Noise." Pts. I and II. Bell Syst. Tech. Jour., Vol. XXIII, No. 3, July 1944, pp. 282-332; Pts. III and IV, Vol. XXIV, No. 1, Jan. 1945, pp. 46-155.
3. Houbolt, J. C., Steiner, R., and Pratt, K. G. "Dynamic Response of Airplanes to Atmospheric Turbulence Including Flight Data on Input and Response." NASA Technical Report TR R-199, June 1964.
4. Press, Harry, Meadows, May T., and Hadlock, Ivan. "A Reevaluation of Data on Atmospheric Turbulence and Airplane Gust Loads for Application in Spectral Calculations." NACA Report 1272, 1956.
5. Press, Harry, and Steiner, Roy. "An Approach to the Problem of Estimating Severe and Repeated Gust Loads for Missile Operations. NACA TN 4332, 1958.
6. Hoblit, F. M., Paul, N., Shelton, J. D., and Ashford, F. E. "Development of a Power Spectral Gust Design Procedure For Civil Aircraft." Federal Aviation Agency Technical Report FA-WA-4768, January 1966.
7. Pritchard, F. E., Easterbrook, C. C., and McVehil, G. E. Cornell Aeronautical Laboratory, Inc. "Spectral and Exceedance Probability Models of Atmospheric Turbulence For Use In Aircraft Design and Operation." Technical Report AFFDL-TR-65-122, November 1965.
8. Peloubet, R. P. and Haller, R. L. "Application of a Power Spectral Gust Design Procedure to Bomber Aircraft." Technical Report AFFDL-TR-66-35, June 1966.
9. Latz, R. N.; The Boeing Company. "KC-135 Power Spectral Vertical Gust Load Analysis." Vol. II. Technical Report AFFDL-TR-66-57.
10. Hwang, Chintsun, Kamberg, B. D., Pi, W. S., and Cross, A.K., Northrup Corporation. "Design Calculations on Proven Trainer and Fighter Aircraft for the Verification of a Gust Design Procedure." Technical Report AFFDL-TR-66-82, July 1966.
11. Houbolt, J. C., and Steiner, R. "Prediction of Gust Loads In Airplane and Missile Operations." WADC Technical Report 59-507, U.S. Air Force, Aug. 11-13, 1959.

TABLE I. EQUATIONS FOR UNIVERSAL BENDING CURVES

AGE	FIG.	INHERENT FUNCTION $u_1(\alpha)$; $1 - \frac{u_1}{\alpha}$	INHERENT FUNCTION $u_2(\alpha)$; $2 - \frac{u_2}{\alpha}$	CROSSING FUNCTION $\frac{u_2}{u_1}$; $2 - \frac{u_2}{\alpha}$
1	1(a)	$\sqrt{\frac{2}{\alpha}}$	$\frac{2}{\alpha} K_0(\alpha)$	
2	1(a)	$\sqrt{2} \cdot \alpha^{-1/2}$		Numerical Integration
3	1(a)	$5.5\alpha - 3.33\sqrt{\alpha}$		Numerical Integration
4	1(b)	$\sqrt{\frac{2}{\alpha}} \left(\frac{2}{\alpha} K_0(\alpha) - \frac{2}{\alpha} \right)$	$\left(\frac{2}{\alpha} K_0(\alpha) - \sqrt{2} K_1(\sqrt{2}\alpha) \right)$	$\left(\frac{2}{\alpha} K_0(\alpha) - \sqrt{2} \right)$
5	1(c)			$\left[\frac{2}{\alpha} \left(\frac{2}{\alpha} K_0(\alpha) \right) \right]_{\alpha=0}$
6	2(a)	$\frac{2(\alpha-1)^{3/2}}{\Gamma(\alpha)} - (2\alpha-1) \cdot \frac{2}{\alpha^2}$	$\frac{2}{\sqrt{\alpha}} \frac{\Gamma(\alpha+1/2)}{\Gamma(\alpha)} \left[1 + \frac{2}{\Gamma(\alpha-1/2)} \right]^{2\alpha-1/2}$	$\left[2 + \frac{2}{\Gamma(\alpha-1/2)} \right]^{2\alpha}$
7	2(b)	$\frac{2\alpha}{\Gamma(\alpha)} \alpha^{-2\alpha-1} e^{-\alpha^2}$	$\frac{2}{\sqrt{\alpha}} \frac{\Gamma(\alpha+1/2)}{\Gamma(\alpha)} \left(\frac{2}{\alpha} \right)^{2\alpha-1/2} \frac{2}{\Gamma(\alpha-1/2)}$	$\left[\frac{2}{\alpha} \right]^{2\alpha}$
8	2(c)	$\frac{2}{\sqrt{\alpha}} \left(\alpha - 2 \right) \frac{\Gamma(\alpha+1/2)}{\Gamma(\alpha)} \left(\frac{2}{\alpha} \right)^{2\alpha-1/2}$	$\frac{2}{\sqrt{\alpha}} \frac{\Gamma(\alpha+1/2)}{\Gamma(\alpha)} \left(\frac{2}{\alpha} \right)^{2\alpha-1/2} \frac{2}{\Gamma(\alpha-1/2)}$	$\frac{2^{2\alpha-1/2}}{\sqrt{\alpha}} \left(\frac{2}{\alpha} \right)^{2\alpha} \frac{\Gamma(\alpha+1/2)}{\Gamma(\alpha-1/2)}$
9	2	$\sqrt{\frac{2}{\alpha}} \left(1 - \alpha \right) \frac{2}{\alpha} \left(\frac{2}{\alpha} \right)^{2\alpha-1/2}$	$\frac{2}{\alpha} \left\{ (1 - \alpha) K_0(2\alpha) + \alpha K_0(1.414\alpha) \right\}$	$\left(\frac{2}{\alpha} \right)^{2\alpha}$
10	2	$\sqrt{\frac{2}{\alpha}} \left[.989 \frac{2}{\alpha} + .0166 \frac{2}{\alpha} + .772\alpha^2 + .001 \frac{2}{\alpha} \right]$	$\frac{2}{\alpha} \left[.989 K_0(2\alpha) + .0166 K_0\left(\frac{2}{\alpha}\alpha\right) + .001 K_0\left(\frac{2}{\alpha}\alpha\right) \right]$	$\left(\frac{2}{\alpha} \right)^{2\alpha}$
11	2	$\sqrt{\frac{2}{\alpha}} \left(1 - \alpha \right) \frac{2}{\alpha} \left(\frac{2}{\alpha} \right)^{2\alpha-1/2}$	$\frac{2}{\alpha} \left\{ (1 - \alpha) K_0(2\alpha) + \alpha K_0(1.414\alpha) \right\}$	$\left(\frac{2}{\alpha} \right)^{2\alpha}$
12	2	$\sqrt{\frac{2}{\alpha}} \left[.989 \frac{2}{\alpha} + .0166 \frac{2}{\alpha} + .772\alpha^2 + .001 \frac{2}{\alpha} \right]$	$\frac{2}{\alpha} \left[.989 K_0(2\alpha) + .0166 K_0\left(\frac{2}{\alpha}\alpha\right) + .001 K_0\left(\frac{2}{\alpha}\alpha\right) \right]$	$\left(\frac{2}{\alpha} \right)^{2\alpha}$
13	2	$\sqrt{\frac{2}{\alpha}} \left(1 - \alpha \right) \frac{2}{\alpha} \left(\frac{2}{\alpha} \right)^{2\alpha-1/2}$	$\frac{2}{\alpha} \left\{ (1 - \alpha) K_0(2\alpha) + \alpha K_0(1.414\alpha) - 3.46\alpha K_1(3.46\alpha) \right\}$	$\left(\frac{2}{\alpha} \right)^{2\alpha}$

$K_0(\alpha)$ - MODIFIED BESSEL FUNCTION
 $K_1(\alpha)$ - PARABOLIC CYLINDER FUNCTION

TABLE I - Reanalysis of Airline Data
(a) Basic Results

Operation	Route	Av. Alt.	A*	N ₀	P	σ_x	σ_c^*	α	x_1
1	Northern transcontinental	5000	.022	1.153	.1625	.075	3.4	7.55	.566
2	Rocky Mountains North & South	8000	.0212	1.04	.4135	.0758	3.58	9.8	.743
3	Southern transcontinental	5000	.0174	1.0	.0696	.0732	4.2	7.4	.542
4	90 percent east of Mississippi River	10,000	.0185	.9	.0325	.0673	3.64	6.1	.41
5	New York to Europe and South America	12,500	.01535	.898	.00775	.0682	4.44	6.22	.423
6	San Francisco to Honolulu	12,500	.01453	.851	.00512	.0652	4.48	6.13	.4
7	Northern transcontinental	12,500	.01564	.917	.0214	.061	3.9	6.37	.388
8	Southern transcontinental	12,100	.0192	.998	.0452	.0578	3.01	6.55	.378

* Based on $L = 1000$ ft.

TABLE II - Concluded
 (b) A and σ_c for Various L Values

Operation	L = 500		1000		1500		2000 ft.	
	A	σ_c	A	σ_c	A	σ_c	A	σ_c
1	.0273	2.7	.022	3.4	.0192	3.89	.0175	4.28
2	.0267	2.84	.0212	3.58	.0186	4.09	.0168	4.51
3	.0219	3.34	.0174	4.2	.0152	4.80	.0138	5.28
4	.0233	2.89	.0185	3.64	.0162	4.16	.0147	4.58
5	.0193	3.53	.01535	4.44	.0134	5.08	.0122	5.59
6	.0183	3.56	.01453	4.48	.0127	5.12	.0115	5.64
7	.0197	3.10	.01564	3.9	.0137	4.46	.0124	4.91
8	.0242	2.39	.0192	3.01	.0168	3.44	.0152	3.79

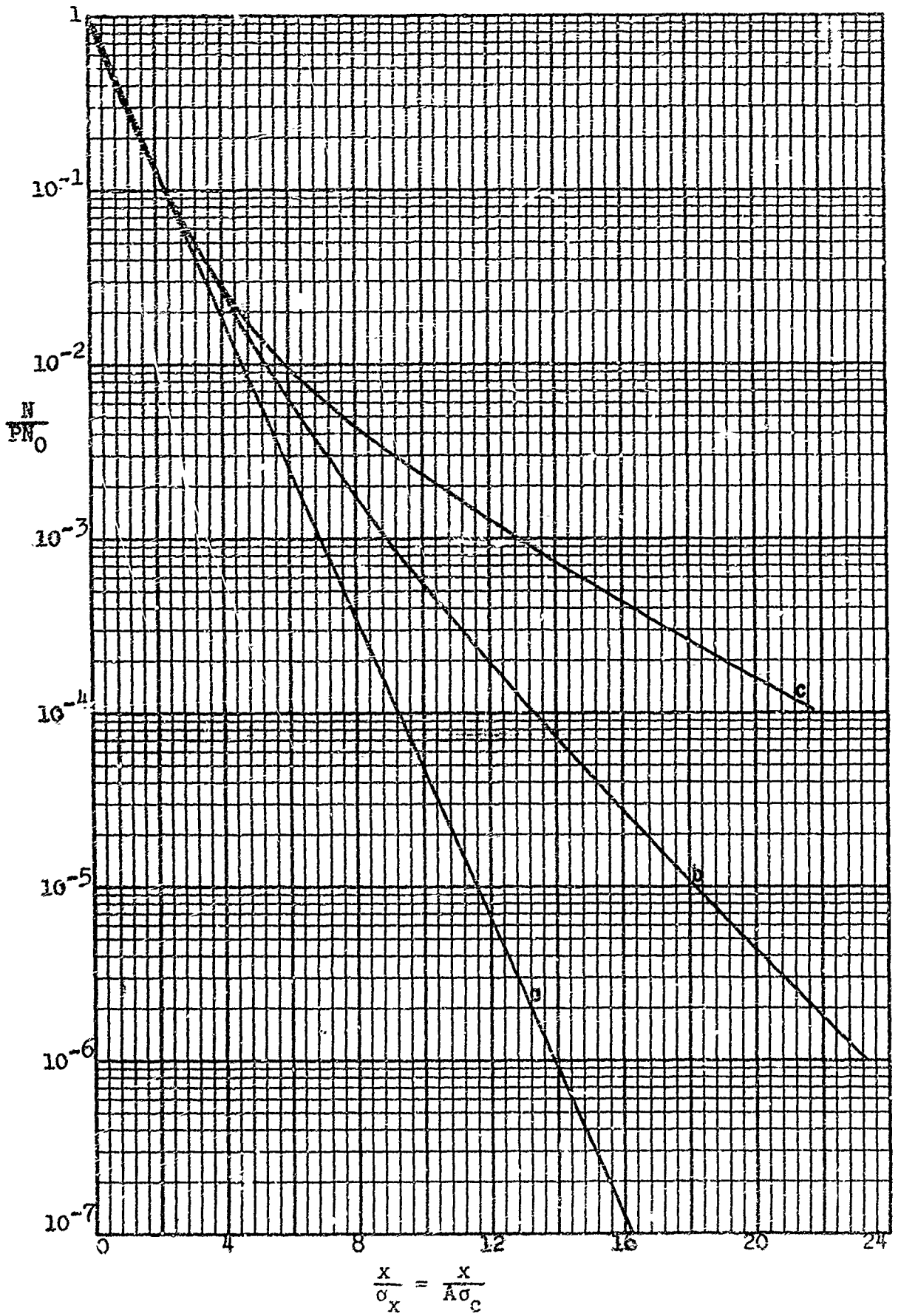


Figure 1(a). Universal Exceedance Curves: Cases a, b, and c

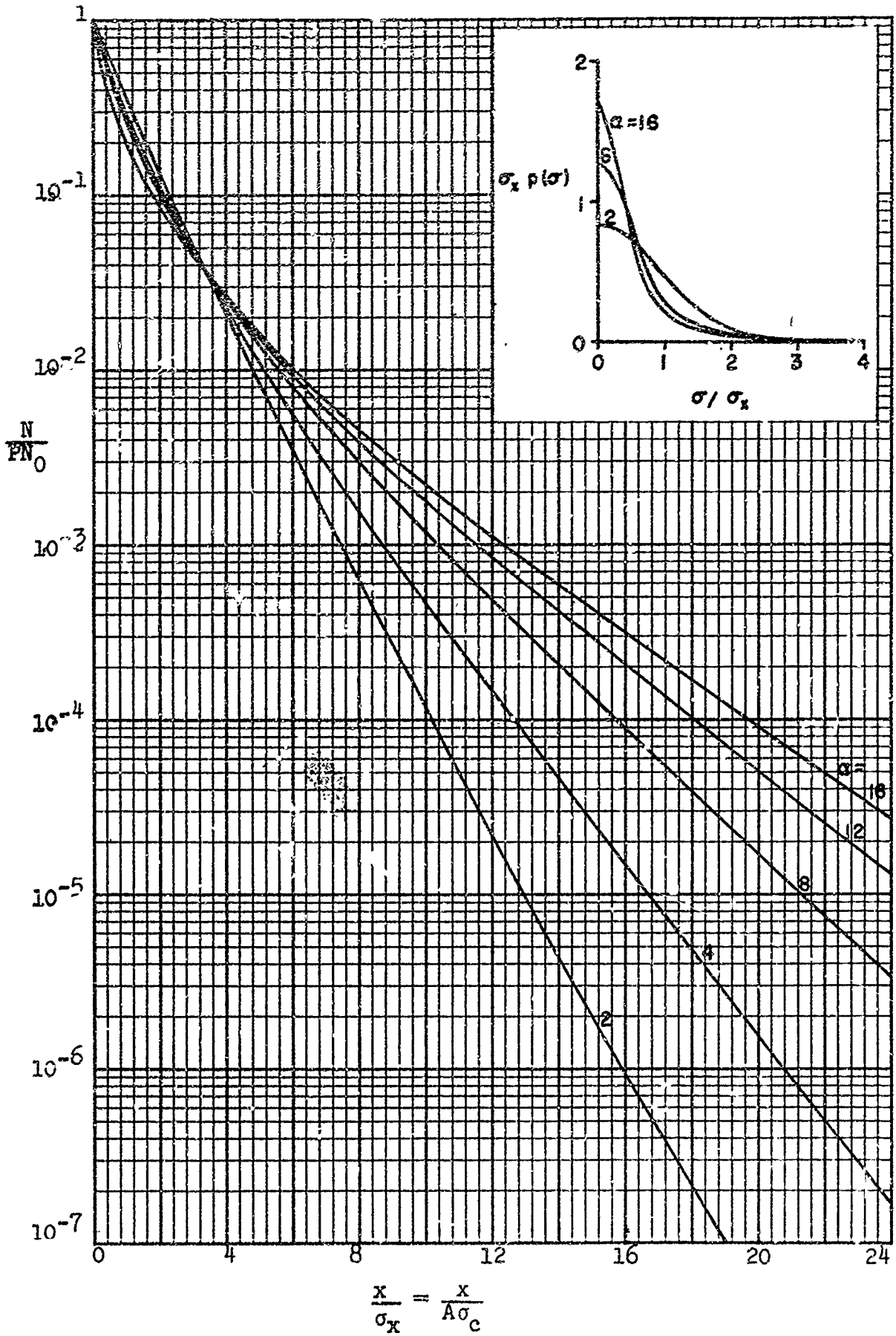


Figure 1(b). Universal Exceedance Curves: Case d

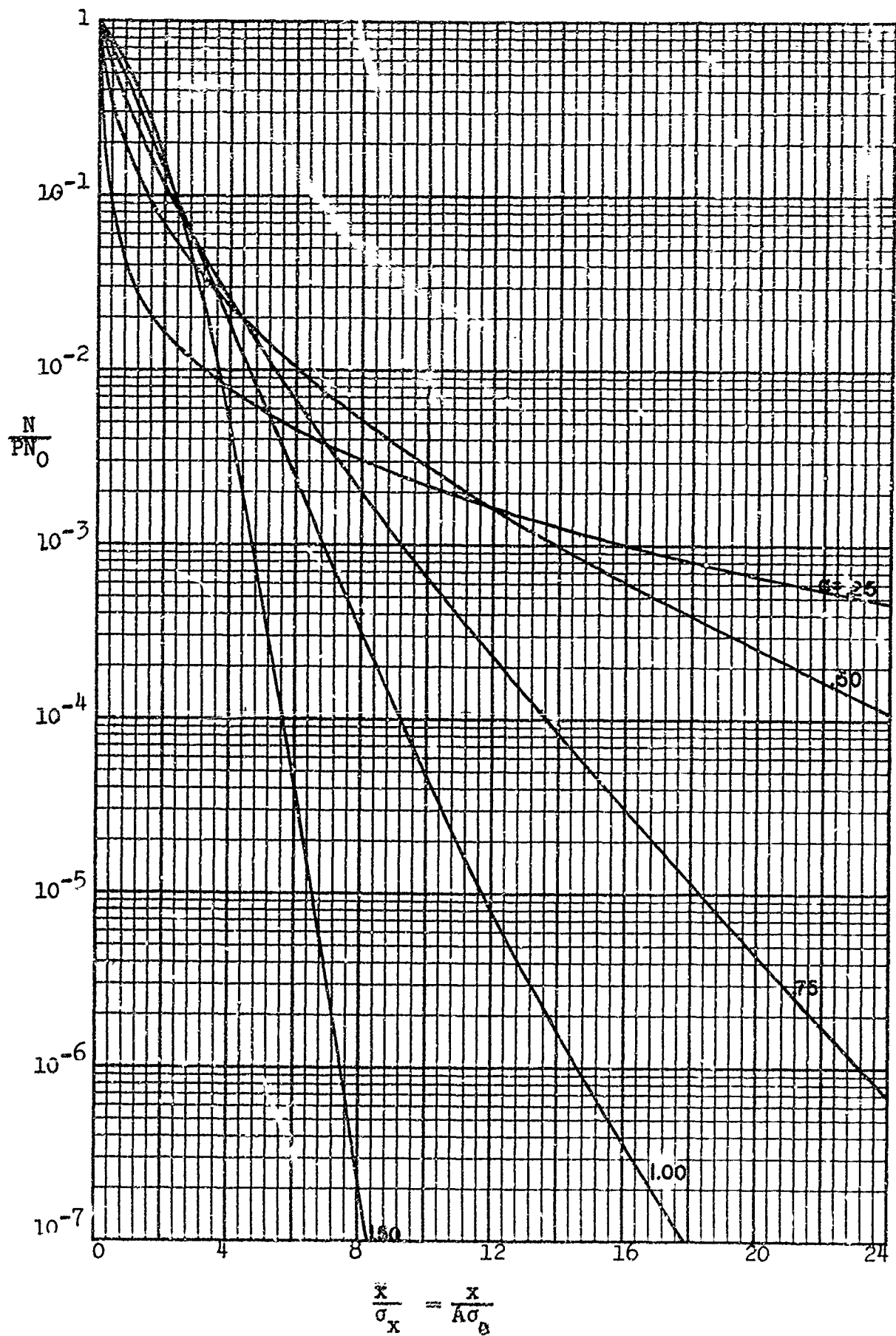


Figure 1(c). Universal Exceedance Curves: Case e

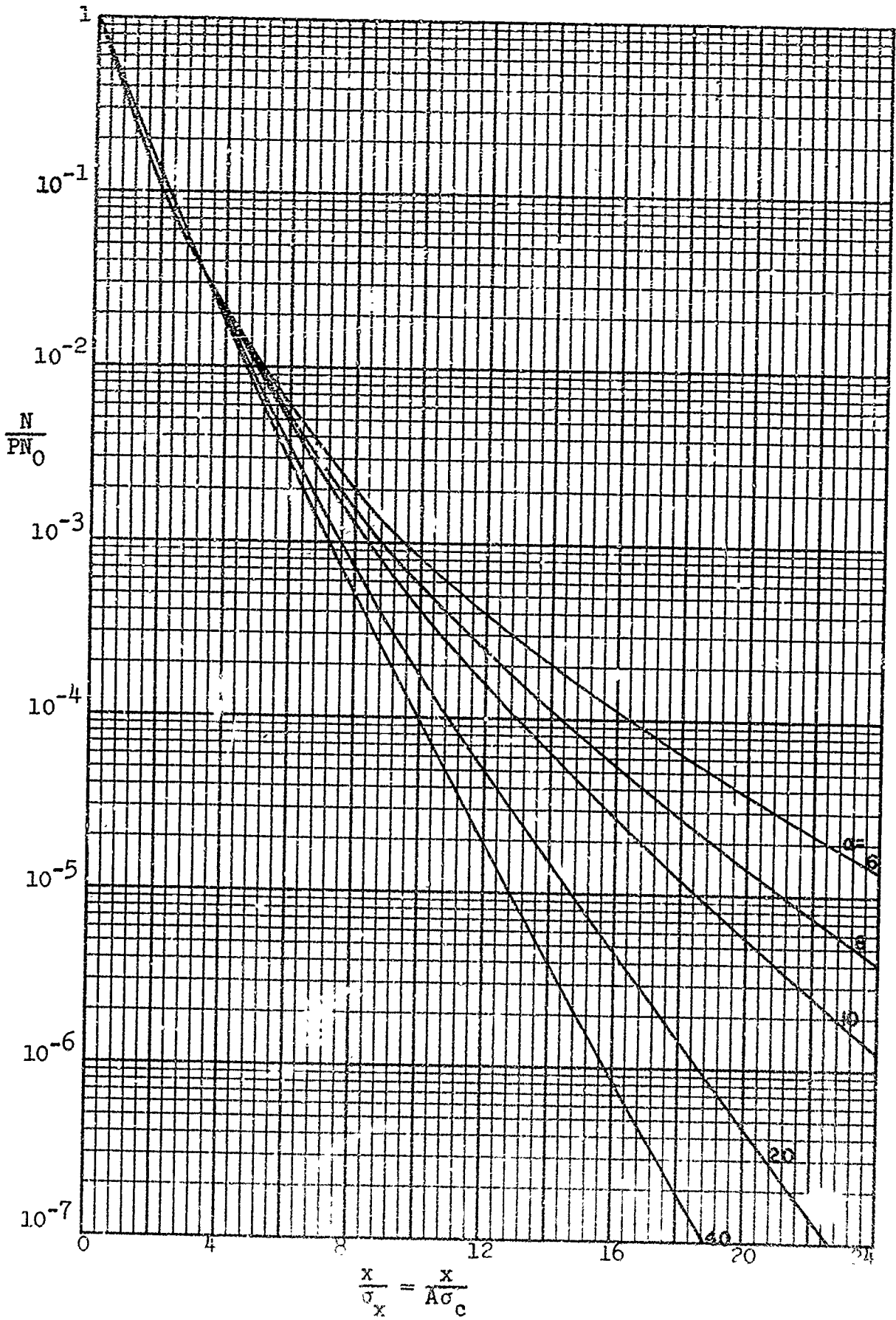


Figure 1(d). Universal Exceedance Curves: Case f

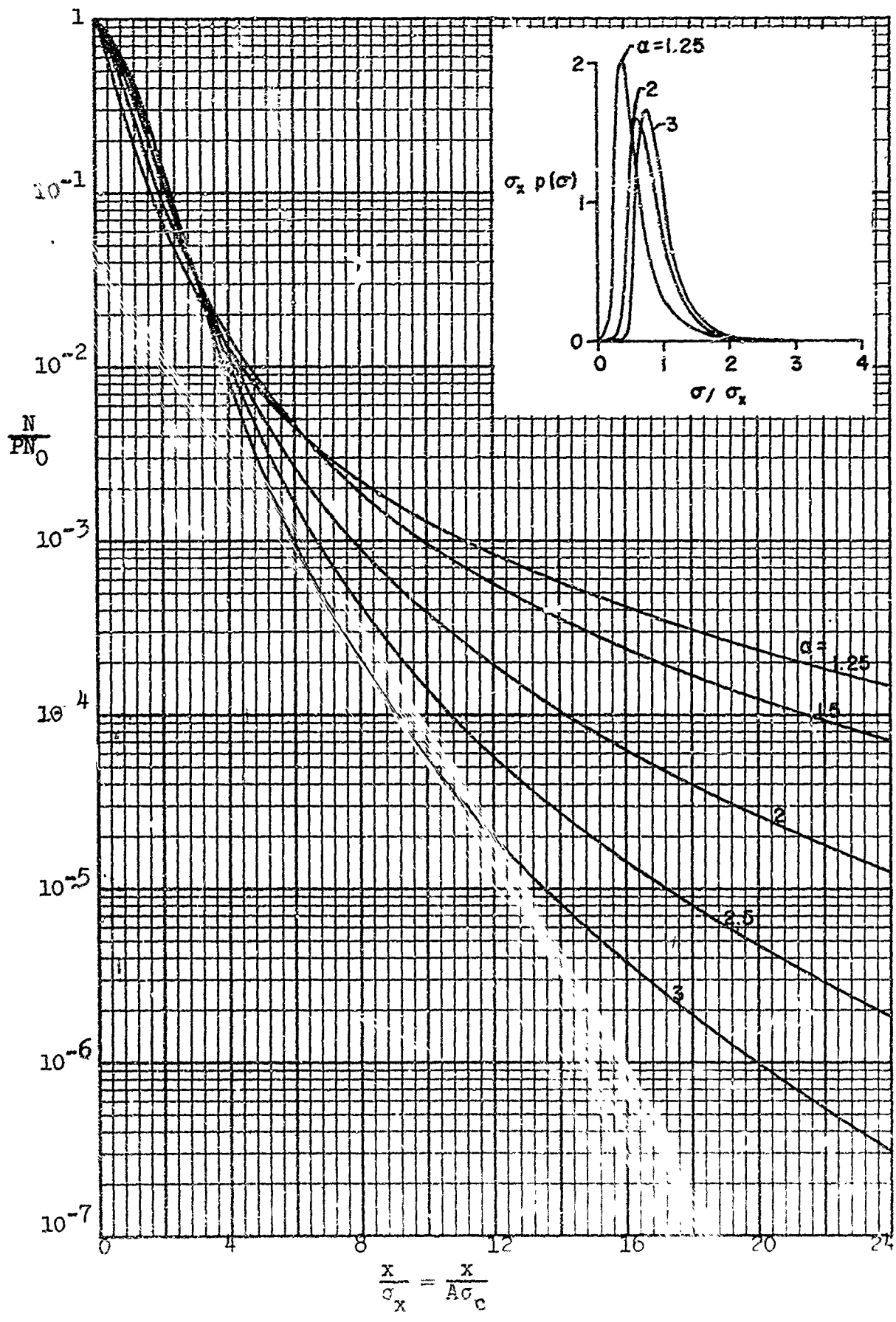


Figure 1(e). Universal Exceedance Curves. Case

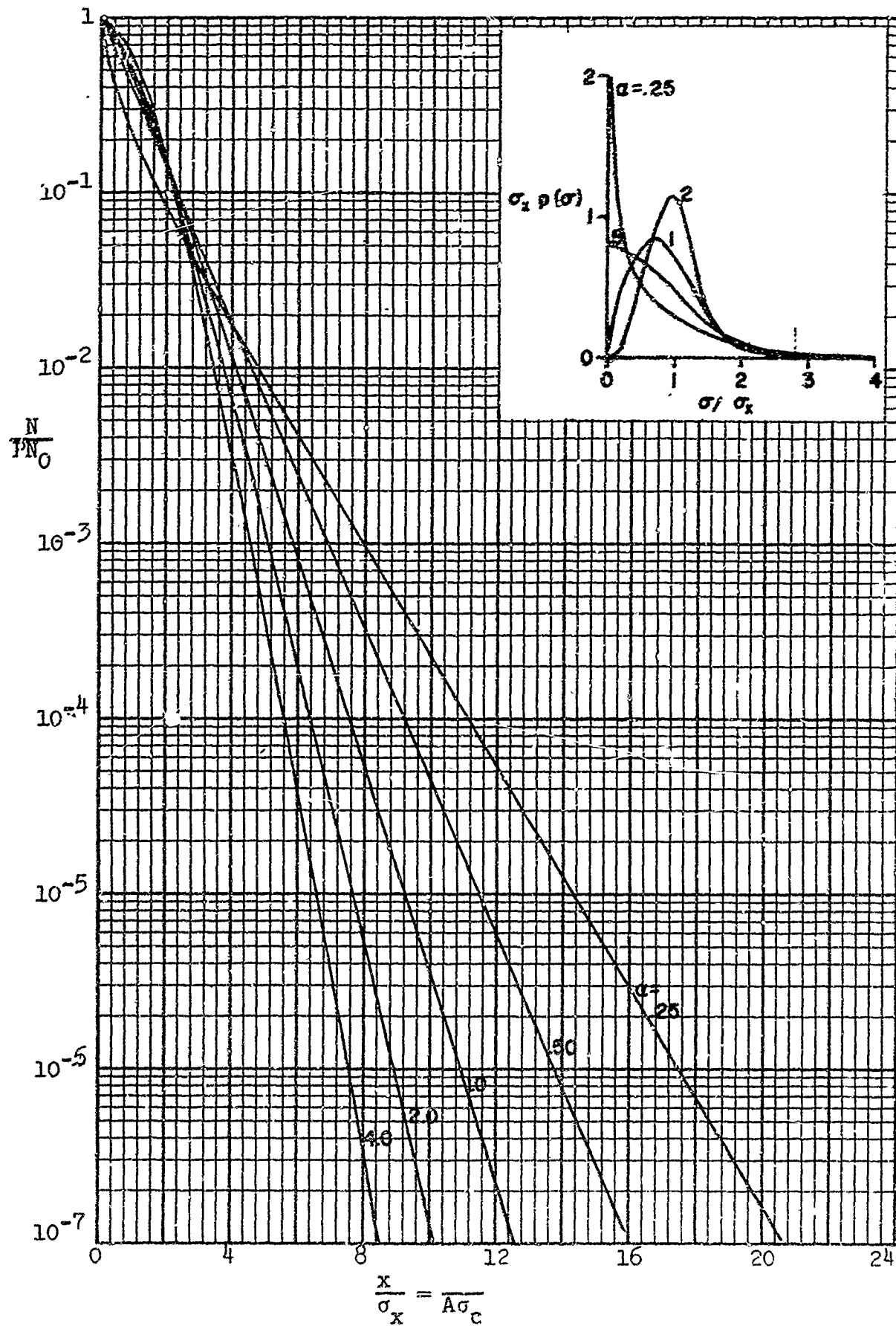


Figure 1(f). Universal Exceedance Curves: Case h

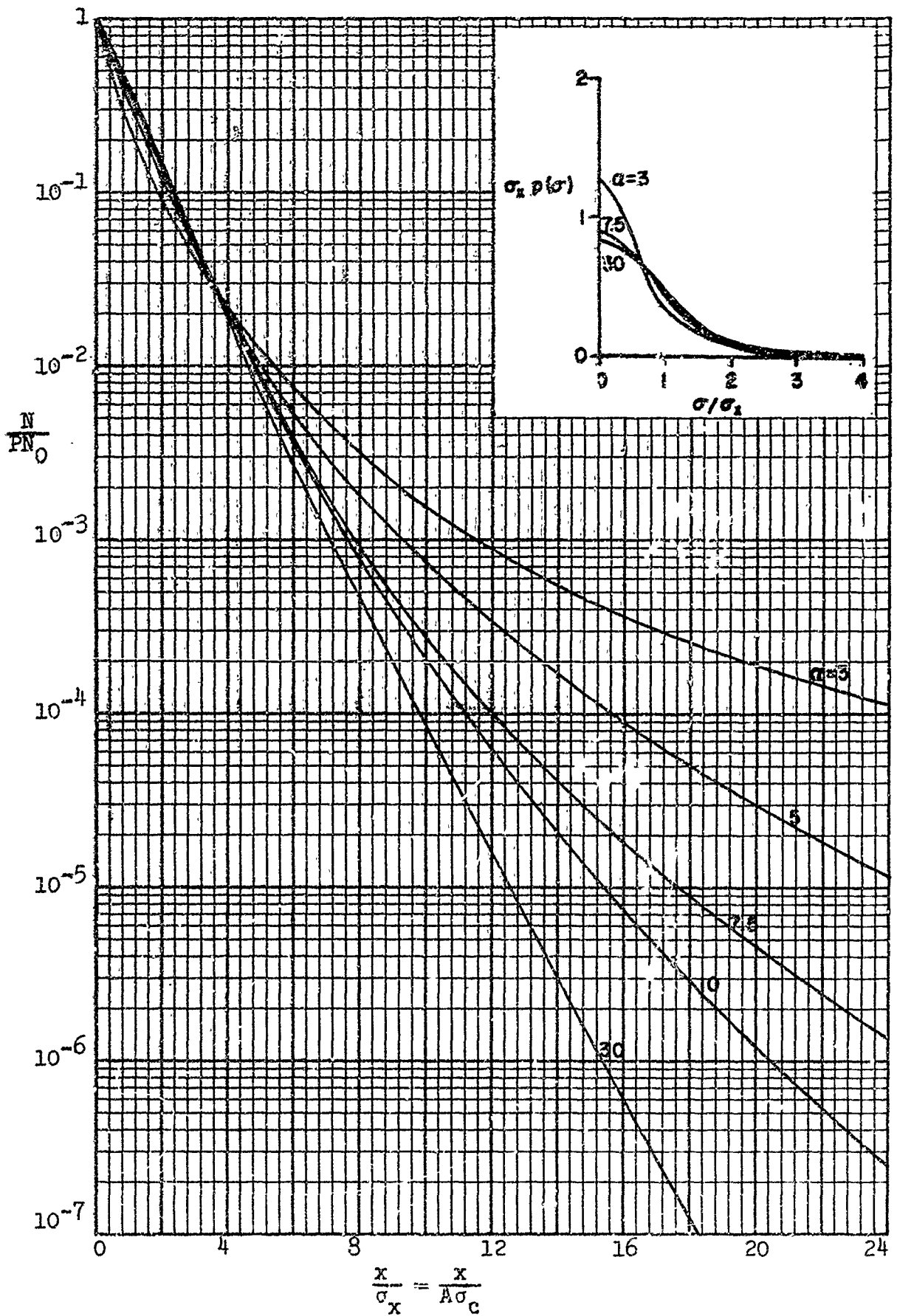


Figure 1(g). Universal Exceedance Curves: Case 1

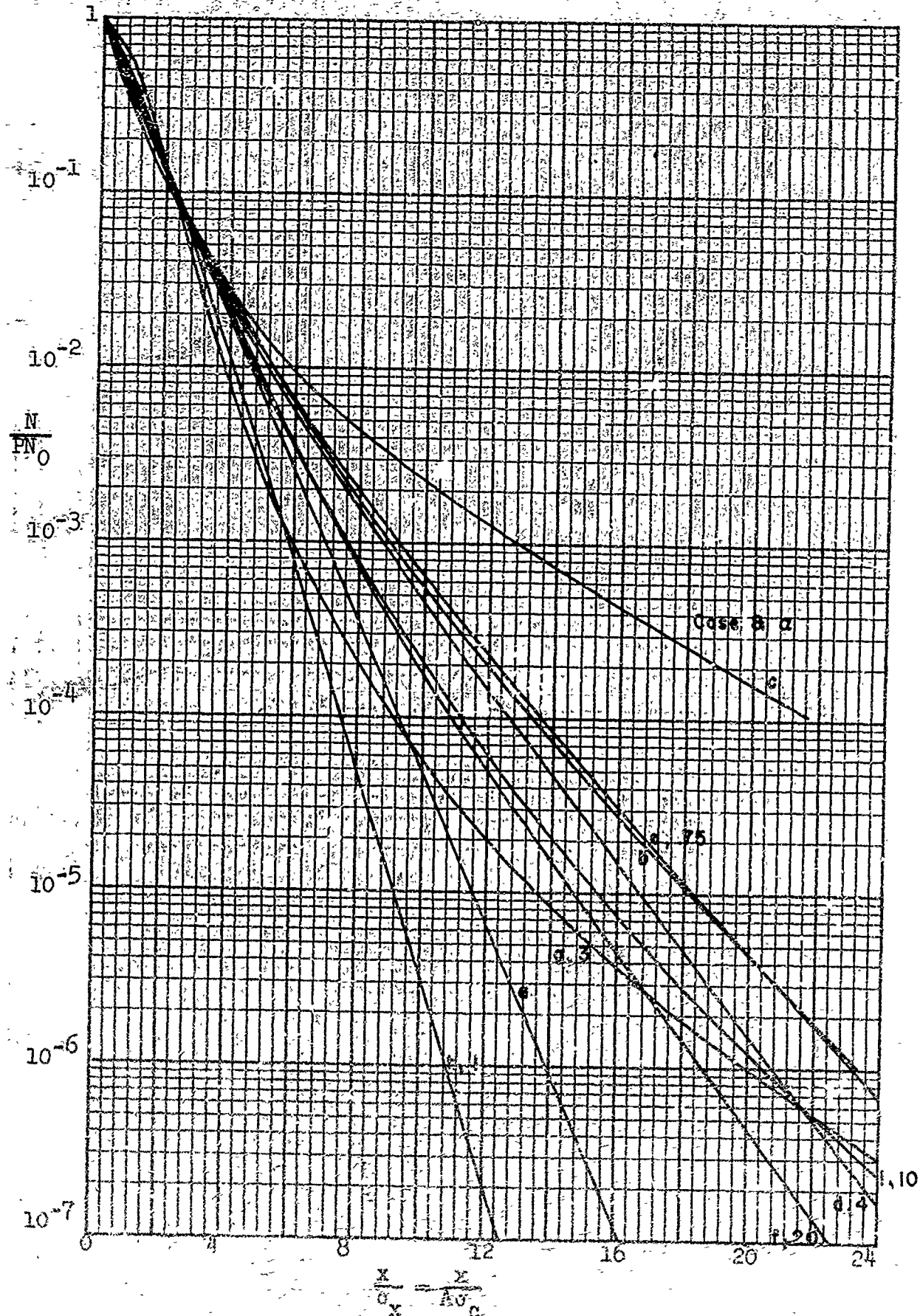


Figure 2. Comparison of Different Possible Exceedance Curves

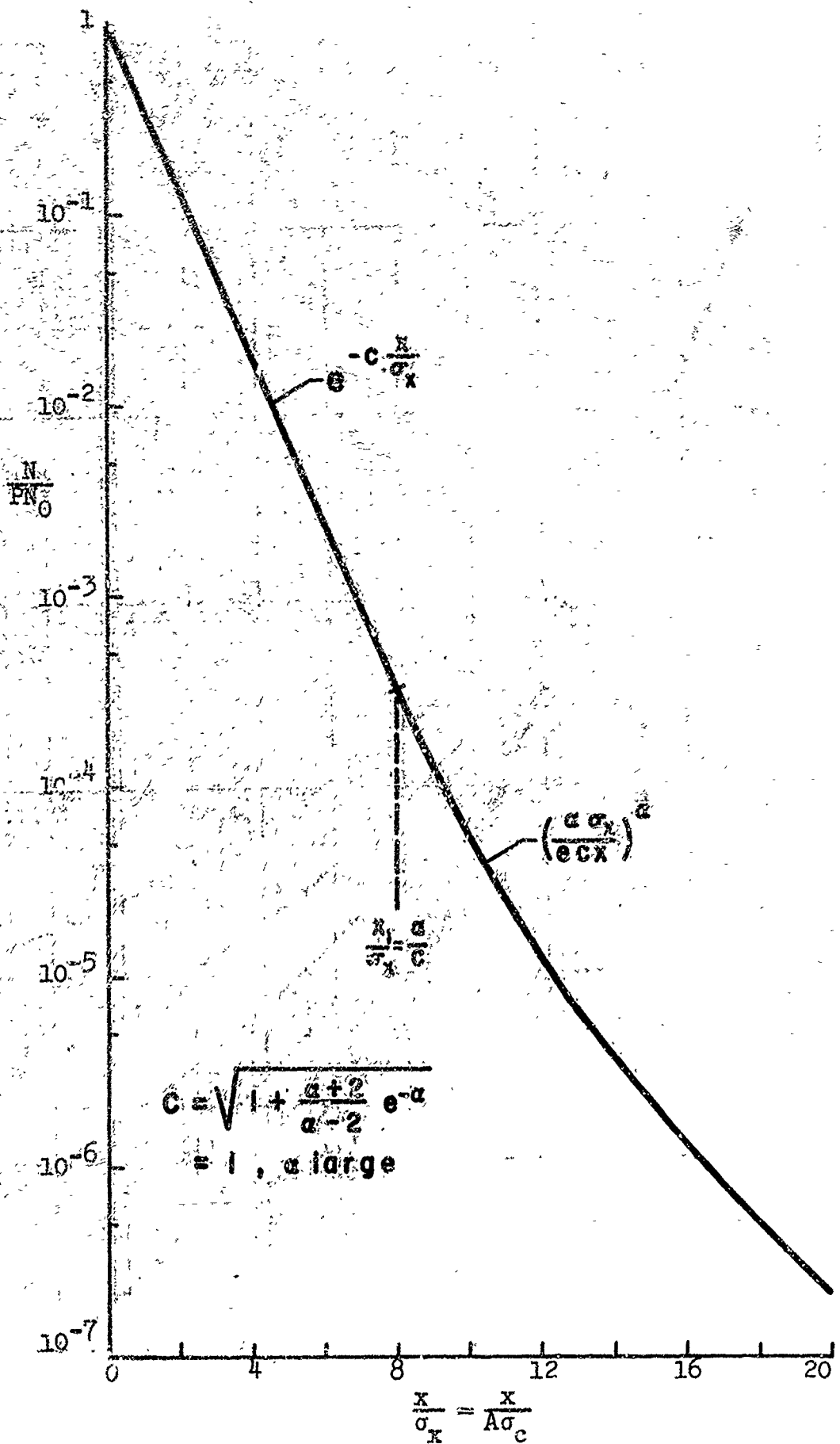


Figure 3. A Composite "Universal" Exceedance Curve: Case j

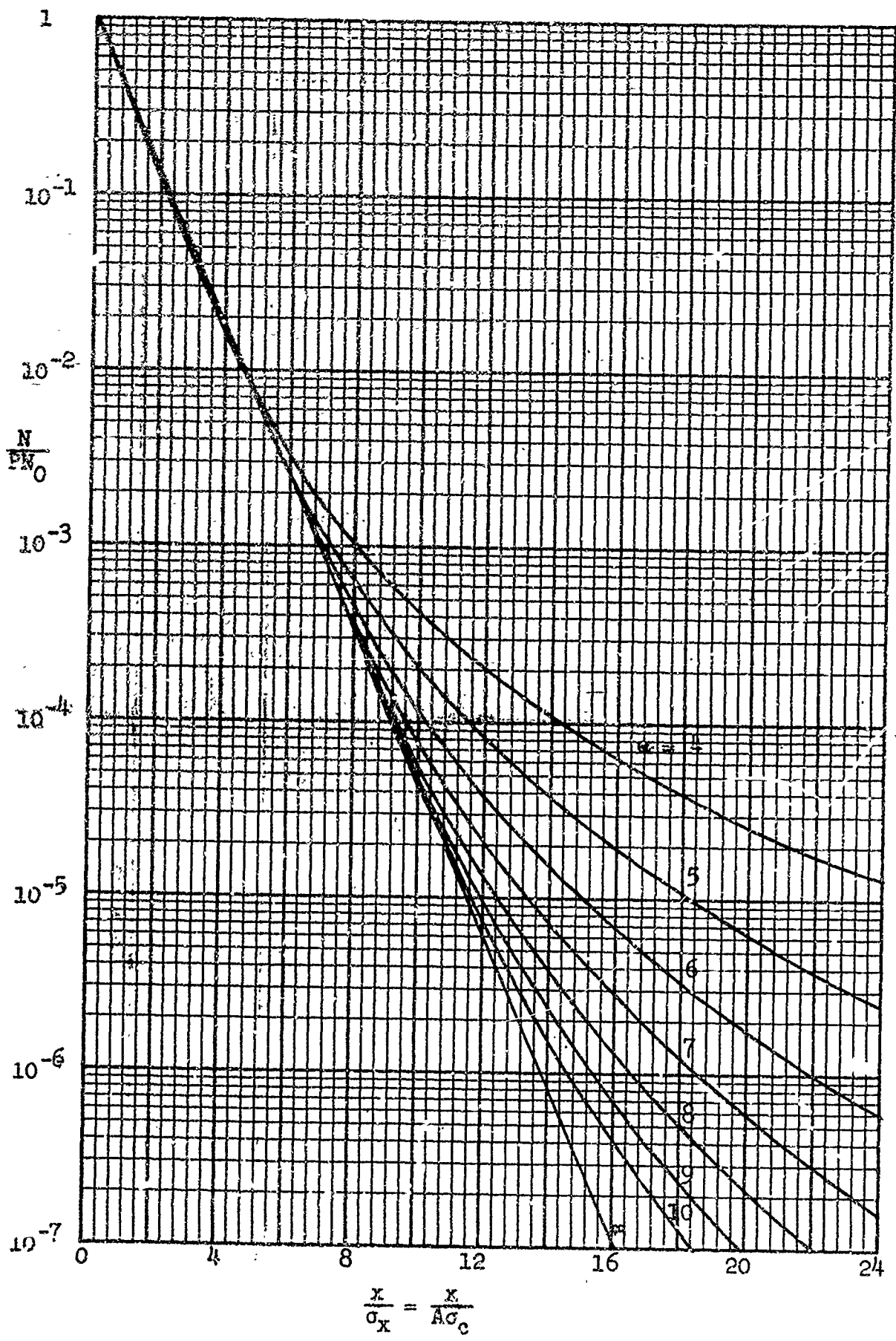


Figure 4. The Case j Composite Universal Exceedance Curve for Various α

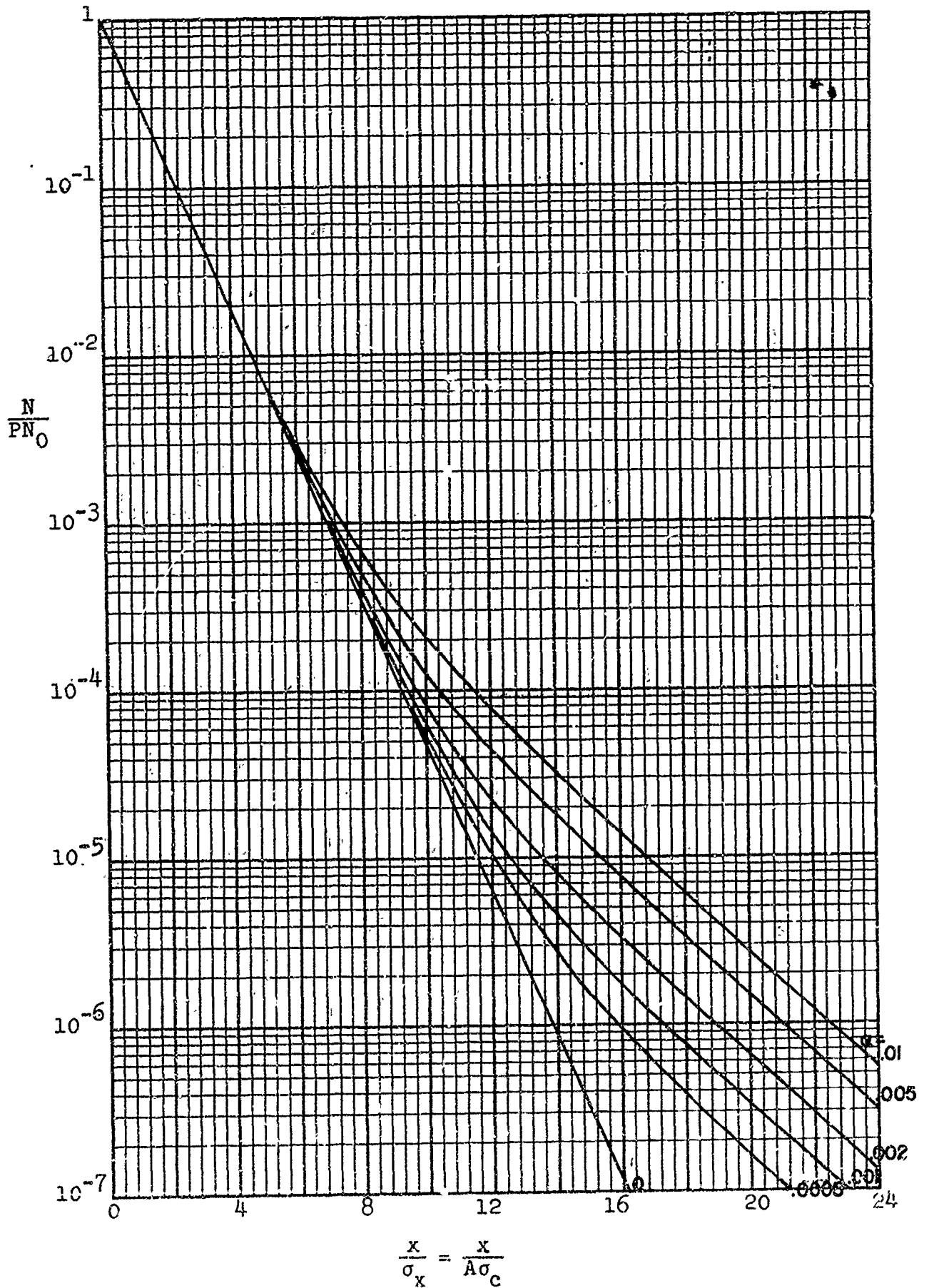


Figure 5. Case k Composite Exceedance Curves

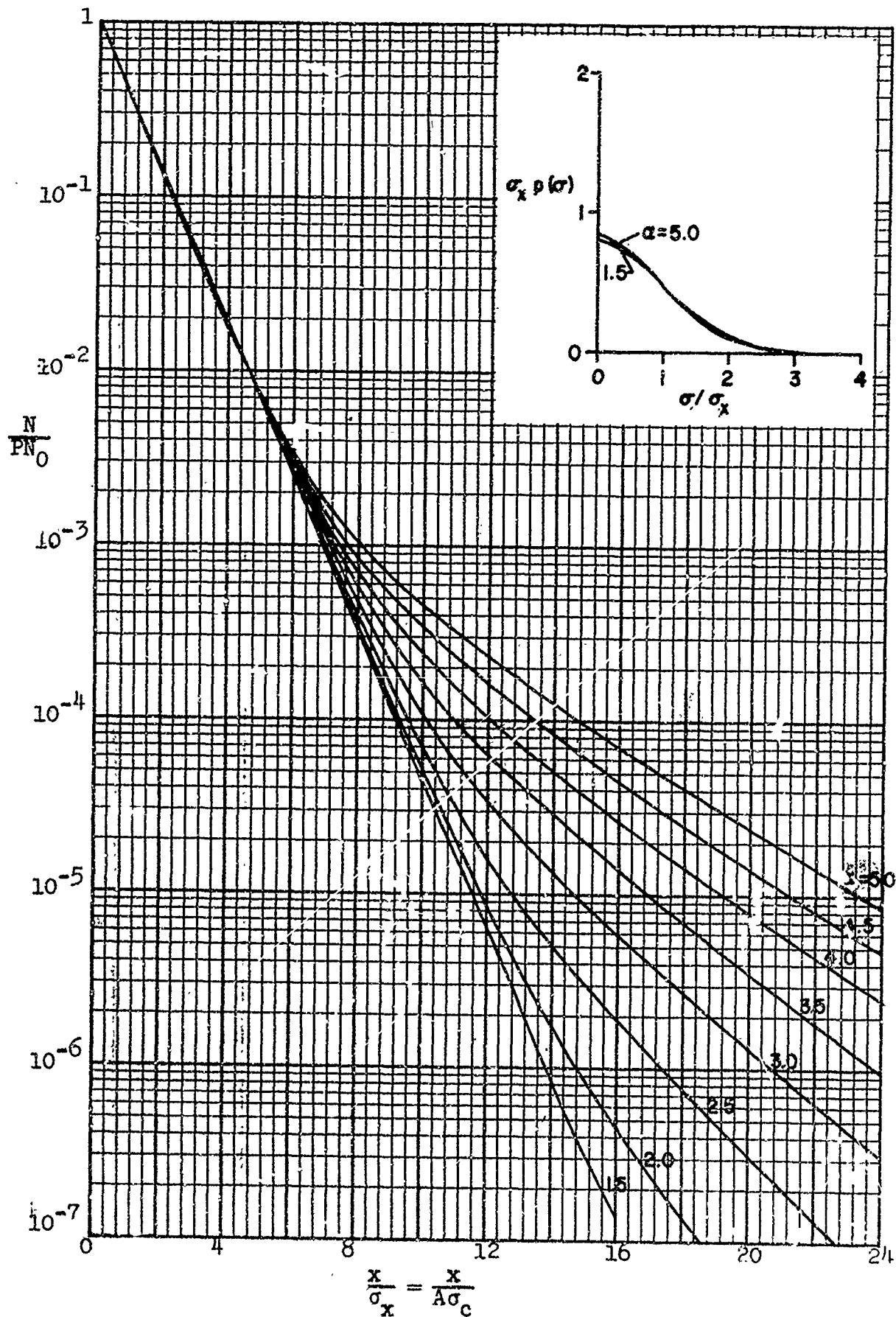


Figure 6. Case 3 Composite Exceedance Curves

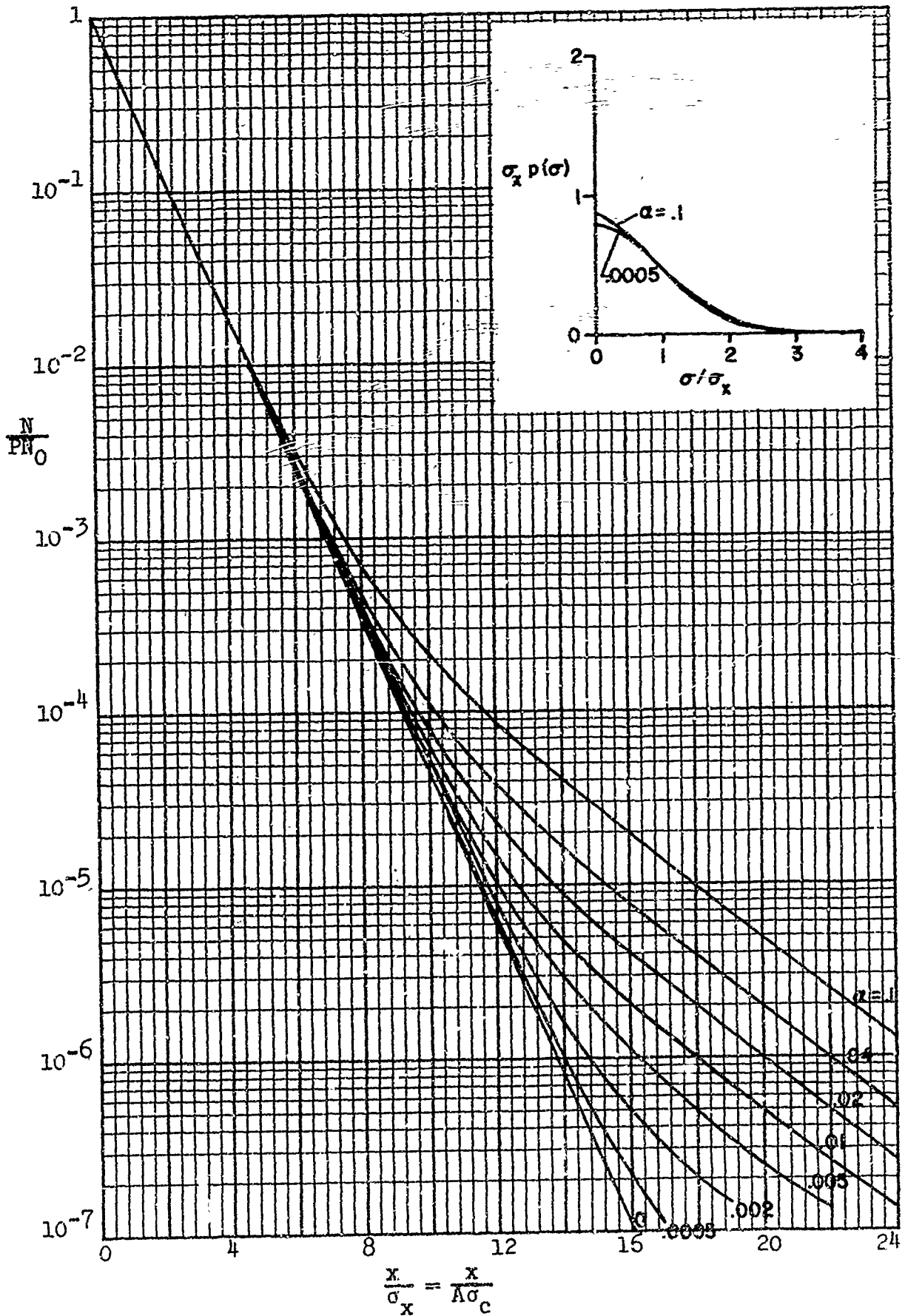


Figure 7. Exceedance Curve Obtained by Superposition: Case m

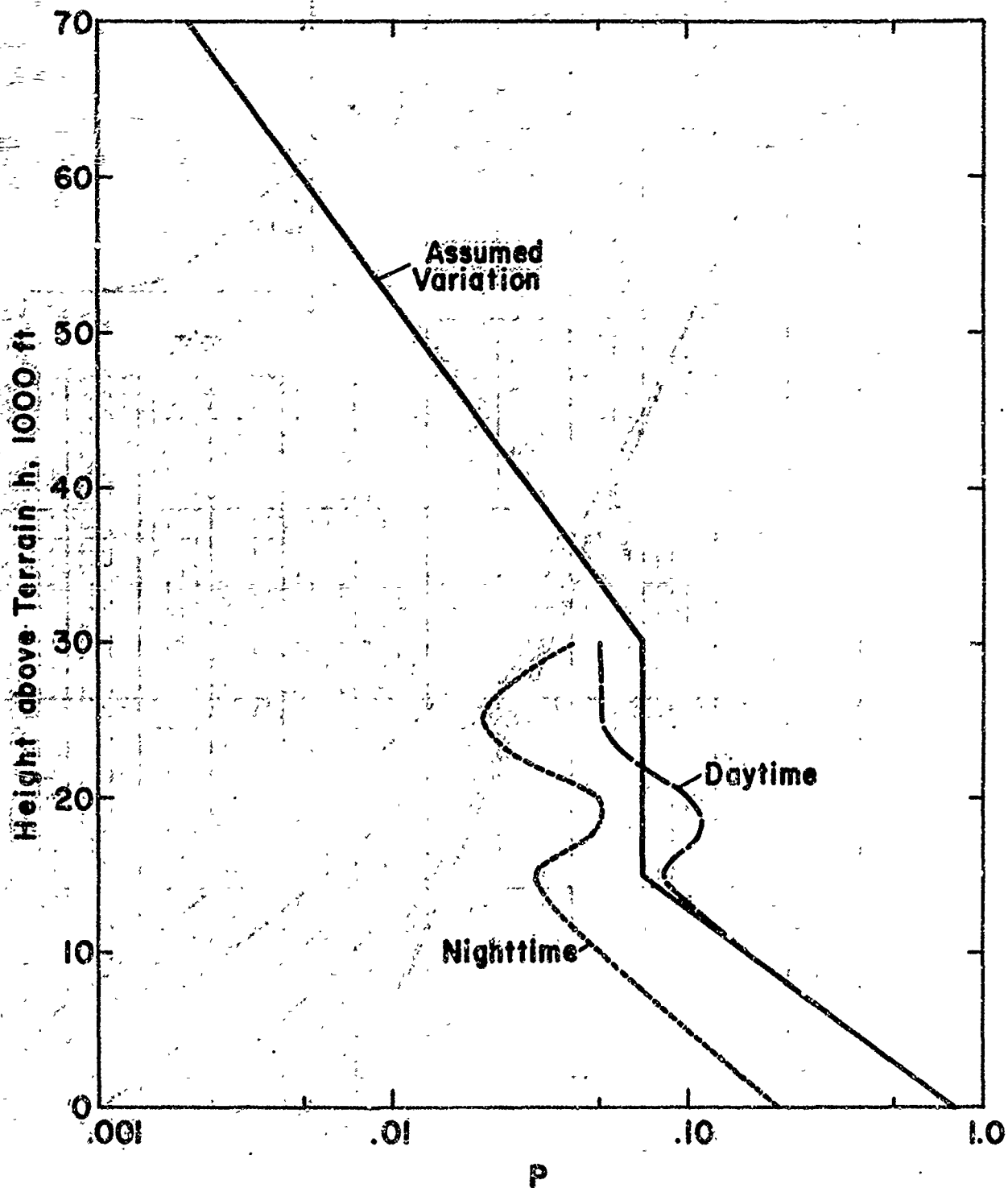


Figure 8. Variation of P with Altitude

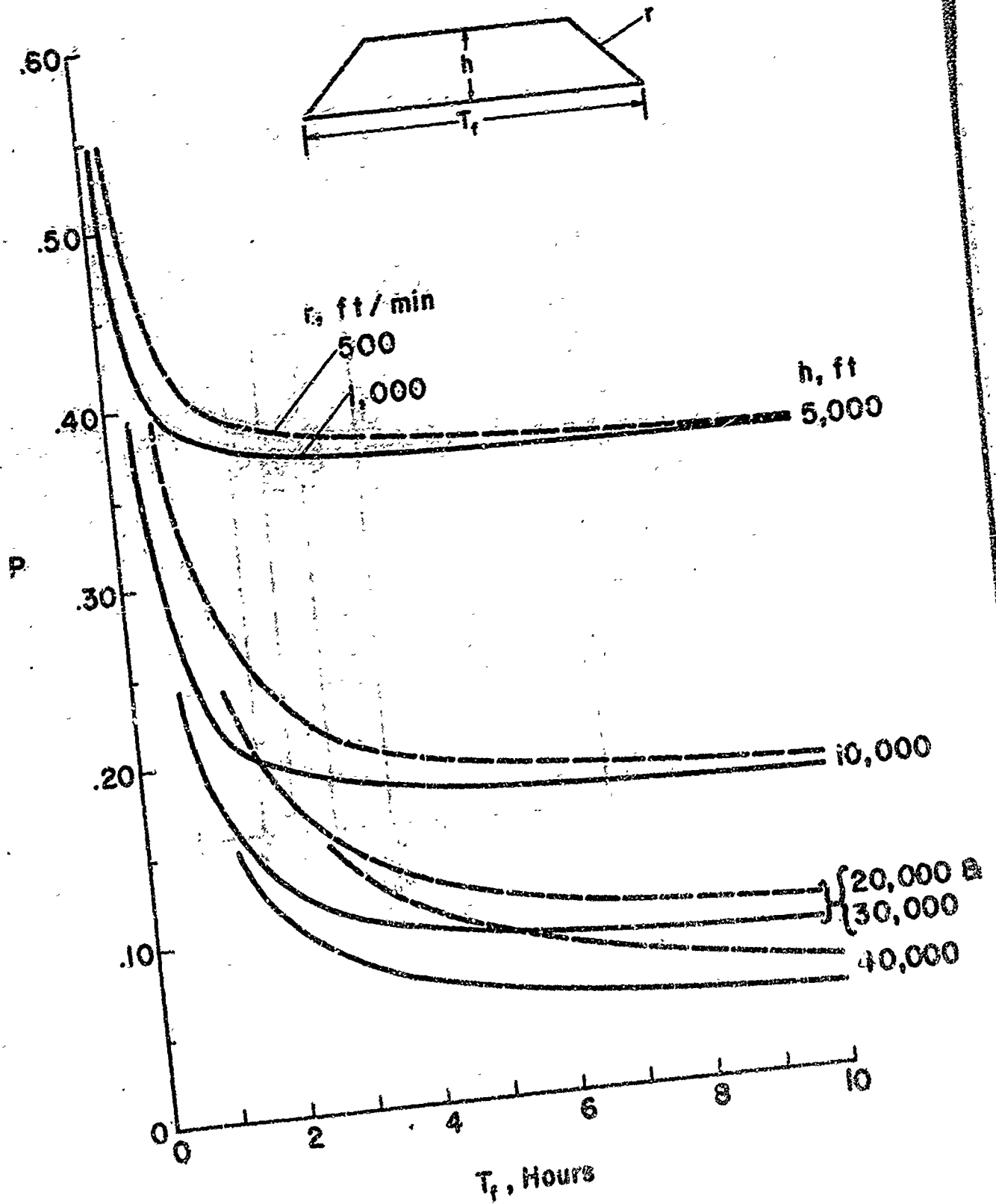


Figure 9. Proportion of Time in Turbulence for a Given Type Mission

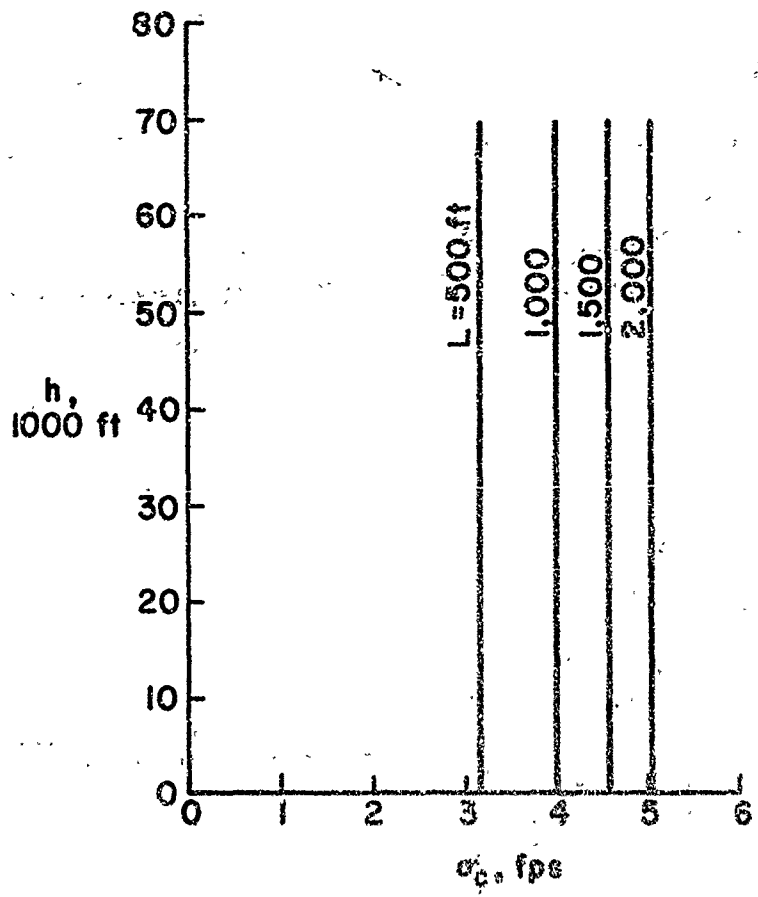


Figure 10. Tentative σ_c Values

	8000 ft. 325 Kt.			6000 ft. 325 Kt.			
				2500 ft. 350 Kt.			
	1	2	3	4	5	6	7
T =	4	22	4	15	2	6	4
P =	.41	.22	.34	.54	.40	.30	.49
$\frac{A_n}{A_1} =$	1	1.163	1.41	1.53	1.25	1.47	1.745
$\sigma_c =$	σ_c	σ_c	σ_c	σ_c	σ_c	σ_c	σ_c

$$T = \sum_{n=1}^7 T_n = 57$$

$$P = \frac{1}{T} \sum_{n=1}^7 P_n T_n = .36$$

$$\frac{A_c^2}{A_1^2} = \sum_{n=1}^7 \frac{P_n T_n}{PT} \cdot \frac{A_n^2}{A_1^2}$$

$$= \left\{ (.08)(1) + (.236)(1.35) + (.0664)(1.99) + (.395)(2.34) \right. \\ \left. + (.039)(1.57) + (.0878)(2.16) + (.0955)(3.05) \right\}$$

$$= \left\{ .08 + .319 + .133 + .926 + .0615 + .189 + .292 \right\}$$

$$= 2.005$$

$$\frac{A_c}{A_1} = 1.416$$

Figure 11. Example Showing Evaluation of Composite A_c

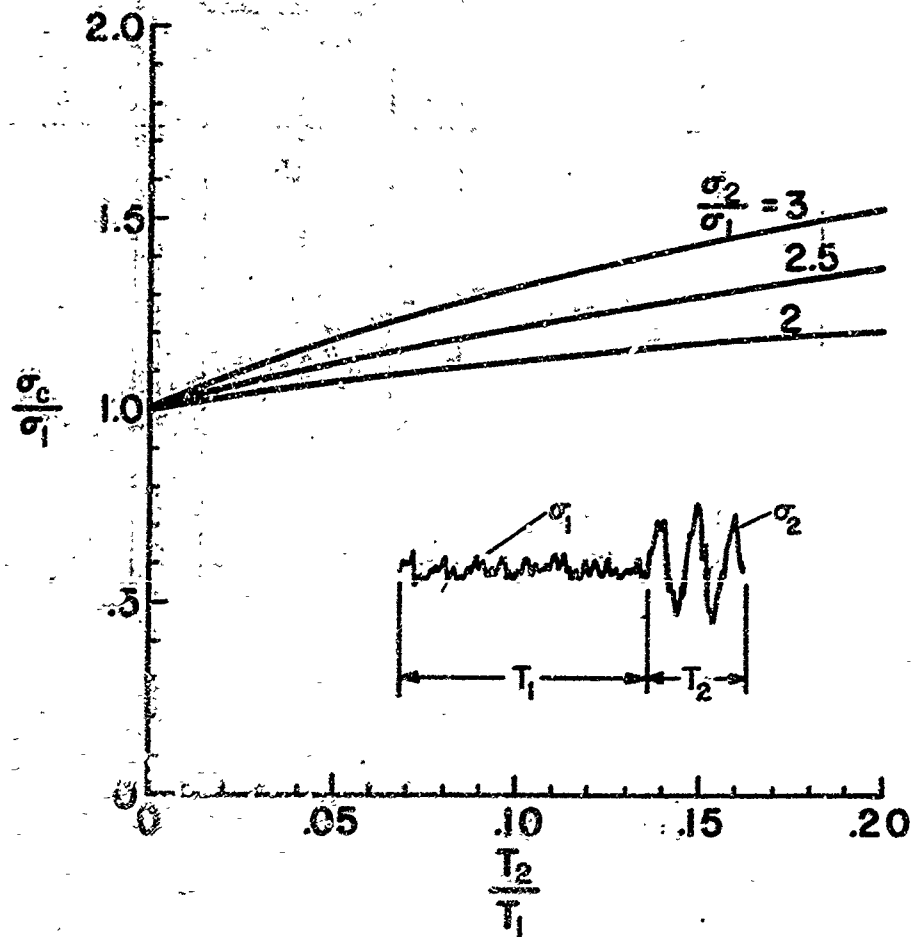


Figure 12. σ_c Increase Due to Increased Severe Turbulence Encounter

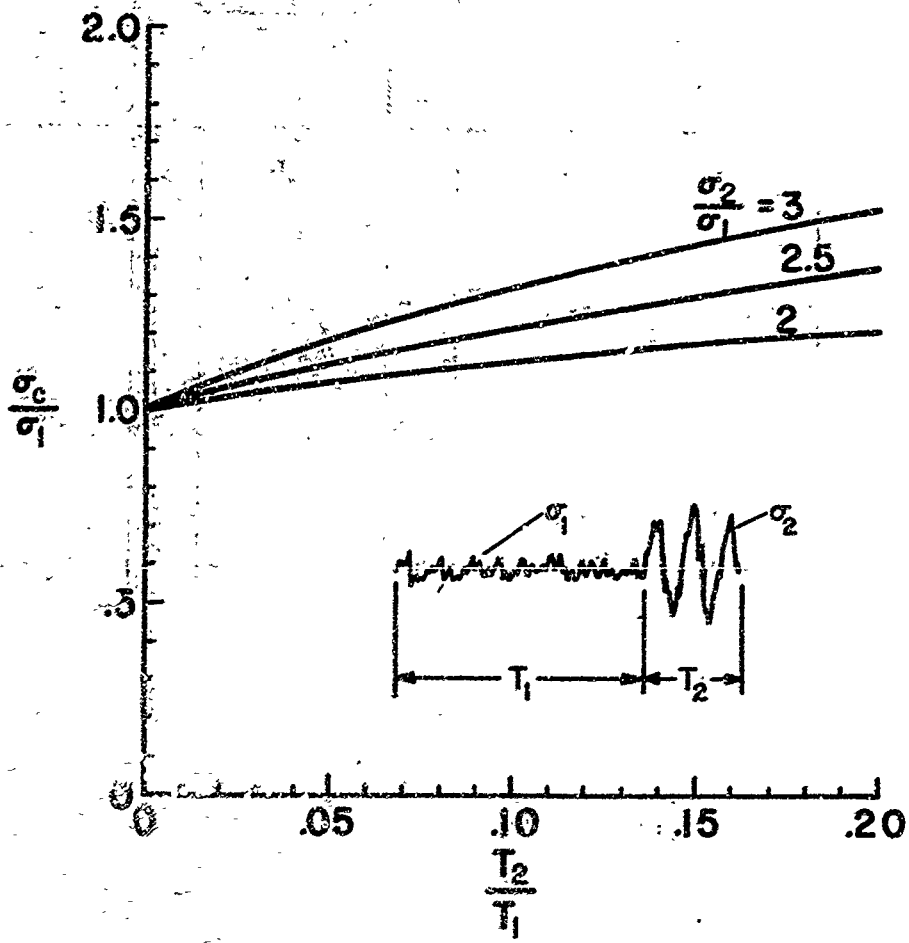


Figure 12. σ_c Increase Due to Increased Severe Turbulence Encounter

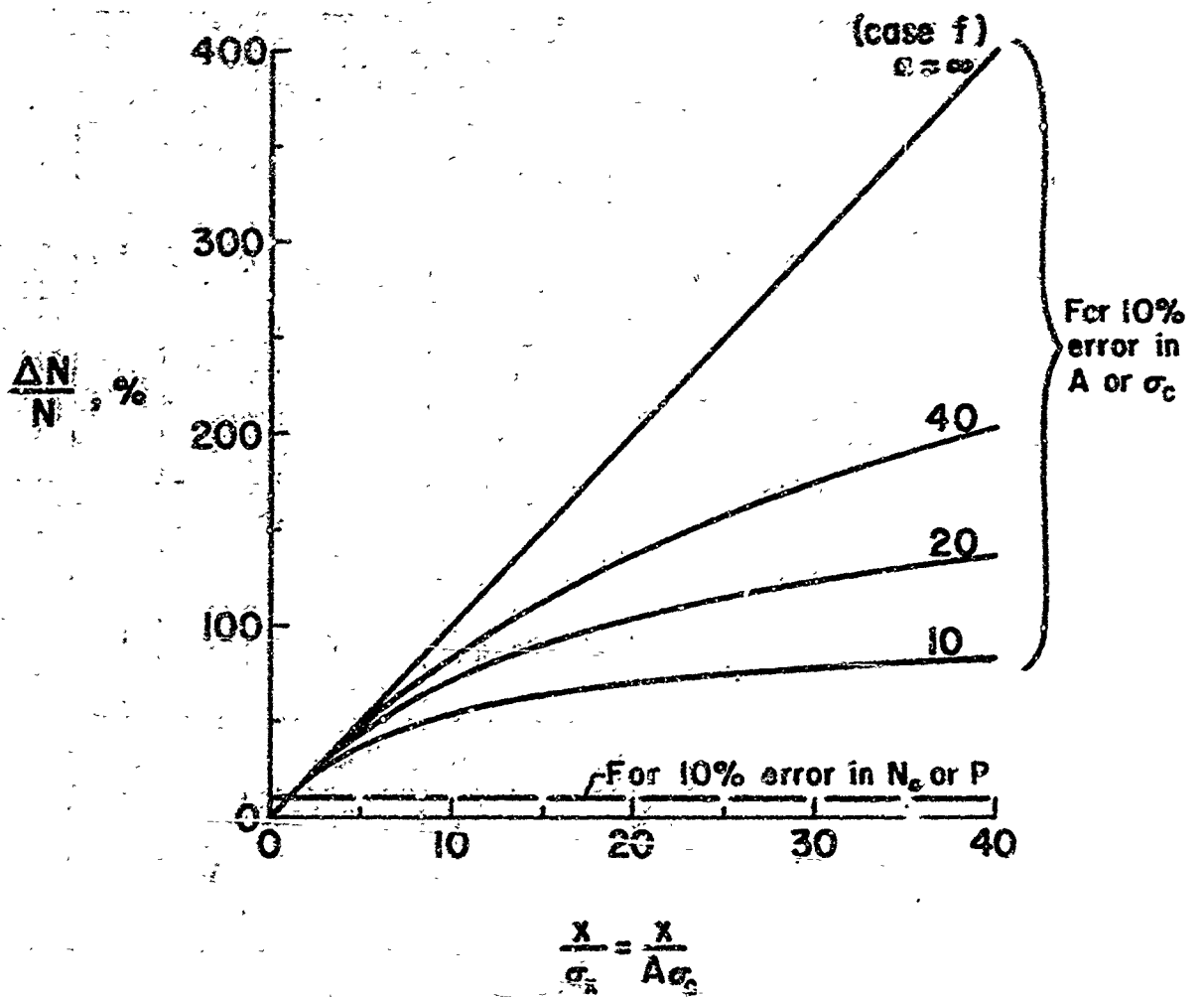


Figure 13. Sensitivity of N to Errors in A , σ_c , N_0 and P

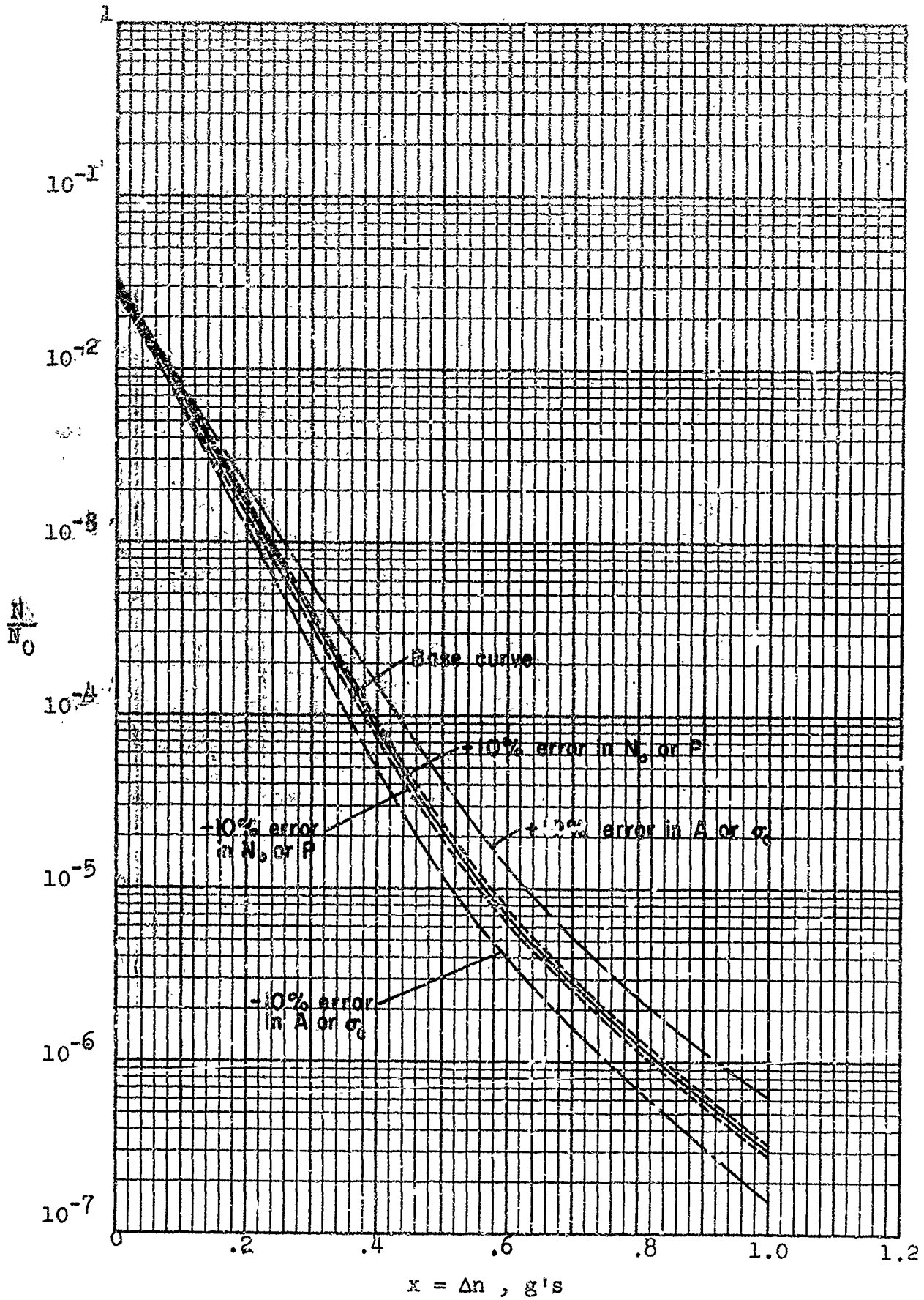


Figure 14. Example Exceedance Curves Illustrating Effect of Errors

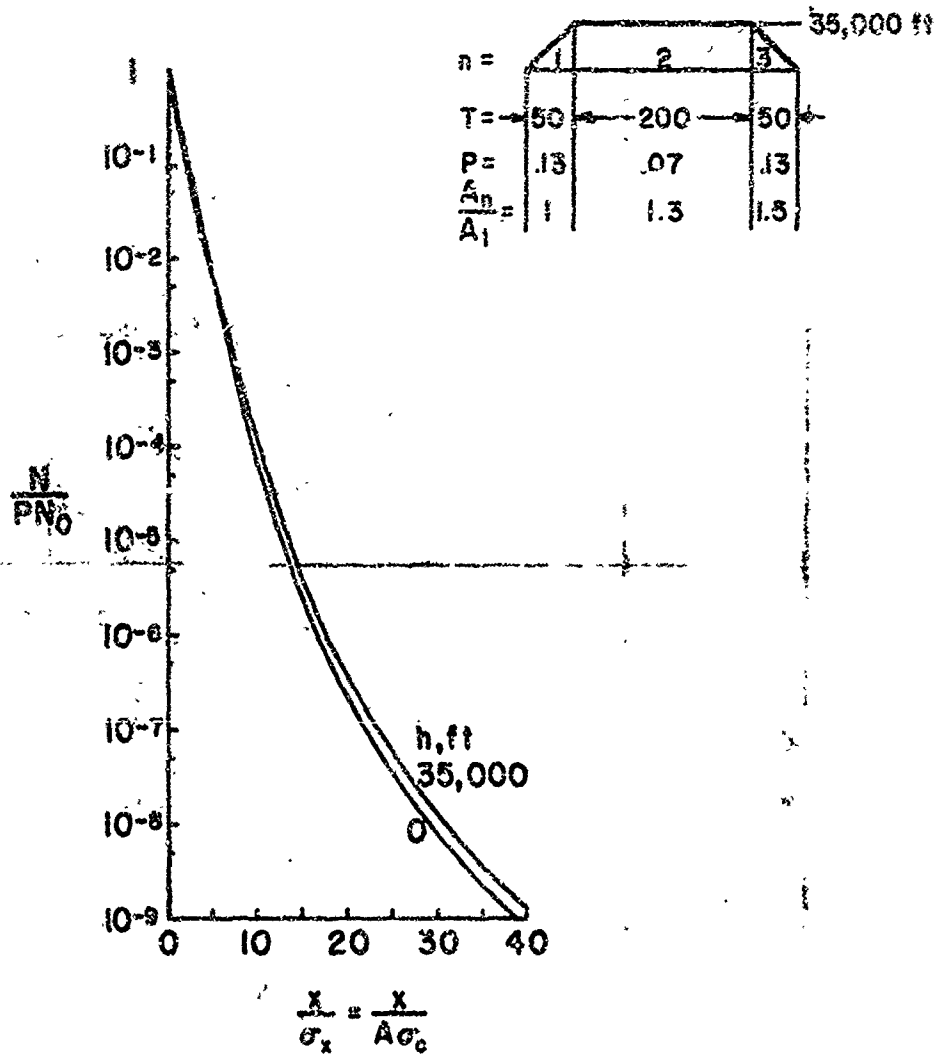
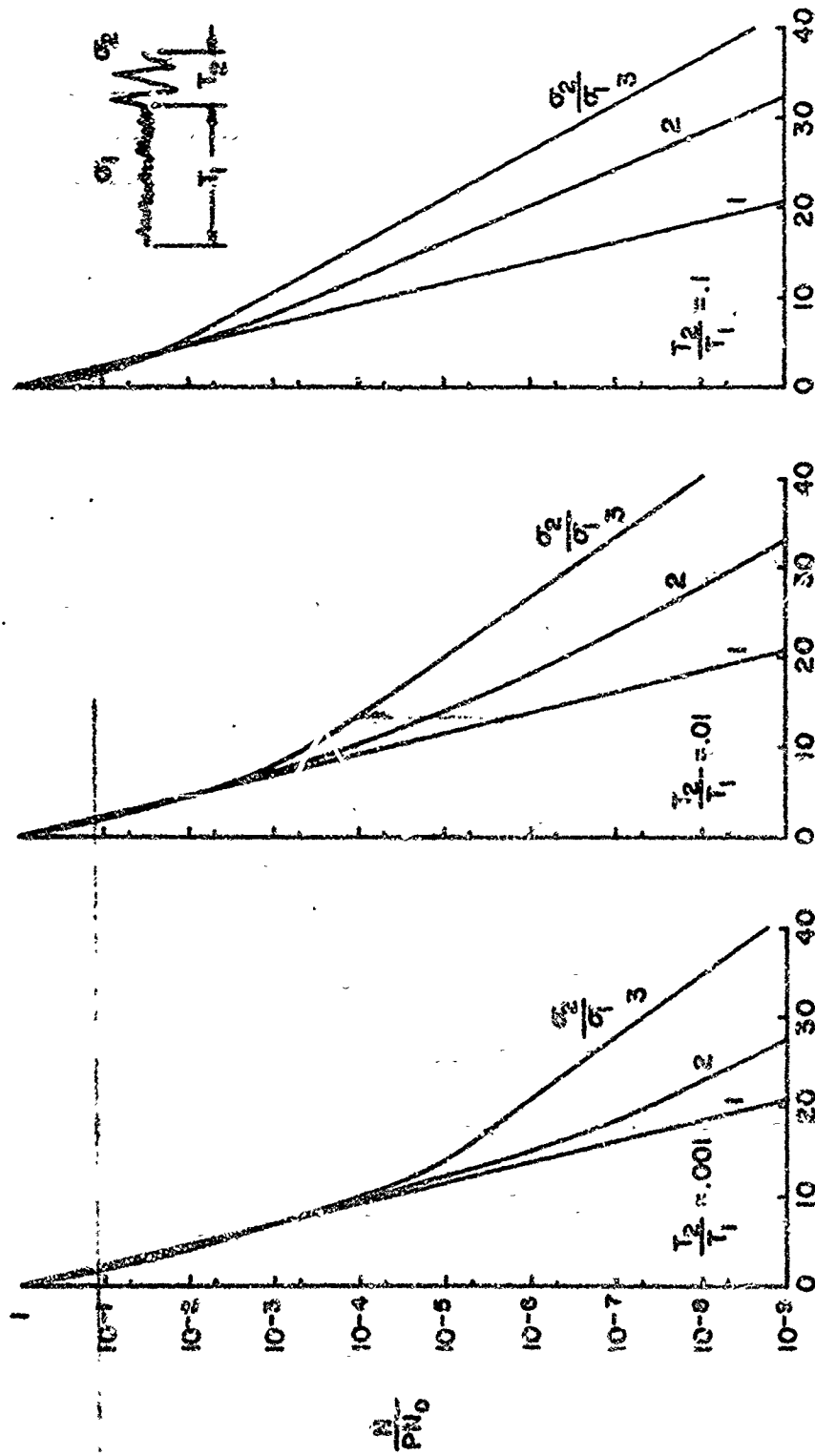


Figure 15. Effect of Altitude on Universal Curve Shape



$$\frac{x}{A\sigma_0} = \frac{x}{A\sigma_0}$$

Figure 16a. Effect of Increased Severe Turbulence Encounter on Universal Curve Shape

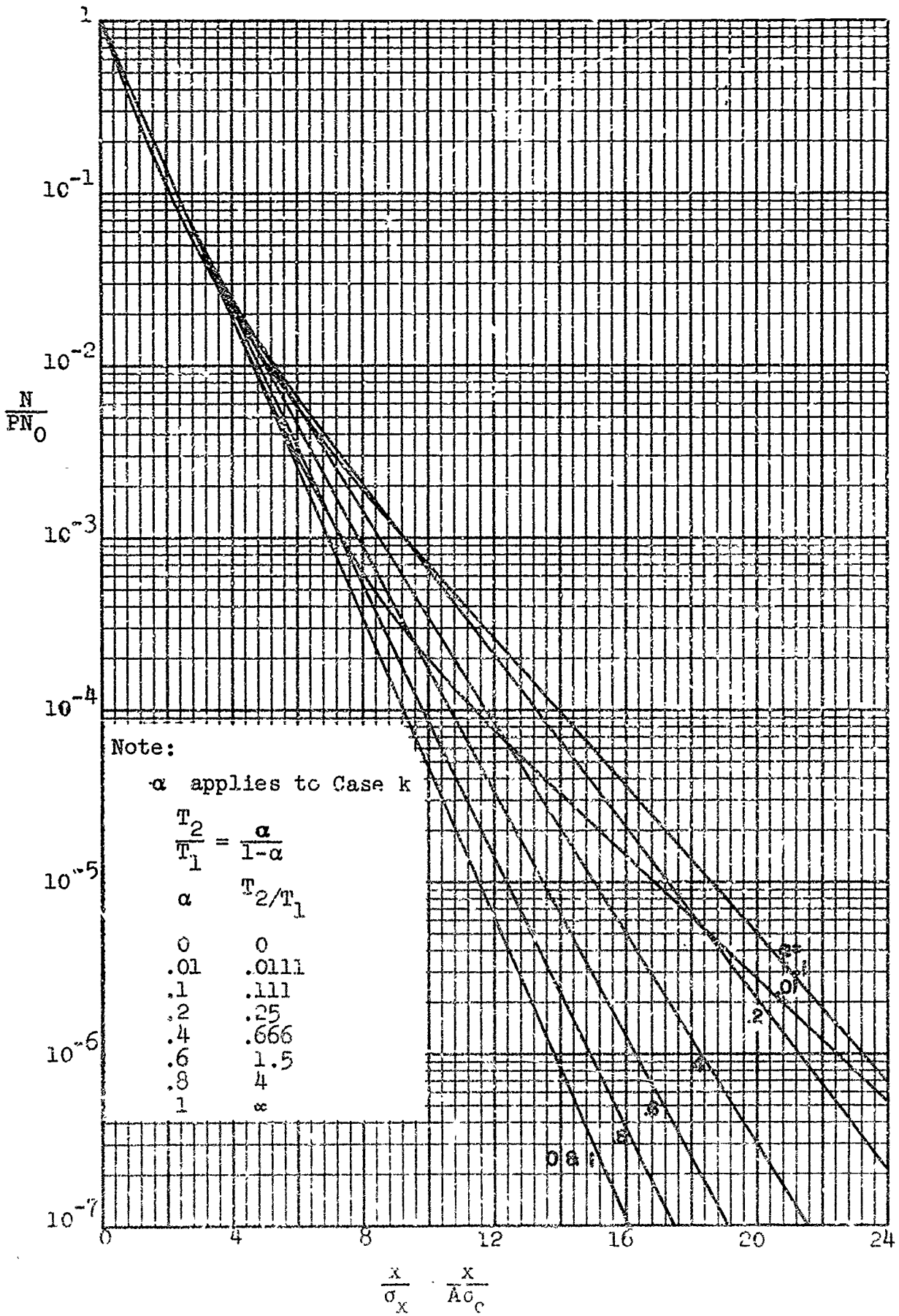


Figure 16b. Concluded

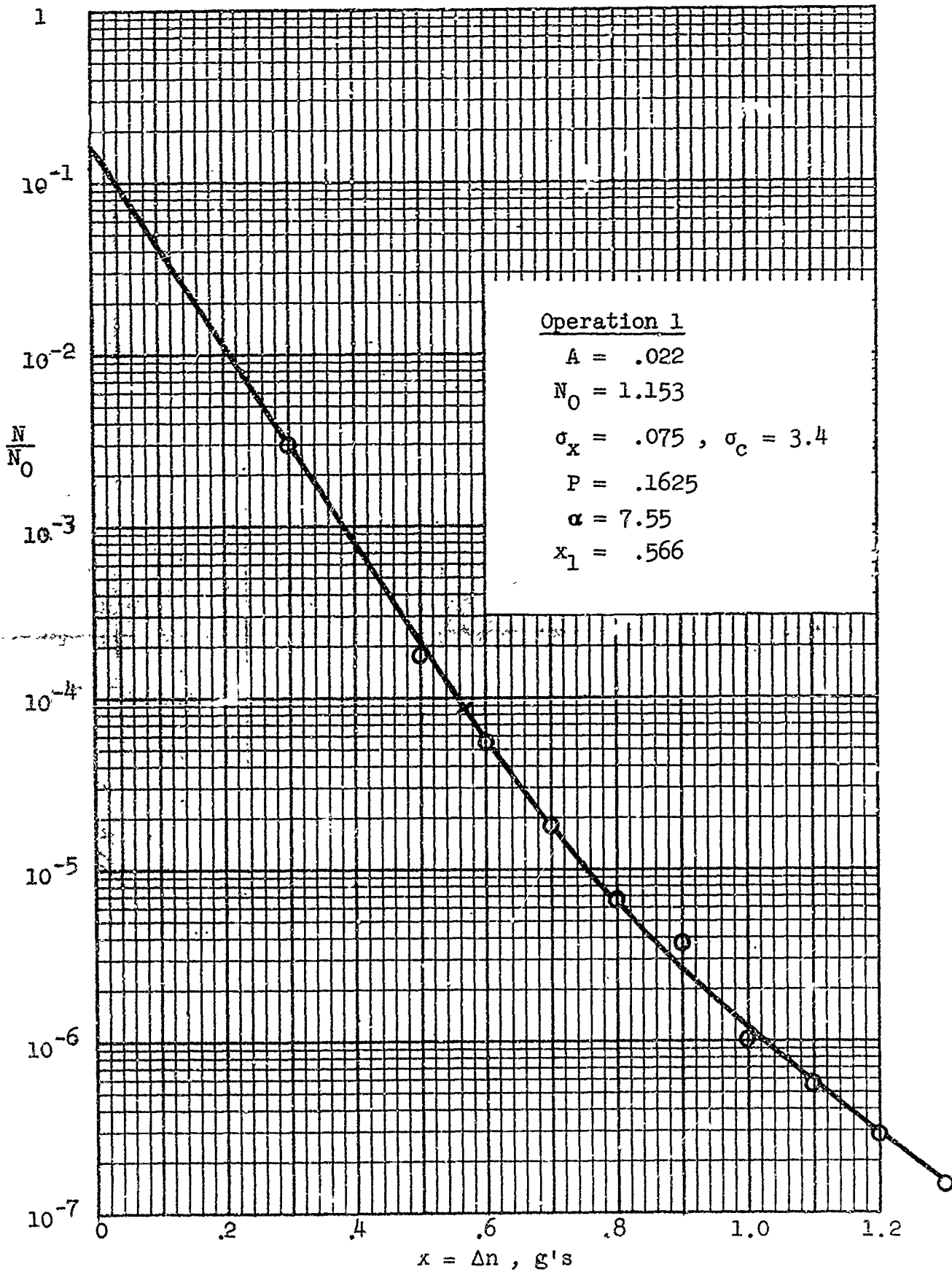


Figure 17a. Reanalysis of airline operations data

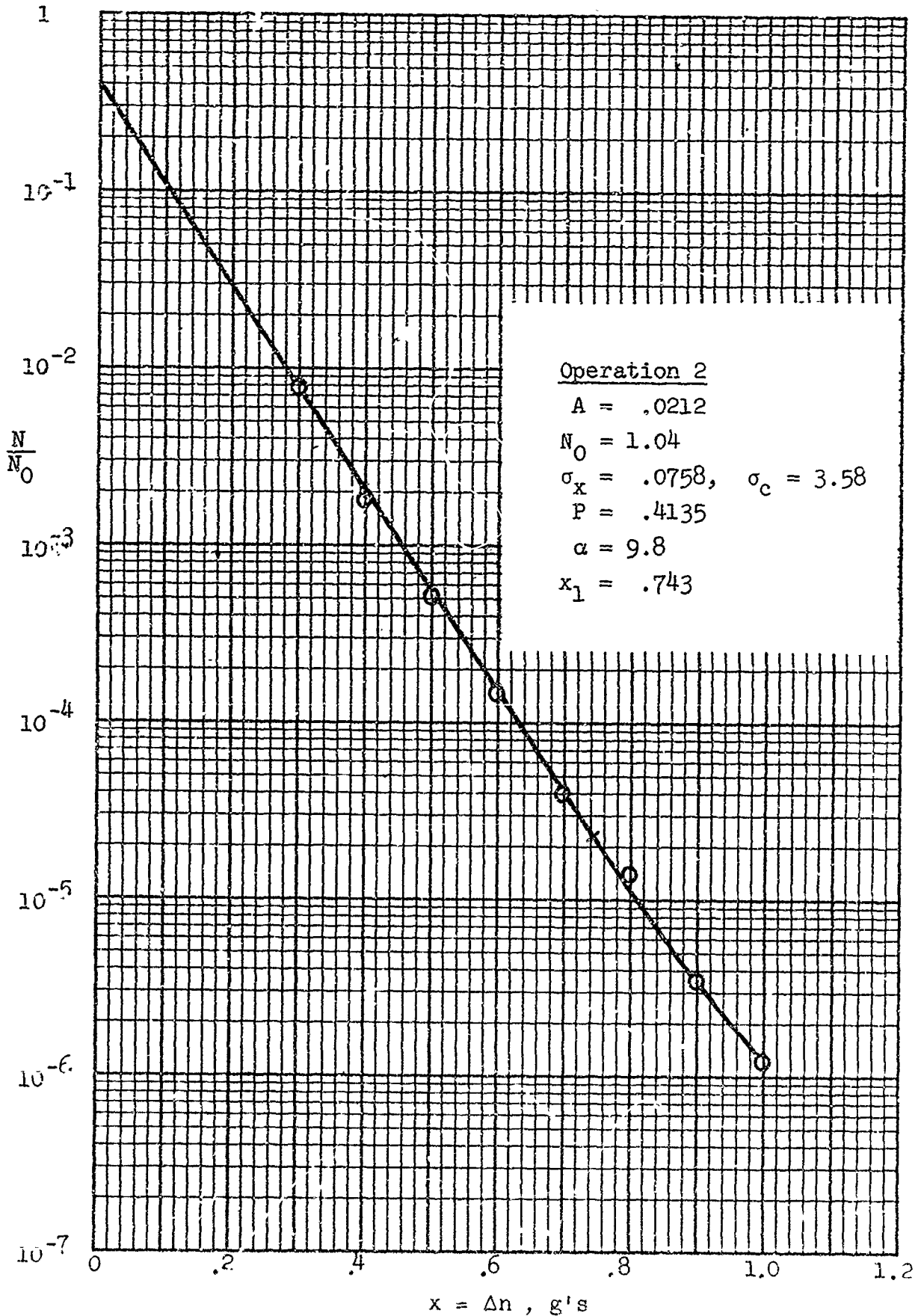


Figure 17b. continued 93

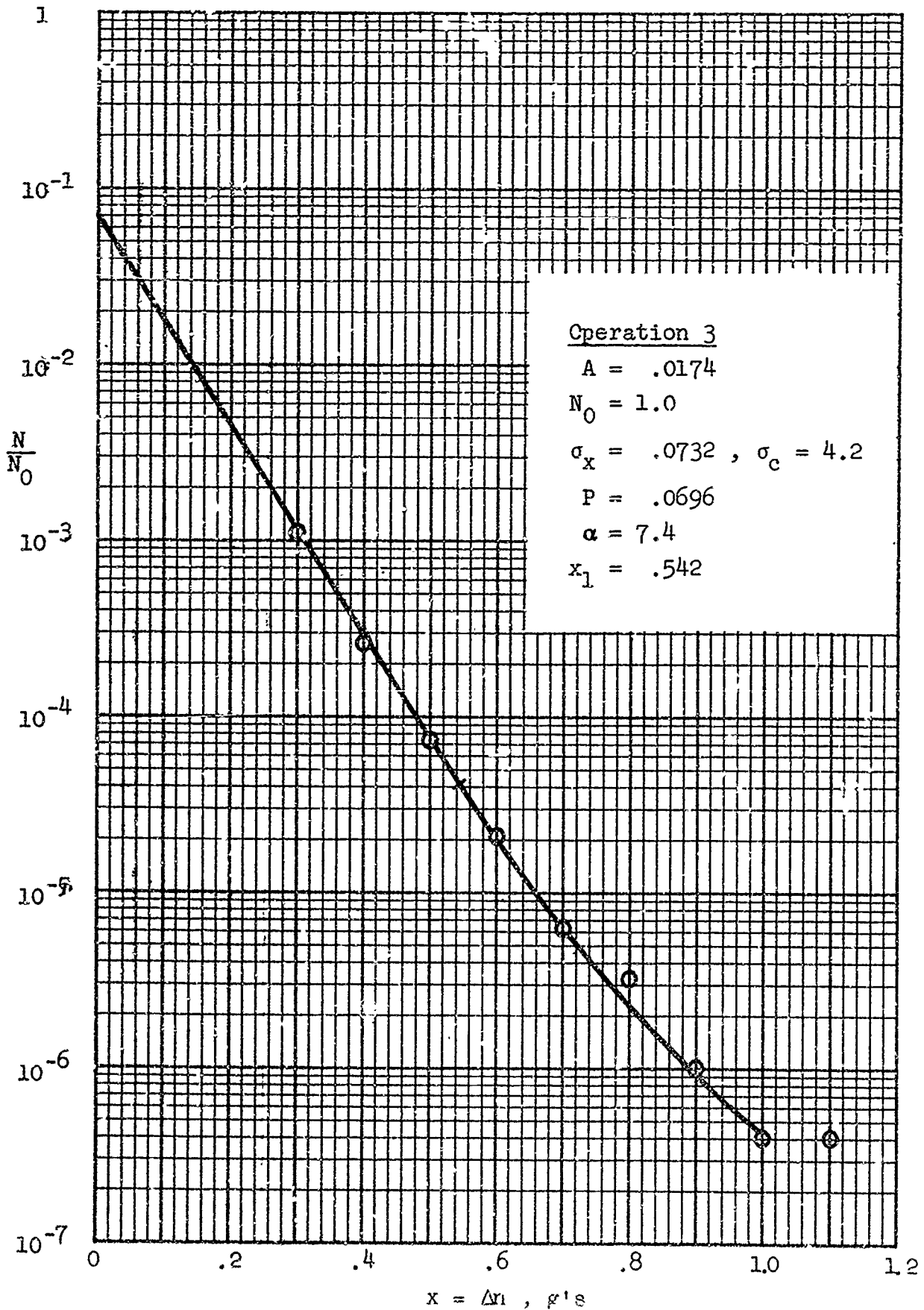


Figure 17c. continued 94

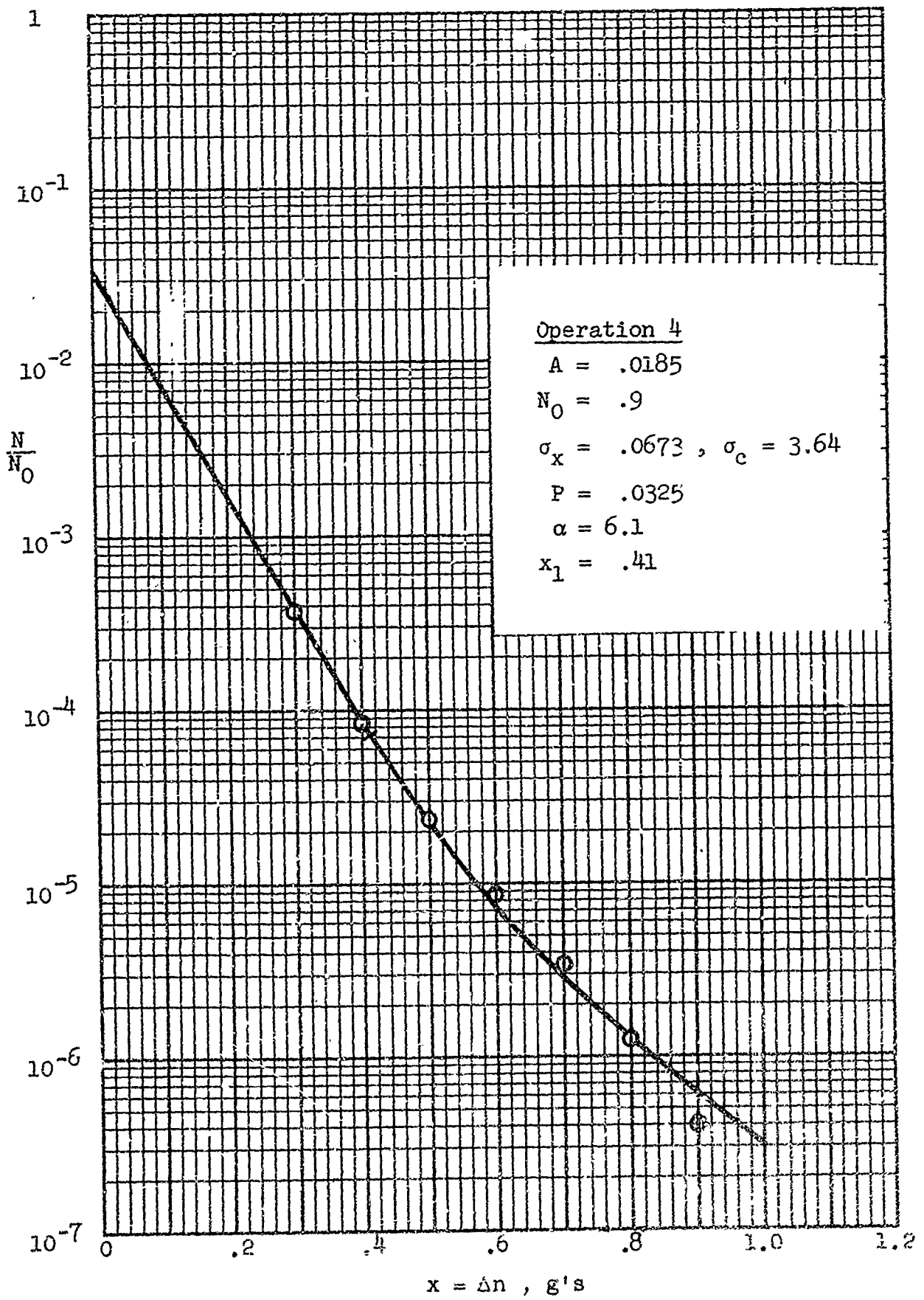


Figure 17d. continued 95

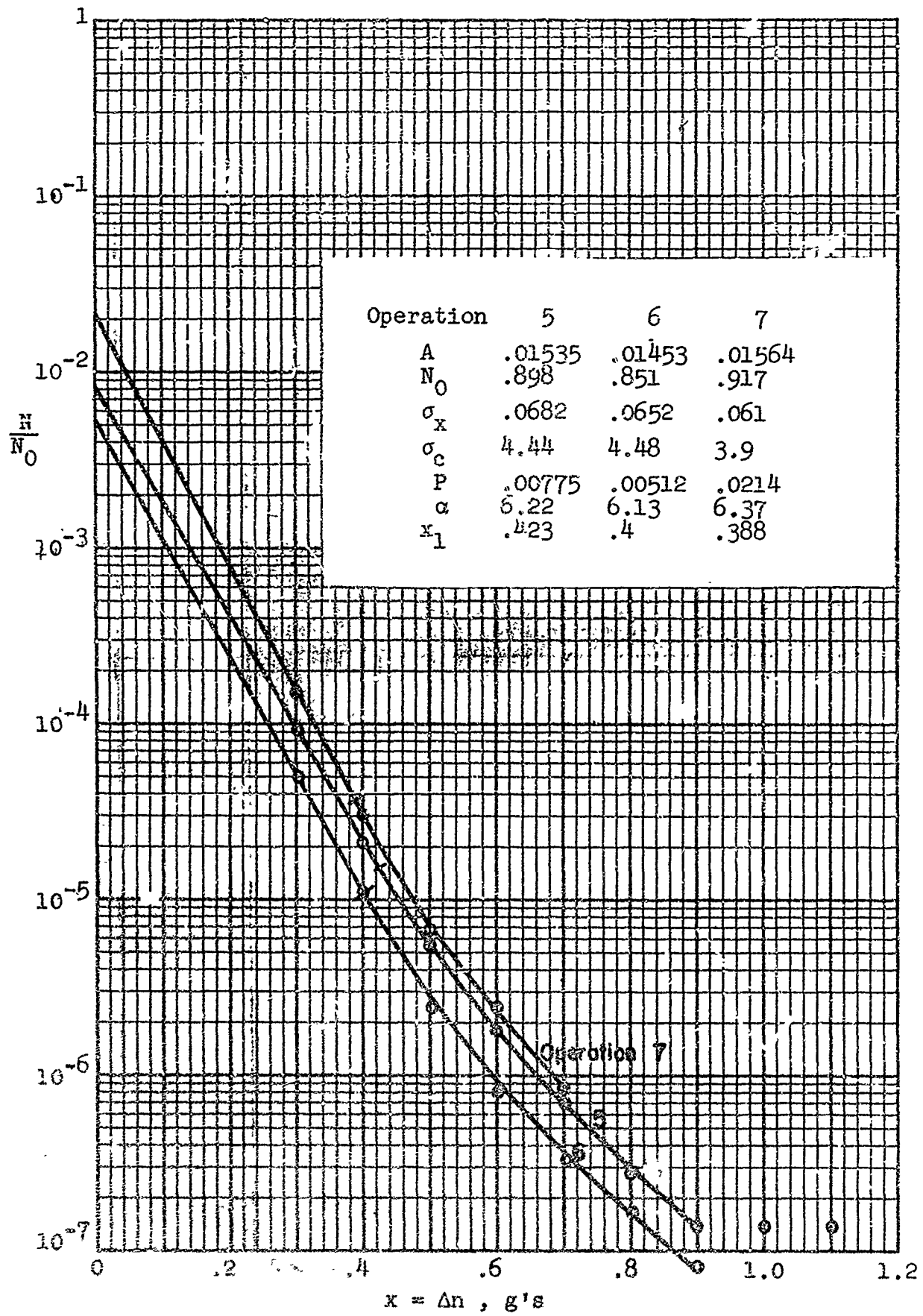


Figure 17e. continued

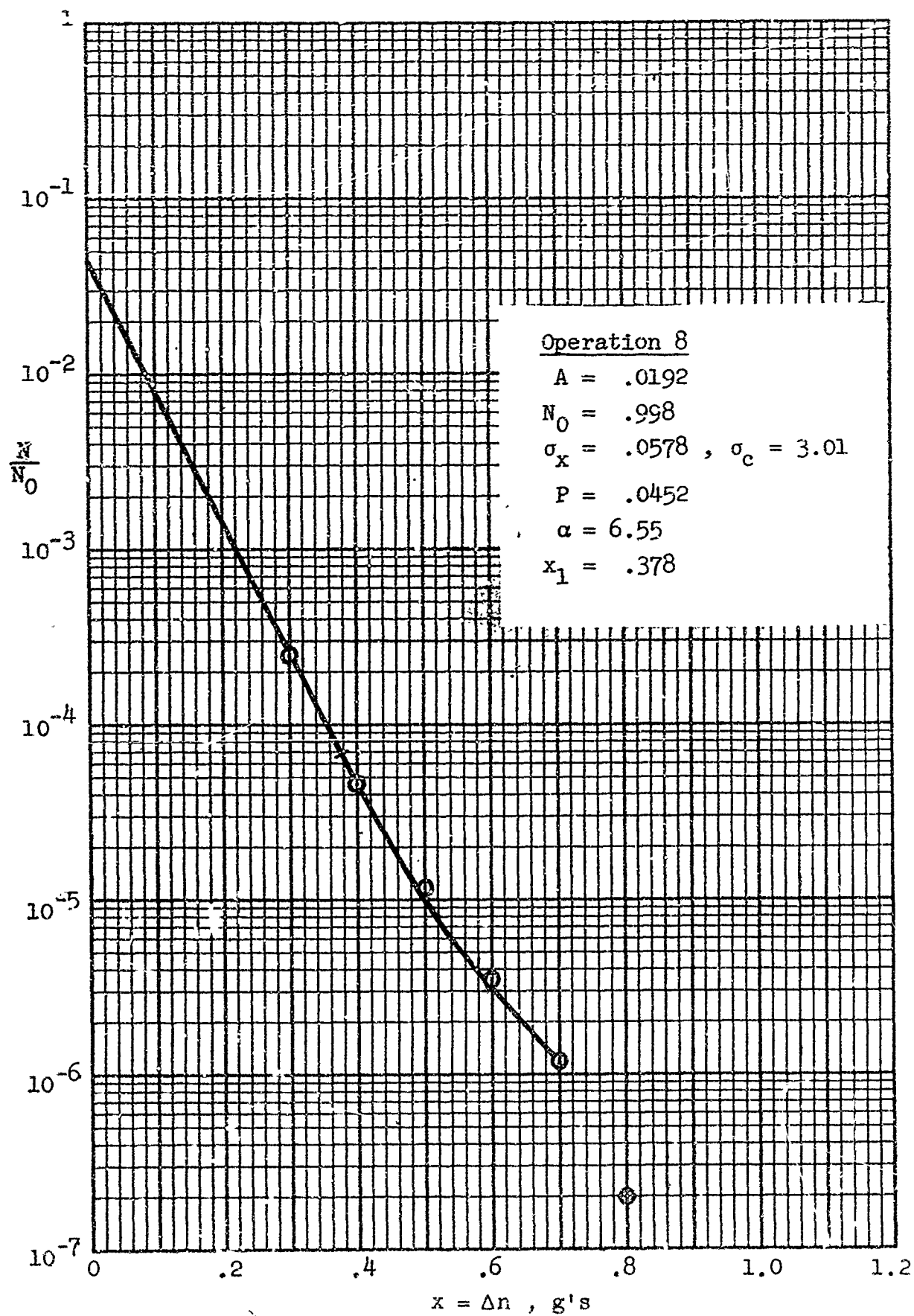


Figure 17f. concluded 97

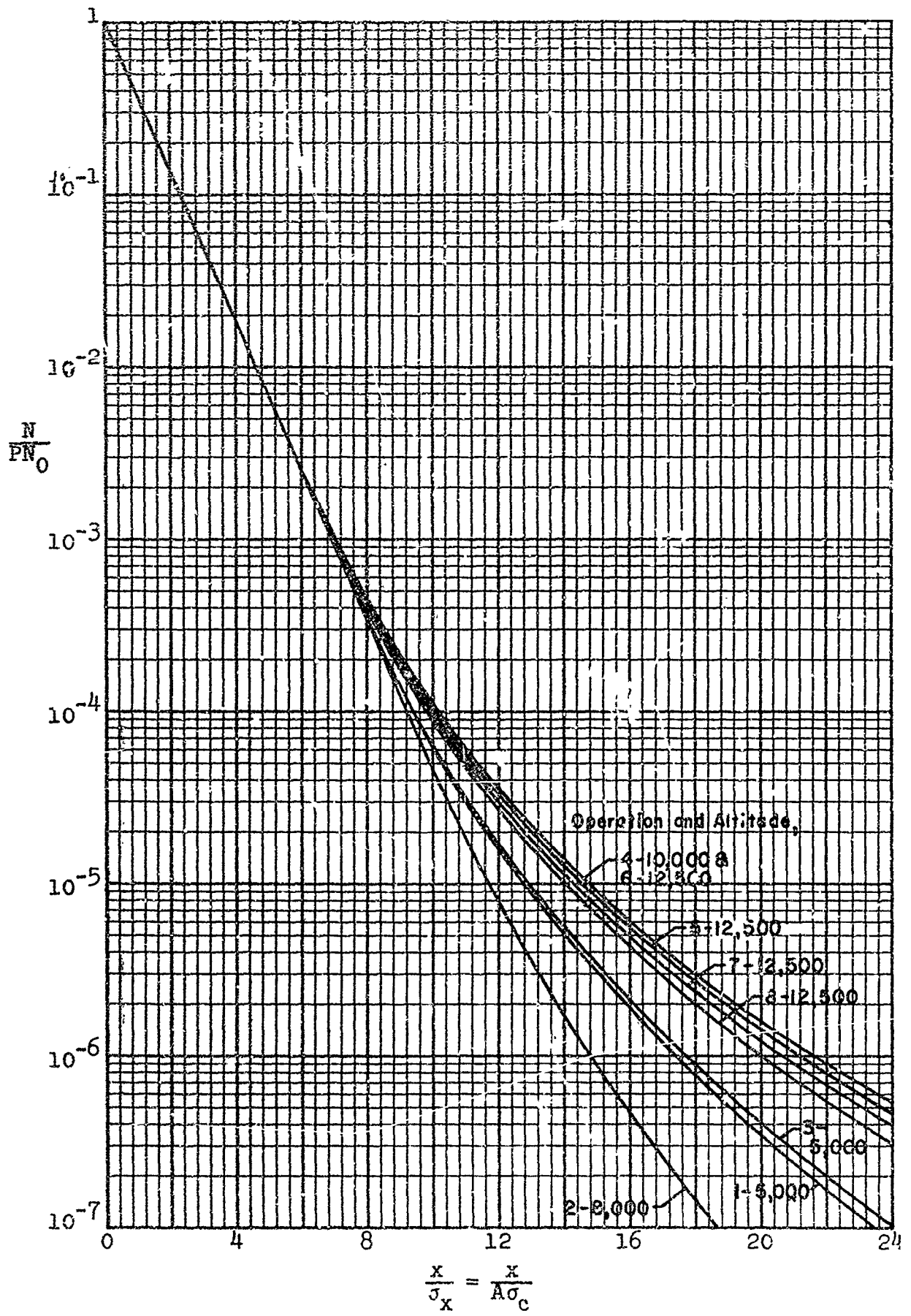


Figure 18. Generalized Exceedance Curves as Derived From the Flight Data

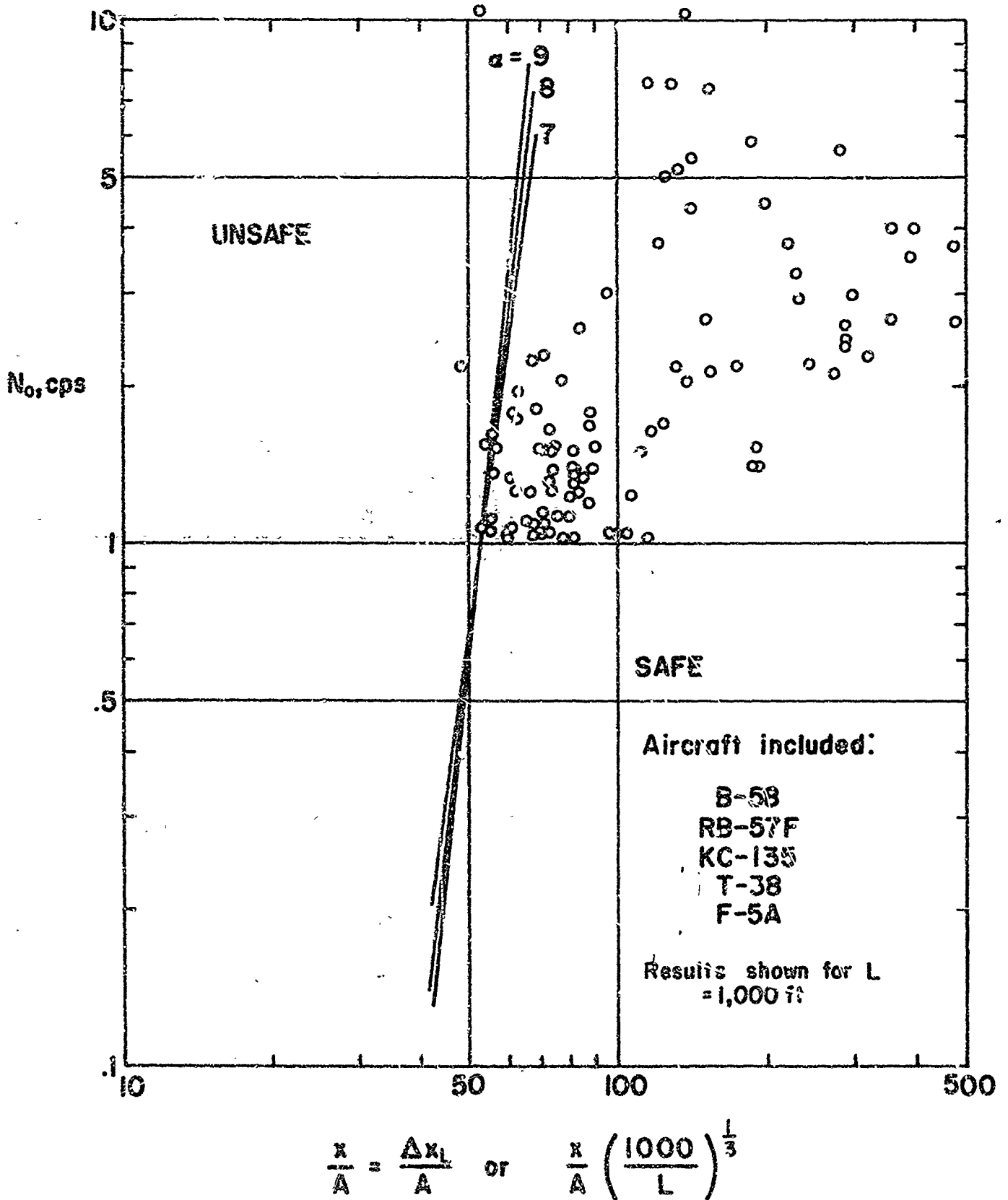
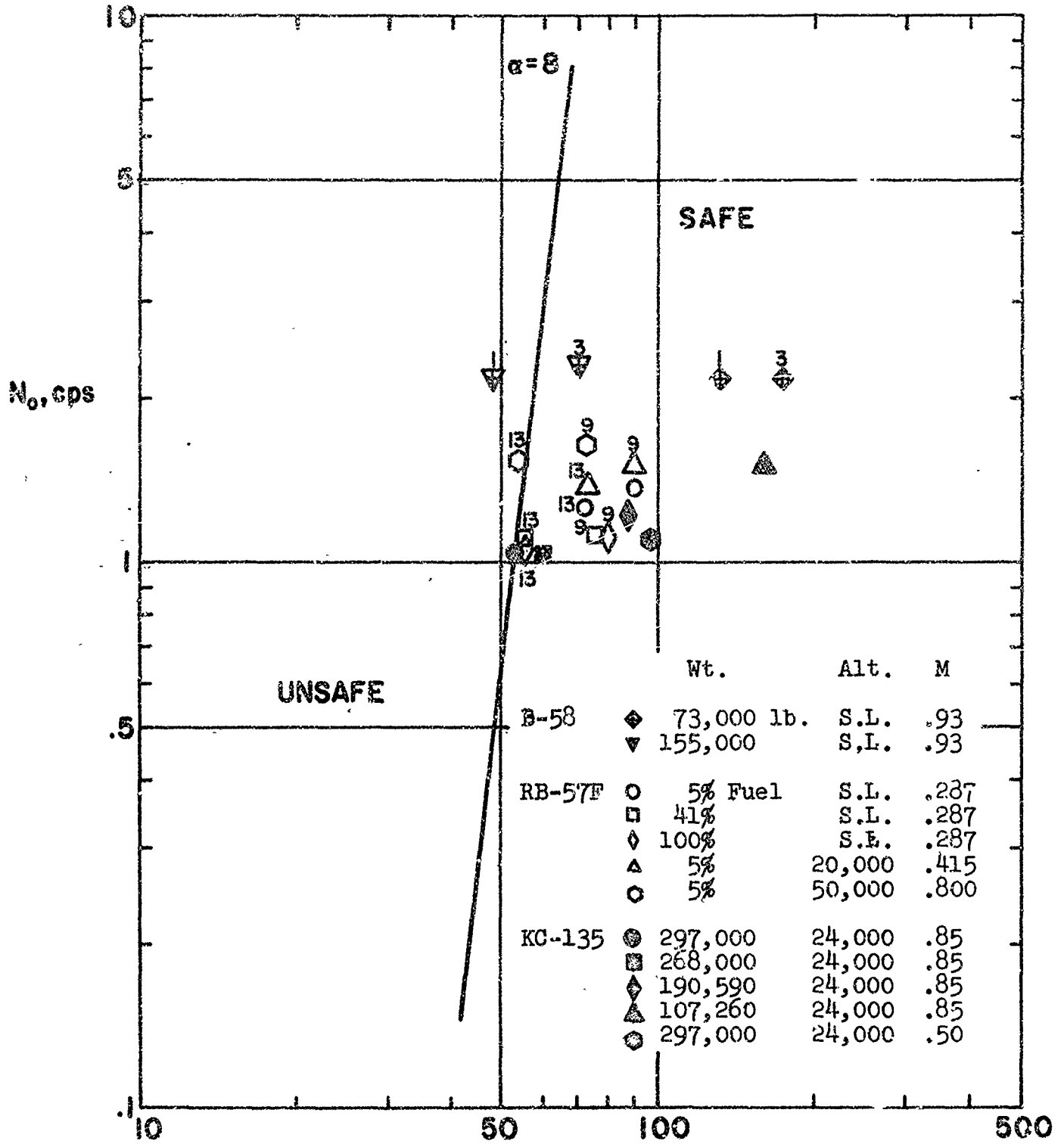


Figure 19. Airplane Computational Results for N_0 vs. $\frac{x}{A}$ Approach



$$\frac{x}{A} = \frac{\Delta x_1}{A} \quad \text{or} \quad \frac{x}{A} \left(\frac{1000}{L} \right)^{\frac{1}{3}}$$

Figure 20. Illustrative N_0 vs. $\frac{x}{A}$ Dependence on Flight Conditions

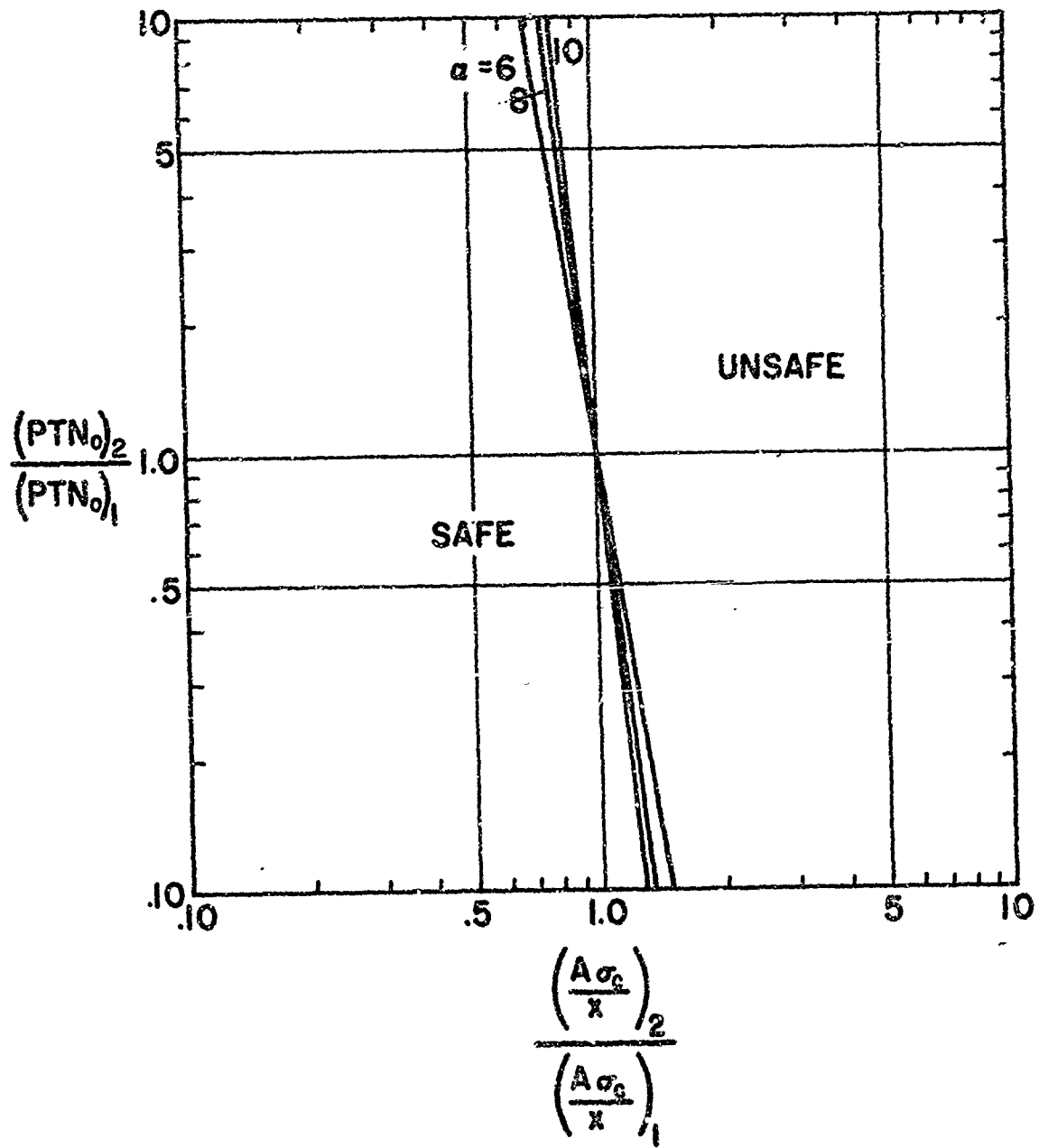


Figure 21. Gust Design by Comparison (Note, Stresswise Adding Metal Lowers A)

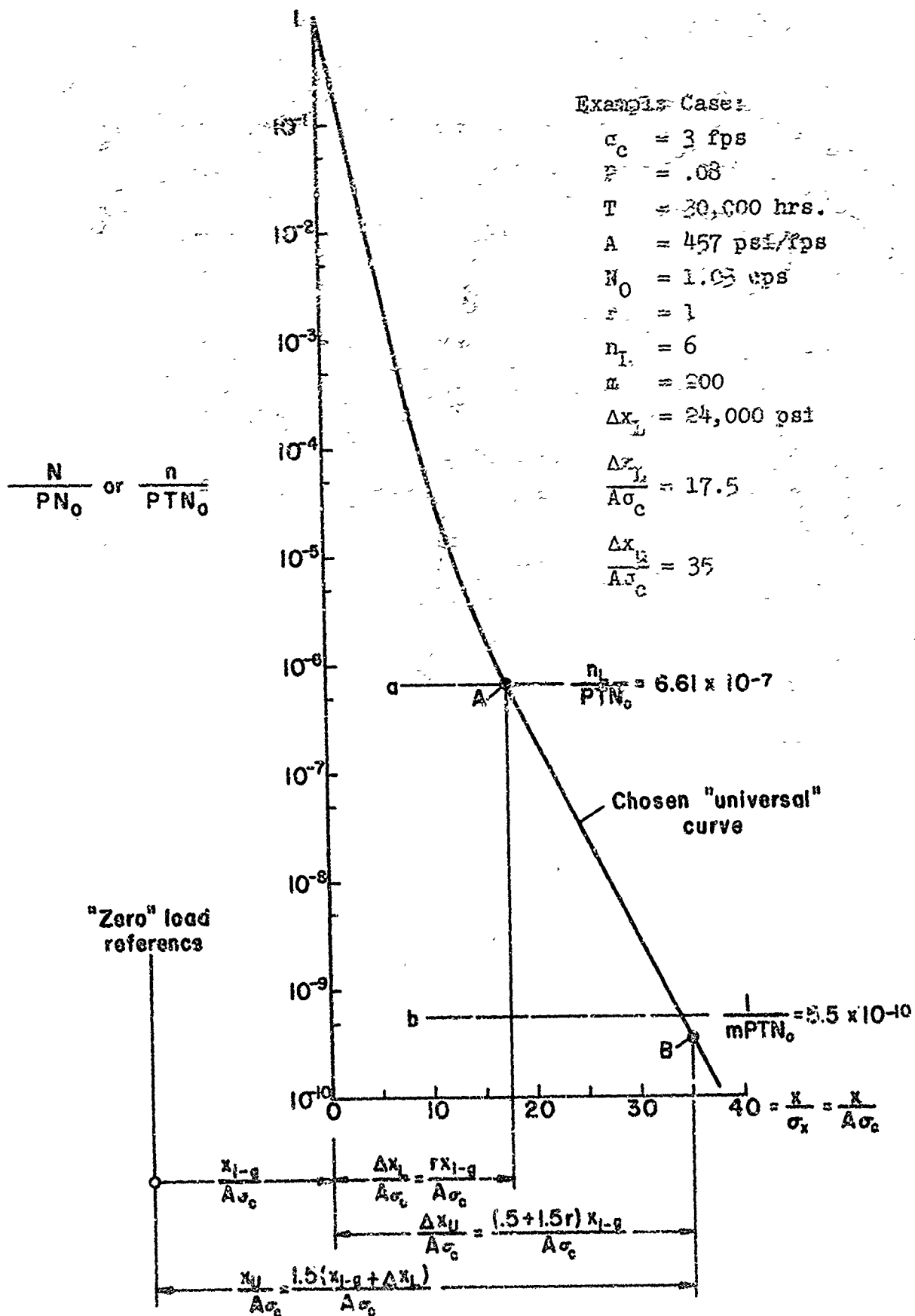


Figure 22. Design Based on Stipulated σ_c , P , and T

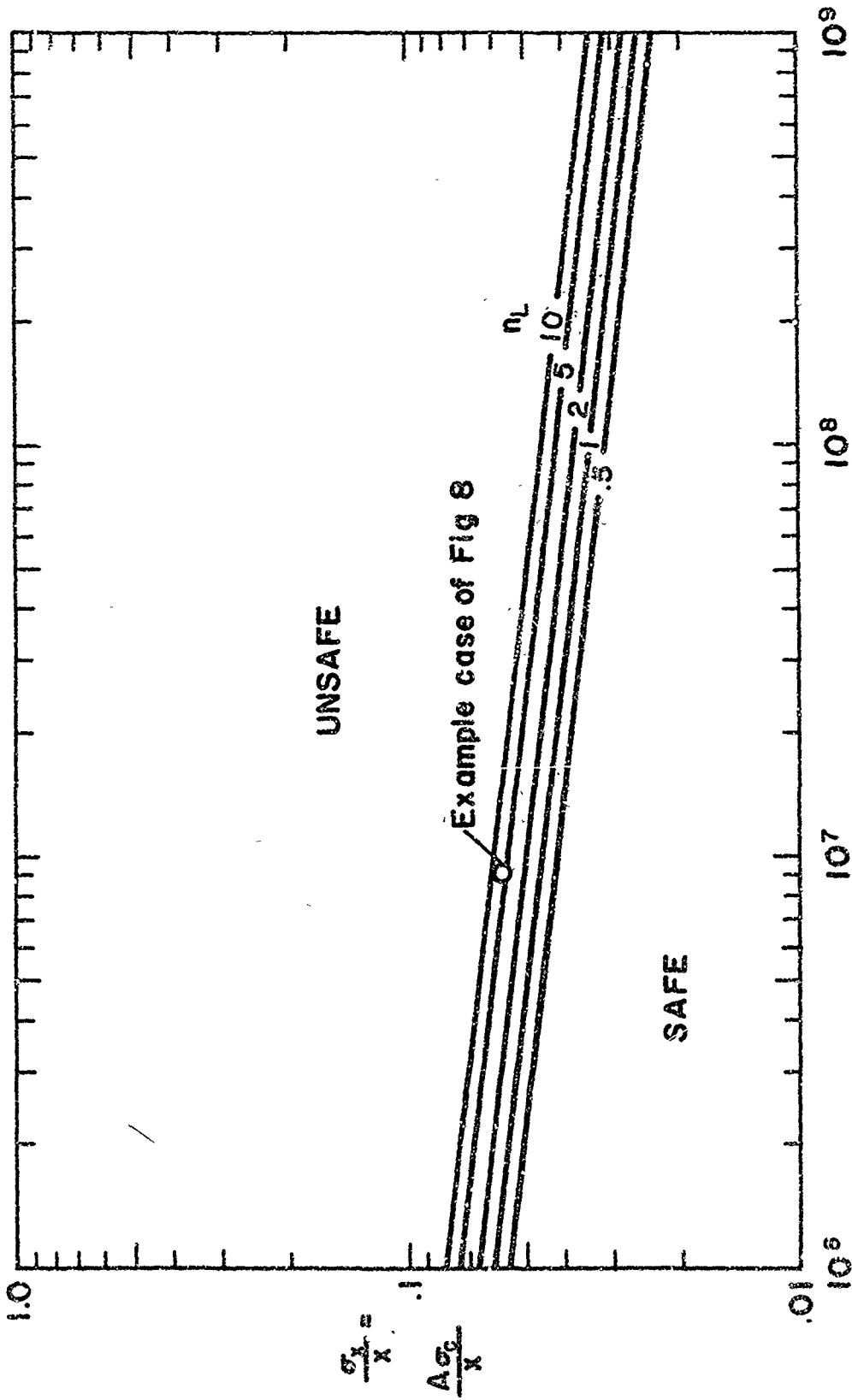


Figure 23. Master Design Chart for Load Exceedance

Number of upward zero crossings, $n_0 = PTN_0$

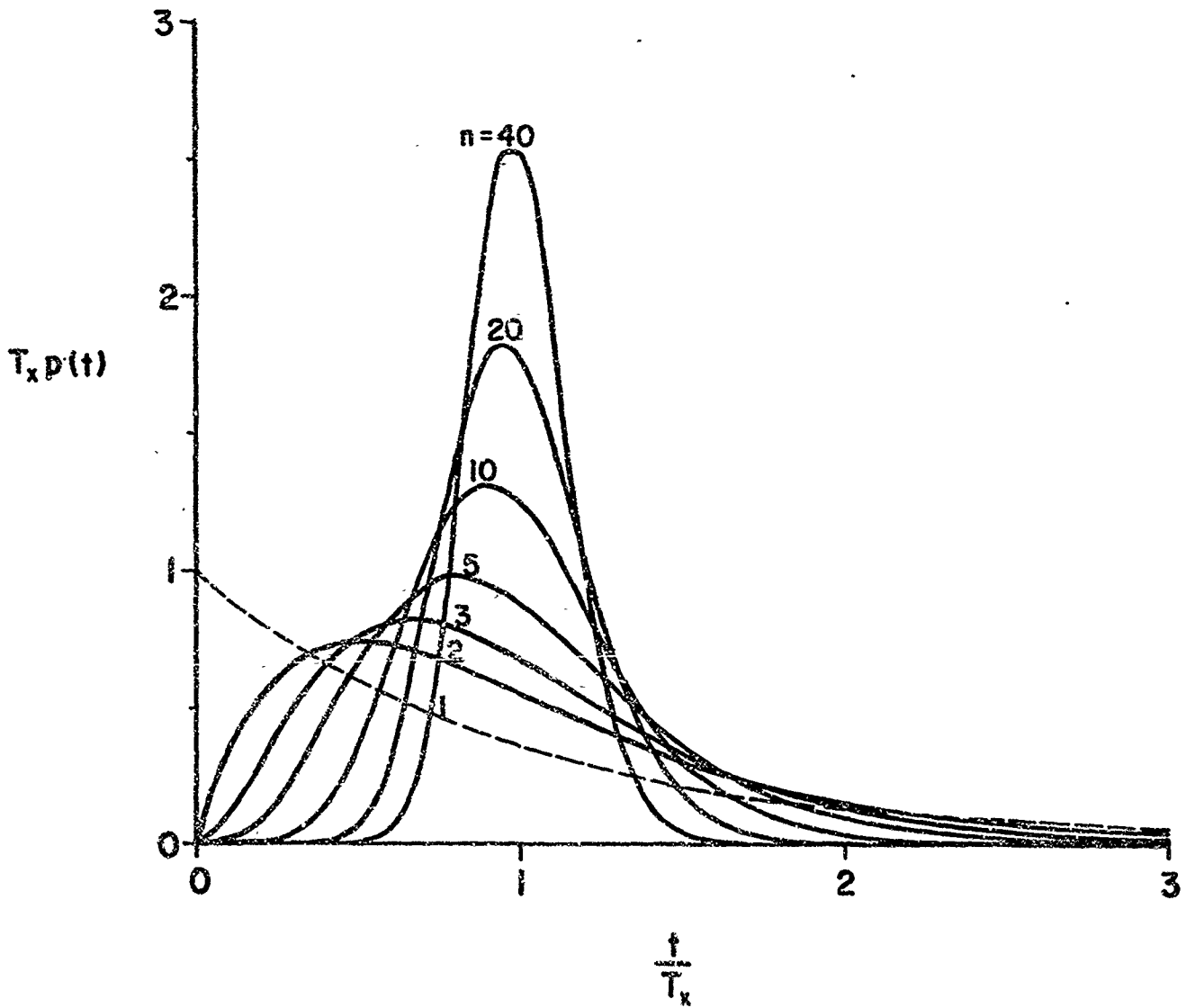


Figure 24a. Distribution Function for Repeat Time; Case a

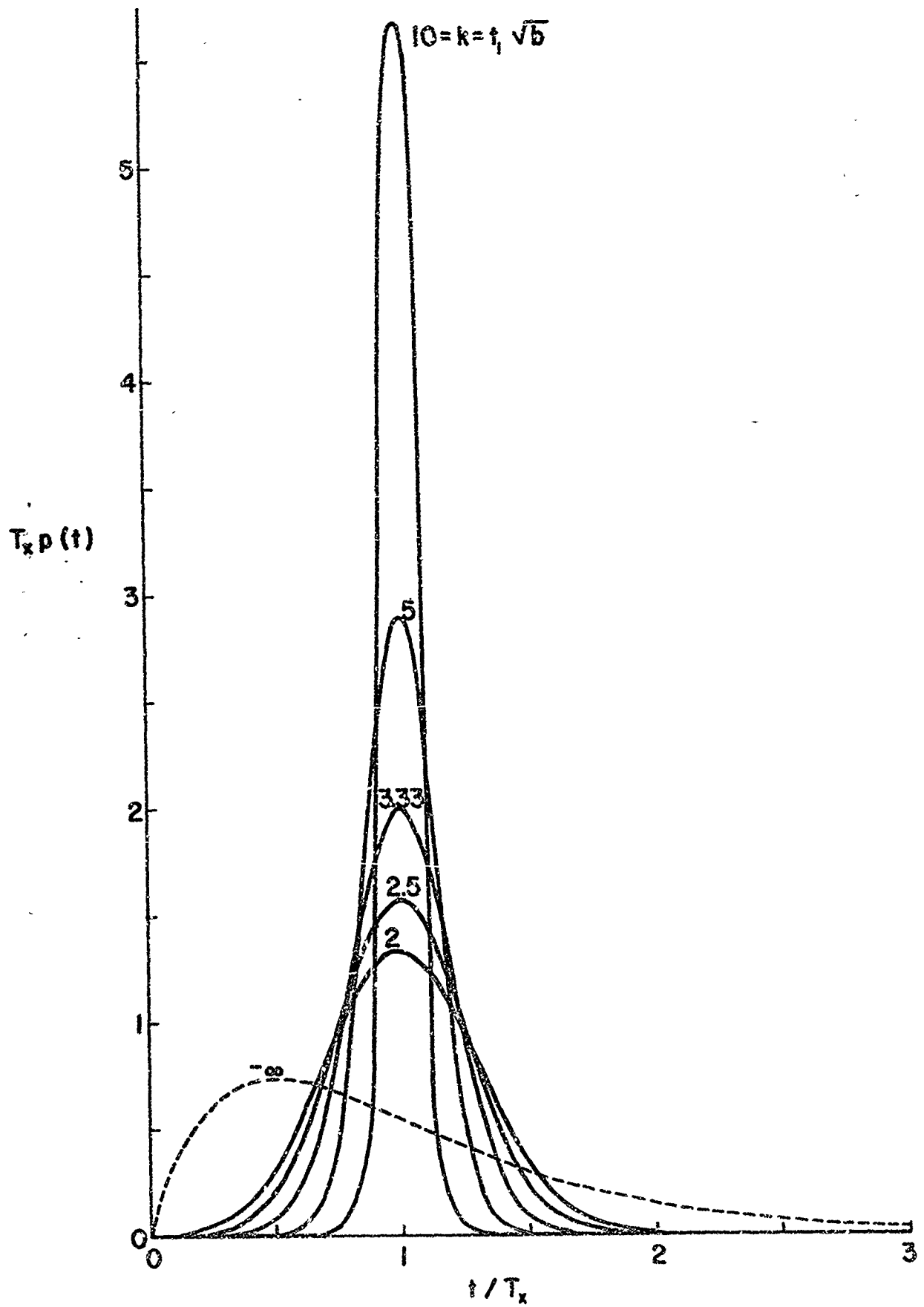
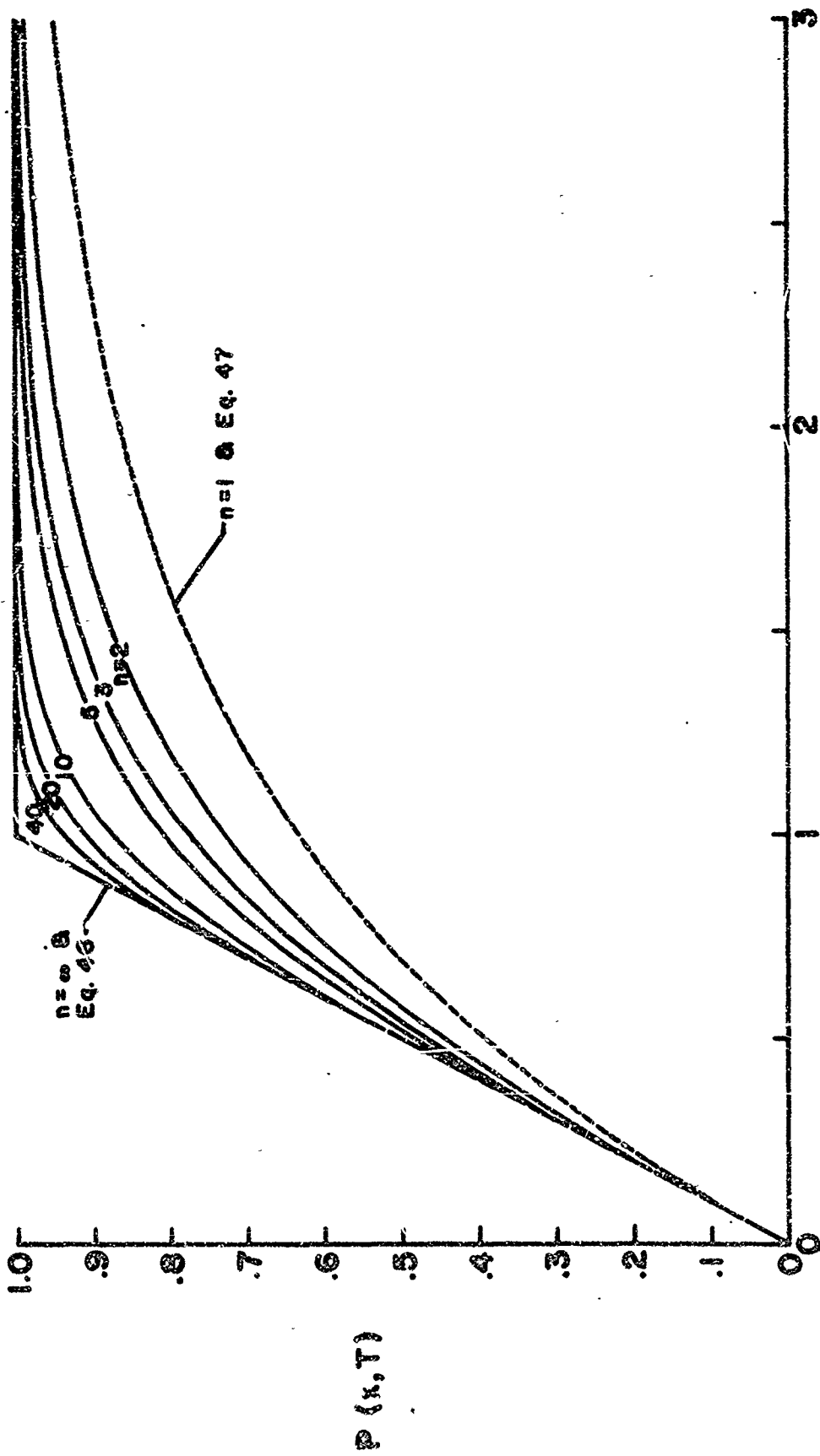


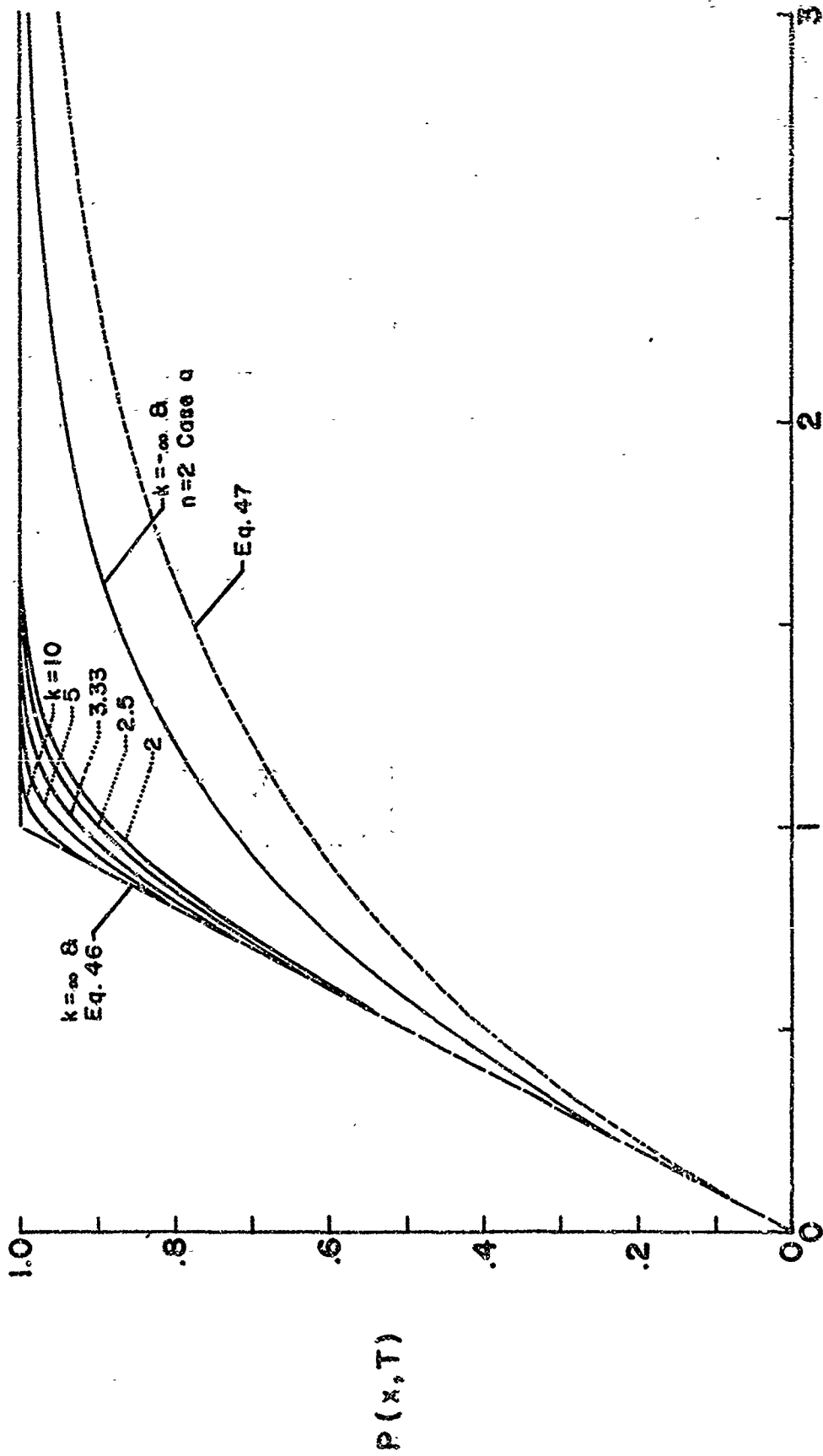
Figure 24b. Distribution Function for Repeat Time; Case b



$$\frac{T}{T_x} = TPN_0 f\left(\frac{x}{\sigma_x}\right)$$

Figure 25a. Probability of Exceeding Load Level x in Time T ; Case a.

$P(x, T)$



$$\frac{T}{T_x} = TPN_0 f\left(\frac{x}{\sigma_x}\right)$$

Figure 25b. Probability of Exceeding Load Level x in Time T ; Case b

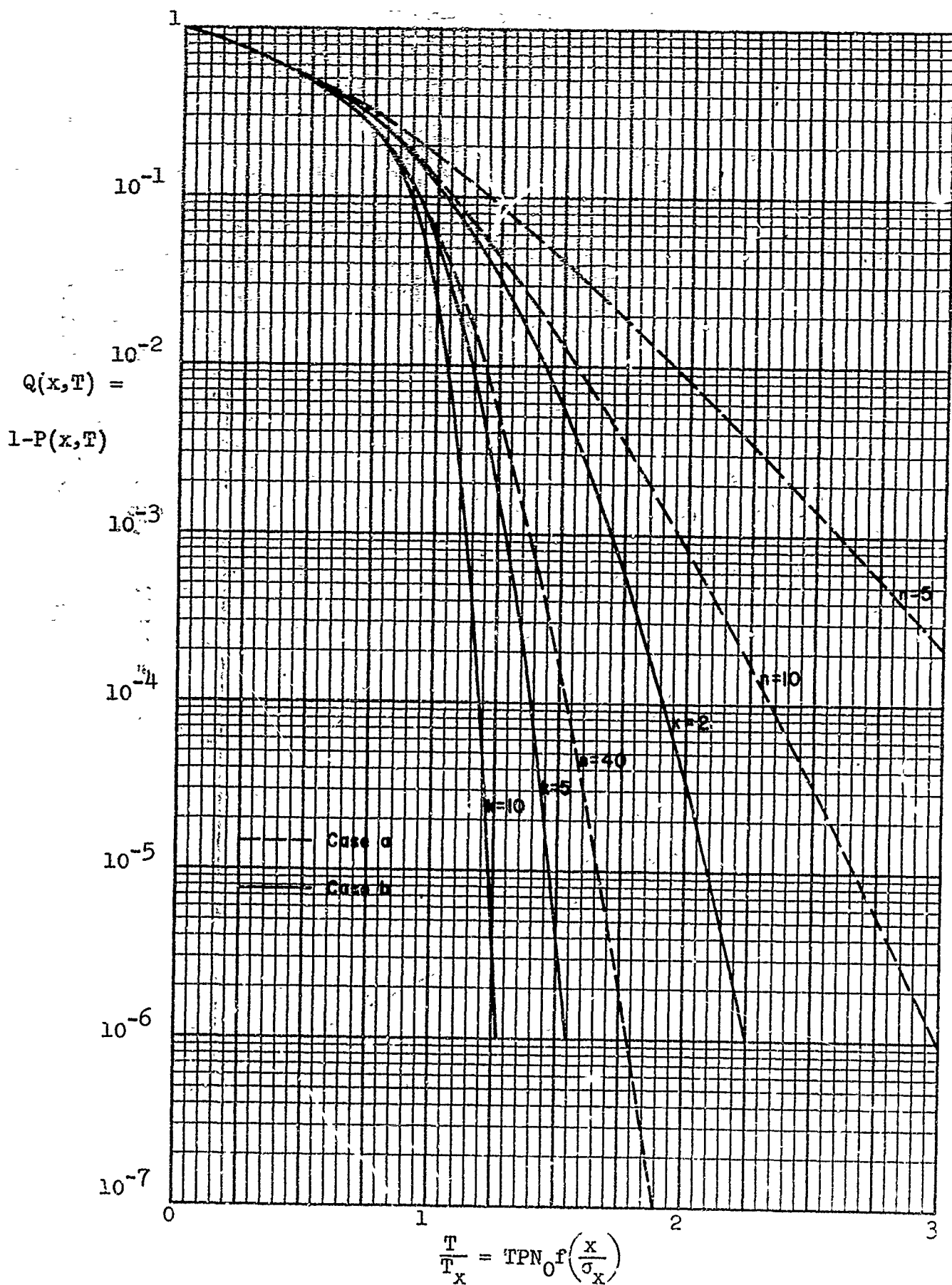
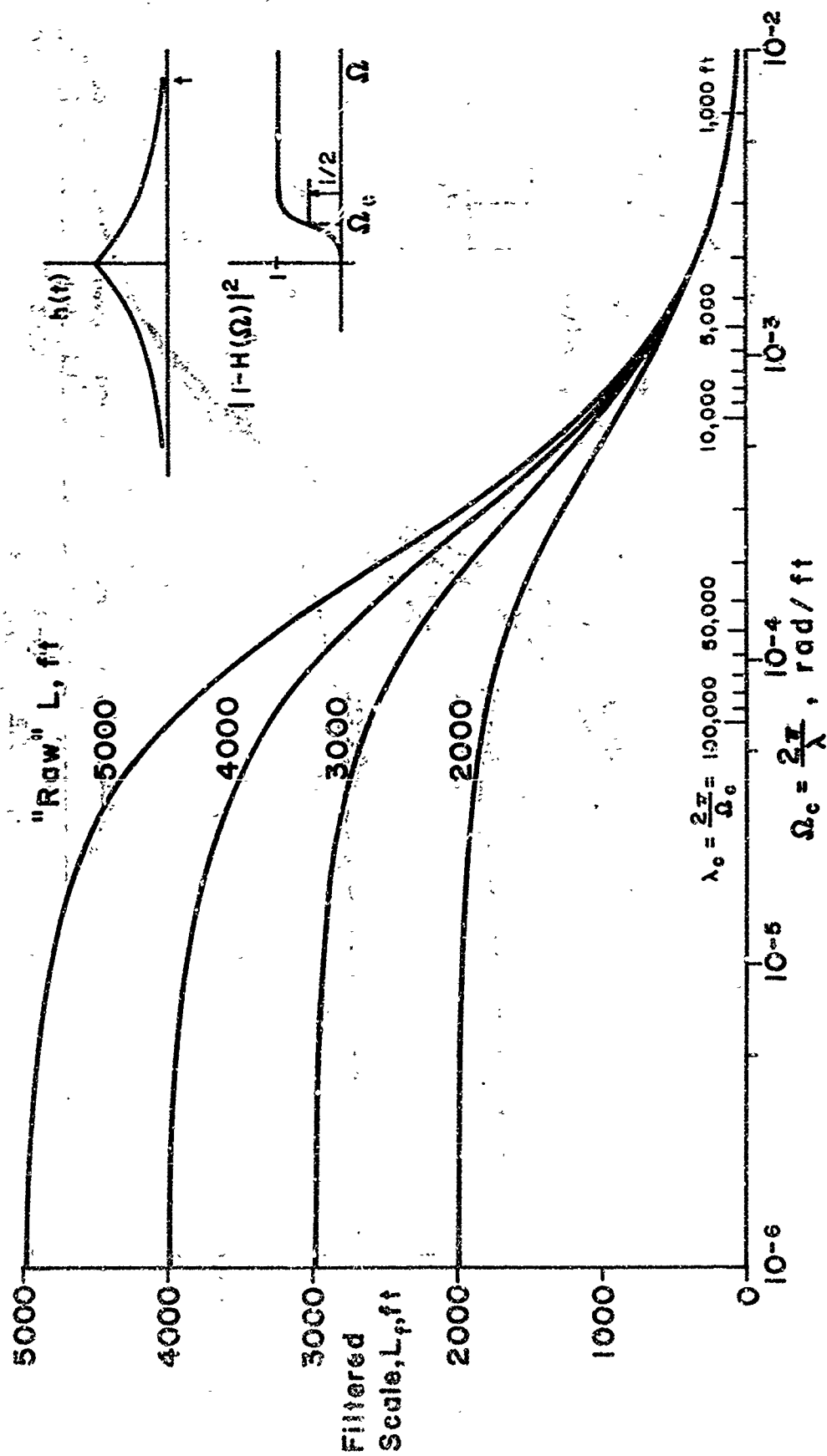
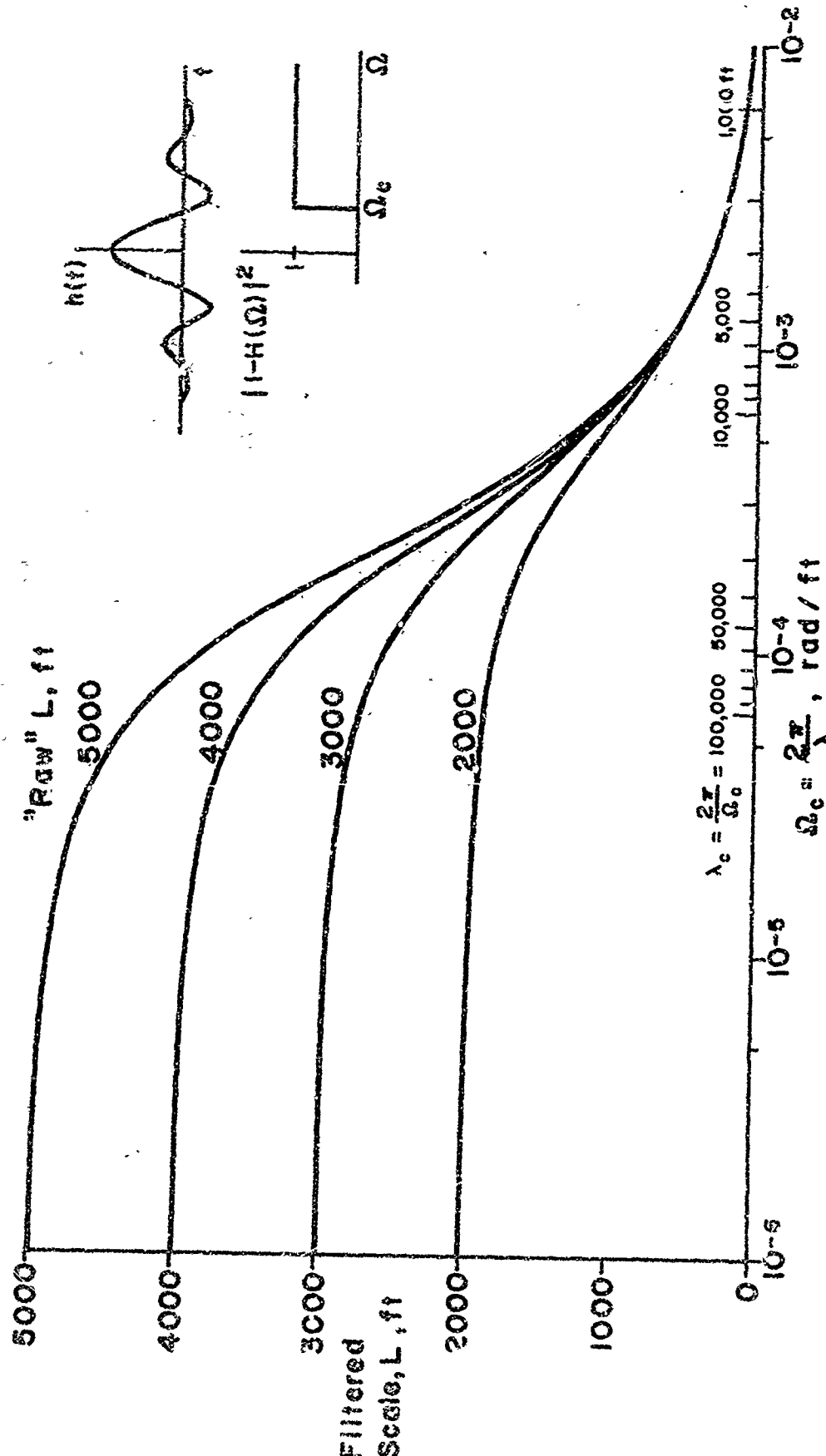


Figure 26. Probability of Not Exceeding Load Level x in Time T



(a) Gradual cutoff

Figure 27(a) Effect of Filtering on L Values



(b) Sharp cutoff

Figure 27. Concluded

Unclassified

Security Classification

DOCUMENT CONTROL DATA - R & D

(Security classification of title, body of abstract and indexing annotation must be entered - even if the overall report is classified)

1. ORIGINATING ACTIVITY (Corporate author) Aeronautical Research Associates of Princeton, Inc. Princeton, New Jersey 08540		1a. REPORT SECURITY CLASSIFICATION Unclassified	
		2a. GROUP	
3. REPORT TITLE Gust Design Procedures Based on Power Spectral Techniques			
4. DESCRIPTIVE NOTES (Type of report and inclusive dates) Final Report: July 1965 - April 1967			
5. AUTHOR(S) (First name, middle initial, last name) John C. Houbolt			
6. REPORT DATE	7a. TOTAL NO. OF PAGES 110	7b. NO. OF REFS 11	
8a. CONTRACT OR GRANT NO. AF33(615)-2878	8b. ORIGINATOR'S REPORT NUMBER(S) ARAP Report No. 106		
8c. PROJECT NO.	8d. OTHER REPORT NO(S) (Any other numbers that may be assigned this report) AFFDL-TR-67-74		
9. DISTRIBUTION STATEMENT This document is subject to specific export controls and each transmittal to foreign governments or foreign nationals may be made only with prior approval of AFFDL(FDTR), Wright-Patterson AFB, Ohio 45433			
11. SUPPLEMENTARY NOTES		12. SPONSORING MILITARY ACTIVITY AFFDL (FDTR) Wright-Patterson AFB, Ohio 45433	
13. ABSTRACT Further developments of gust design procedures based on power spectral techniques are presented. A number of topics are considered, and presentation is in the nature of a series of interrelated small reports under one cover. Generalized load exceedance curves are considered theoretically, and certain significant properties of these curves are established. It is shown that response and design considerations may be expressed in terms of three basic parameters: P the proportion of time in turbulence, σ_c the gust severity, and a shape parameter which defines the generalized exceedance curves. Over a dozen different families of theoretical exceedance curves are generated. The basic response and environmental parameters that are of concern in design are discussed, and the use of composite values of these parameters as might be involved in mission considerations is shown. The composite gust intensity value σ_c , and the related scale value, L, still represent unsettled questions. A reexamination of some previous airline operational data in terms of generalized exceedance curves is included. Recommendations on four specific design procedures are given. One of the design procedures, based primarily on the response parameters A and N_0 , incorporates the results of computational studies that were performed on certain existing aircraft as a means for establishing design boundaries. The problem of determining the probability of exceeding given load levels in flights of (continued on reverse side)			

DD FORM 1 NOV 55 1473

Unclassified

Security Classification

14. KEY WORDS	LINK A		LINK B		LINK C	
	ROLE	WT	ROLE	WT	ROLE	WT
gust design procedures power spectral techniques atmospheric turbulence aircraft dynamic response gust spectra scale value discrete gust design exceedance curves probability density probability of exceeding aircraft operational statistics						
13. Abstract (Cont'd) specified duration is investigated. Areas and parameters which are considered to have weakness or uncertainty are indicated, and recommendations are accordingly made for appropriate future research effort. Consideration of the effect of filtering on deduced scale value is included in an Appendix.						